Synthesis and characterization of anion exchange blend membranes for vanadium redox flow battery applications

Von der Fakultät Energie-, Verfahrens- und Biotechnik der Universität Stuttgart
zur Erlangung der Würde eines Doktors der Ingenieurwissenschaft (Dr.-Ing.)
genehmigte Abhandlung

Vorgelegt von
Hyeongrae Cho
aus Seocheon, Südkorea

Hauptberichter: Prof. Dr. rer. nat. Andreas Friedrich
Mitberichter: Prof. Dr. Qingfeng Li
Prüfungsvorsitzender: Prof. Dr. -Ing. Ulrich Nieken

Tag der mündlichen Prüfung: 07.12.2021

Institut für Chemische Verfahrenstechnik der Universität Stuttgart

2021

Contents

Erklärung

Hiermit versichere ich, dass ich die vorliegende Arbeit mit dem Tite

"Synthesis and characterization of anion exchange blend membranes for vanadium redox flow battery applications"

selbstständig verfasst und keine anderen als die angegebenen Quellen und Hilfsmittel benutzt habe, dass alle Stellen der Arbeit, die wörtlich oder sinngemäß aus anderen Quellen übernommen wurden, als solche kenntlich gemacht sind.

Ich versichere außerdem, dass die vorliegende Dissertation nur in diesem und keinem anderen Promotionsverfahren eingereicht wurde und dass diesem Promotionsverfahren keine endgültig gescheiterten Promotionsverfahren vorausgegangen sind.

Declaration of Authorship

I herewith duly declare that I have authored the dissertation

"Synthesis and characterization of anion exchange blend membranes for vanadium redox flow battery applications"

independently and only with use of specified aids. I have mentioned all sources used and cited correctly according to scientific rules.

Stuttgart, __, __, ____ ________________________________

Hyeongrae Cho

Publication of the individual chapters in scientific journals

The present thesis has a cumulative structure, this means the chapters are papers which have been published in scientific journals.

Chapter 3. Application of Novel Anion-Exchange Blend Membranes (AEBMs) to Vanadium Redox Flow Batteries

Hyeongrae Cho, Henning M. Krieg and Jochen A. Kerres

Membranes 2018, 8(2), 33

(H.C. and J.K. conceived and designed the experiments. H.C. performed the experiments. H.C., J.K., and H.K. analysed the data. H.C., J.K., and H.K. wrote the paper.)

Chapter 4. Performances of Anion-Exchange Blend Membranes on Vanadium Redox Flow Batteries

Hyeongrae Cho, Henning M. Krieg and Jochen A. Kerres

Membranes 2019, 9(2), 31

(Conceptualization, H.C., J.A.K.; investigation, H.C.; data analysis, H.C., J.A.K., H.M.K.;

writing-first draft, H.C.; review and editing, J.A.K., H.M.K.)

Chapter 5. Novel Anion Exchange Membrane Based on Poly(Pentafluorostyrene) Substituted with Mercaptotetrazole Pendant Groups and Its Blend with Polybenzimidazole for Vanadium Redox Flow Battery Applications

Hyeongrae Cho, Vladimir Atanasov, Henning M. Krieg and Jochen A. Kerres

Polymers 2020, 12(4), 915

(H.C. and J.A.K. conceived and designed the experiments. H.C. performed the experiments.

H.C., J.A.K., V.A. and H.M.K. analysed the data. H.C. wrote the first draft. J.A.K., V.A. and H.M.K. reviewed and edited the manuscript. All authors have read and agreed to the published version of the manuscript.)

Patent enrollment

One patent has been enrolled during thesis work:

Kationenaustauscher- und Anionenaustauscherpolymere und –(blend)membranen aus hochfluorierte aromatische Gruppen enthaltenden Polymeren mittlels nucleophiler Substitution

AKZ 10 2019 008 024.6

Jochen Kerres, **Hyeongrae Cho**, Vladimir Atanasov

This Patent is still closed due to license change from national (DE) to international (TCP). The patent license is currently under negotiation with company Freudenberg and therefore cannot be present in this dissertation.

Further non-related publications

To complete the publication list these are my further contribution the publications are not content of this thesis.

- Simple fabrication of 12 μm thin nanocomposite fuel cell membranes by direct electrospinning and printing

Matthias Breitwieser, Carolin Klose, Matthias Klingele, Armin Hartmann, Johannes Erben, **Hyeongrae Cho**, Jochen Kerres, Roland Zengerle, Simon Thiele

Journal of Power Sources 337 (2017) 137-144

- Electrospun sulfonated poly(ether ketone) nanofibers as proton conductive reinforcement for durable Nafion composite membranes

Carolin Klose, Matthias Breitwieser, Severin Vierrath, Matthias Klingele, **Hyeongrae Cho**, Andreas Büchler, Jochen Kerres, Simon Thiele

Journal of Power Sources 361 (2017) 237-242

- Electrowinning of Iron from Spent Leaching Solutions Using Novel Anion Exchange Membranes

Wouter Dirk Badenhorst, Cloete Rossouw, **Hyeongrae Cho**, Jochen Kerres, Dolf Bruinsma, Henning Krieg

Membranes 2019, 9(11), 137

Abbreviations

IEM Ion exchange membrane

CEM Cation exchange membrane

AEM Anion exchange membrane

SPEK Sulfonated poly(ether ketone)

Br-PPO Brominated poly (2, 6-dimethyl-1,4-phenylene oxide)

PVDF-HFP Poly(vinylidene fluoride-co-hexafluoropropylene)

S-PEEK Sulfonated poly(ether ether ketone)

PBI Polybenzimidazole

VRFB Vanadium redox flow battery

AEBM Anion exchange blend membrane

PPFSt Poly(pentafluorostyrene)

RFB Redox flow battery

CNT Carbon nano tube

PAN Polyacrylonitrile

CE Coulombic efficiency

VE Voltage efficiency

EE Energy efficiency

NMR Nuclear magnetic resonance

FT-IR Fourier transform infrared spectroscopy

IEC Ion exchange capacity

TGA Thermal gravimetric analysis

DMAc Dimethylacetamide

WU Water uptake

SR Swelling ratio

OCV Open circuit voltage

PBIOO Poly[(1-(4,4′-diphenylether)-5-oxybenzimidazole)-benzimidazole]

F6-PBI Hexafluoropropylidene polybenzimidazole

TMIm 1,2,4,5-tetramethylimidazole

DOS Degree of substitution

PA Phosphoric acid

HT-PEMFC High temperature proton exchange membrane fuel cell

PPFSt Poly(pentafluorostyrene)

ADL Acid doping level

1. Scope of this work

Due to the increasing concerns of fossil fuel using and environmental issues, the world needs to develop renewable energy sources and clean energy conversion devices, e.g. fuel cells, flow batteries and electrolyzers. Vanadium redox flow batteries (VRFBs) are considered promising energy storage system for large scale applications due to their long cycle lives, low cost, design flexibility and safety.

Ion exchange membrane (IEM) is polymeric material composed of ionic head groups as fixed ions in polymeric backbone and transportable ions. Those types of membranes can be used in various applications which are energy related devices mentioned above. Therefore, developments of ion exchange membranes are required with improved properties to increase the efficiency of energy applications.

Aim of this work is to develop ion exchange membranes with improved properties and to display better performances in VRFB compared to commercial reference membranes. Because currently available IEMs in VRFBs are limited due to fast vanadium ions cross-over or/and low ionic conductivity resulting in low performances in the battery. To overcome those drawbacks and to be used in vanadium redox flow battery, ion exchange membranes were developed either by blending or via new synthetic procedures. Thus, novel ion exchange polymers and/or membranes were developed, analyzed and applied in vanadium redox flow battery.

In this dissertation, therefore, polymers synthesis, membranes preparation and applications of ion exchange membranes have been studied. This dissertation is divided into mainly three parts. The first part introduces a general background of the subject regarding ion conducting polymers and applications in vanadium redox flow battery. The second part is the papers published during the thesis work. The last part of this dissertation is overall discussion on the results and summary.

2. Introduction

2.1 Ion exchange membranes (fundamentals of IEMs)

Ion Exchange Membranes (IEMs) conduct ions through the membrane. IEM is generally classified as a Cation Exchange Membranes (CEMs) or an Anion Exchange Membranes (AEMs) depending on the ions which permeate through the membrane. For example, a CEM is composed of negatively charged head groups as fixed ions in the membrane and cations as counter ions that are transportable along with a membrane. While an AEM is consisting of cationic head groups and exchangeable anions [1][2]. IEMs are used in various energy applications such as fuel cells [3], electrolyzers [4], redox flow batteries [5], actuators [6] and solar cells [7].

For CEMs, a most prominent CEM is a perfluorinated polymer membrane, known as Nafion, showing excellent performance such as high thermal and chemical stabilities and superior ionic conductivity due to the hydrophilic-hydrophobic phase separated morphology (**Figure 1,** lamellar microstructures of Nafion were confirmed by SAXS experiments by Kreuer showing wide channels, more separated and good connectivity [8]). Despite of outstanding performance of Nafion membranes, it is still challenges for large scale commercialization due to several shortcomings such as a complex production process, disposal of environmental-unfriendly chemicals, high permeability through the membrane and high price [9]. For this reason, development of alternative membranes has been intensively studied, for example, a-hydrocarbon based CEM, sulfonated arylene main chain ionomers by fine tuning, acid-base blends membranes and cross-linked cation exchange membranes to be applied in electro-chemical devices such as fuel cells and electrolyzers [10].

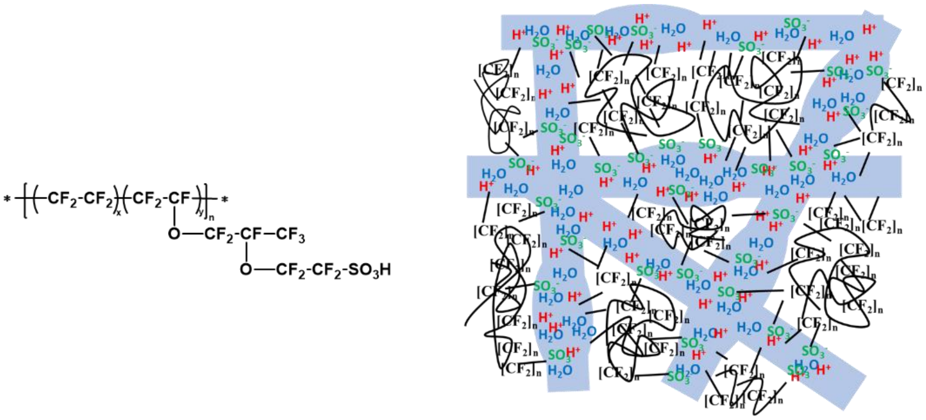

Structure of perfluorinated polymer (Nafion)

Microstructure : Ion channels

Figure 1. Structure of a perfluorinated polymer and its hydrophilic-hydrophobic phase separated microstructure

AEMs can be further defined as non-alkaline anion exchange membranes and alkaline anion exchange membranes depending on counter ions (**Figure 2 (a)**). AEMs possessing anion such as Br^-, Cl^-, I^-, SO_4^{2-} and HSO_4^- are regarded as non-alkaline anion exchange membranes, while OH^-, CO_3^{2-} and HCO_3^- are refined as alkaline anion exchange membranes. Applications are depending on the type of anions for example, SO_4^{2-} or HSO_4^- in vanadium redox flow battery OH^- form in alkaline fuel cell and HCO_3^- form in CO_2 pumps. Anion exchange membranes also can be applied as proton exchange membranes in fuel cells by doping in/with phosphoric acid. The quaternized ammonium head groups of AEM can absorb phosphoric acids via acid base interactions, phosphoric acids can be doped more than one molecule per quaternized head group by hydrogen bonds. Therefore, the phosphoric acid doping level (ADL, how many phosphoric acid molecules per anion exchange group) is important for proton transportation. Along with the doped phosphoric acids, the AEM transports protons through the membrane as described in **Figure 2 (b)** [11][12].

The main challenge of AEM is a low alkaline stability of cationic head groups. Most of cationic head groups are based on quaternary ammonium which are prone to degraded by hydroxide ions. There are possible degradation pathways triggered by hydroxide ions shown in (**Figure 3**). The degradation, nucleophilic substitute induced by hydroxide attack, takes place to a carbon next to nitrogen and formed alcohol and amine. Hofmann elimination can be taken place in the presence of β-hydrogen forming to alkene and amine. Rearrangements such as Sommelet-Hauser rearrangement and Stevens rearrangement are possible that is alkyl groups shift from nitrogen to carbon forming a trimethylamine. To enhance the chemical stability toward hydroxide, polymer designs such as introducing bulky groups providing steric hindrance and electron donating groups are suggested and showed improved chemical stabilities [10].

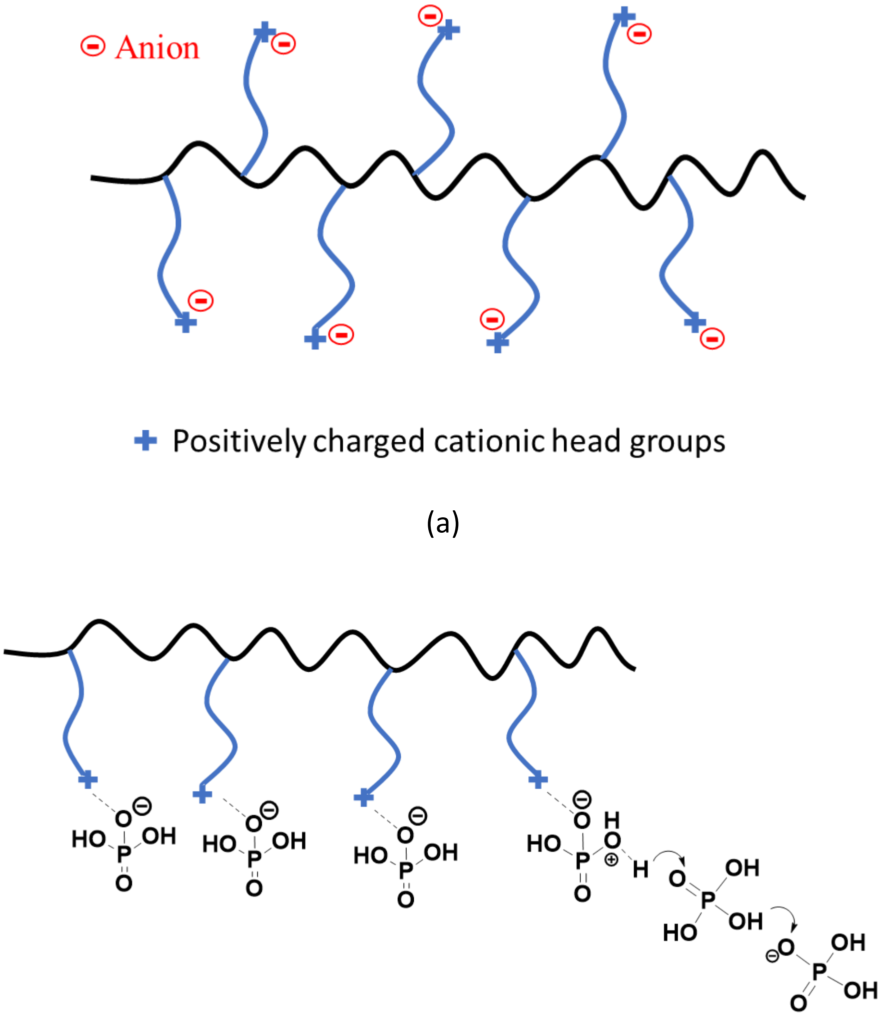

(a)

(b)

Figure 2. Structure of an anion exchange membrane (a) and phosphoric acid doped anion exchange membrane (b)

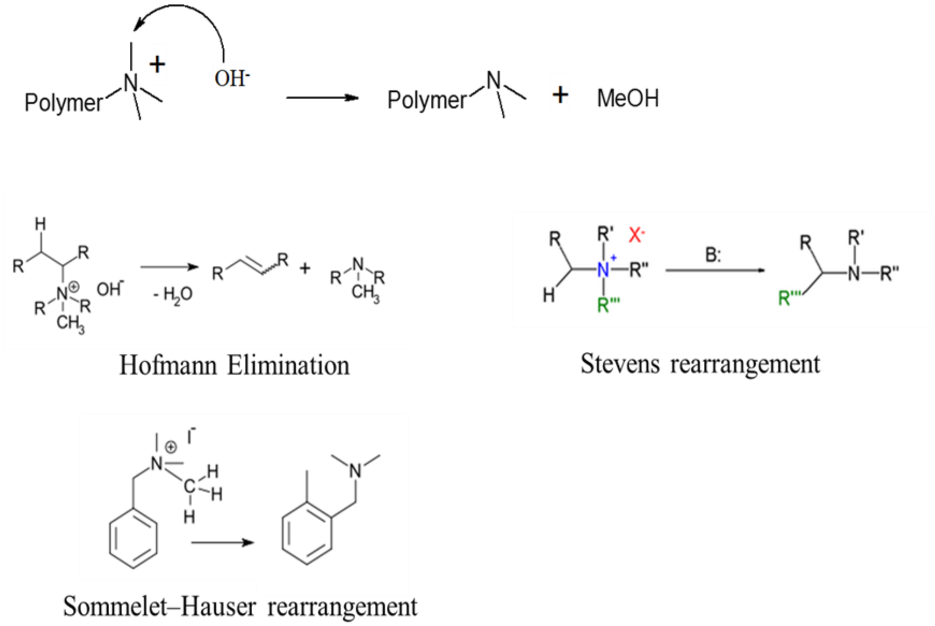

Hofmann Elimination

Stevens rearrangement

Sommelet–Hauser rearrangement

Figure 3. Possible degradation pathways of AEMs

General requirements of IEMs to be applied in electrochemical devices are as follows: 1) sufficient mechanical strength, 2) high ionic conductivity, 3) high chemical and thermal stabilities, 4) no or little fuel or electrolyte cross-over through the membranes.

The typical process to obtain an IEM is to dissolve a polymeric material in an organic solvent and casting on a proper plate, and finally, evaporating the solvent. Then, IEMs are obtained. Meanwhile there are new methods for IEMs preparation to improve the performances of membranes such as (i) blending, (ii) pore filling, (iii) in-situ polymerization and (iv) electrospinning [13]. Polymer blending (i) is an attractive method since this method enhances the chemical and mechanical stability and increases the ionic conductivity [14]. Although this method is simple for IEMs preparation, superior IEMs can be produced by choosing two or more polymers which are thermal-, chemical- and mechanically stable and in an appropriate ratio among the polymers. Pore filling (ii) is a novel way to prepare IEMs. IEMs are generally prepared by filling a polymeric electrolyte into a porous substrate. The porous substrate, therefore, is required chemically and mechanically stable. In this method, IEMs with high selectivity, high ion exchange capacity and low swelling can be prepared [15]. Conventional in-situ polymerization (iii) employs post-modification process which will bring additional cost and toxicity risks resulting in an obstacle to industrial scale commercialization, therefore, in situ polymerization has been achieved without post-modification [16]. In this study, brominated poly (2,6-dimethyl-1,4-phenylene oxide) (Br-PPO) was dissolved in liquid monomers without organic solvents followed by addition of tertiary amines. Then the crosslinked AEMs were obtained by thermal crosslinking during the membrane formation process. Electro-spinning method (iv) for IEM preparation provides unique advantages. A polymer solution in an injector flies to the collector due to the applied electric field in-betweens, subsequently a mat of nanofibers is formed onto collectors [17]. For example, a reinforced cation exchange membrane was prepared by electrospun sulfonated poly(ether ketone) (SPEK) nanofiber followed by filling the fiber mat voids with a Nafion dispersion by inkjet-printing [18]. The reinforced SPEK membrane exhibited 30% higher peak power density in fuel cell test than that of a reference membrane reinforced with a poly(vinylidene fluoride-co-hexafluoropropylene) (PVDF-HFP fiber mat).

2.2 Membranes for VRFBs

For the VRFB applications, both AEM and CEM can be used as a separator. The primary function of the IEM in VRFB is not only conduct ions of supporting electrolytes such as proton or SO_4^{2-} or HSO_4^- but also to prevent cross mixing of vanadium ions between two electrolyte tanks. Nafion membranes, as described in introduction part, are commonly used in VRFBs due to high chemical stability and its superior ionic conductivity [19]. In VRFBs, a Nafion membrane showed high vanadium ions crossover resulting in a fast capacity decay during a charge-discharge cycling test [20]. Therefore, modification of Nafion membranes has been studied and applied in VRFBs. Those membranes have shown improved battery performances, for example, coating with polyethyleneimine, poly(diallyldimethylammonium chloride) and poly(styrene sulfonic acid) and composite membranes with inorganic particles [21][22][23][9]. In spite of efforts to improve performances in VRFBs, however, Nafion membranes are too expensive to facilitate a large scale commercialization [24]. Alternative aromatic hydrocarbon main chain polymers have been studied in VRFBs such as sulfonated poly(ether ether ketone), (S-PEEK) and sulfonated Radel-polymer indicating better performance than Nafion membranes [25][26]. However, these types of membranes are obviously degraded by highly oxidative vanadium (V^{5+}) species forming vanadium radical resulting in aromatic chain scission (**Figure 4**) [27]. The V^{5+} oxidizes phenyl group through a radical mechanism, which resulted in a chain scission of phenyl backbone. The V^{5+} oxidizes the hydroxylated backbone into quinone through a redox mechanism.

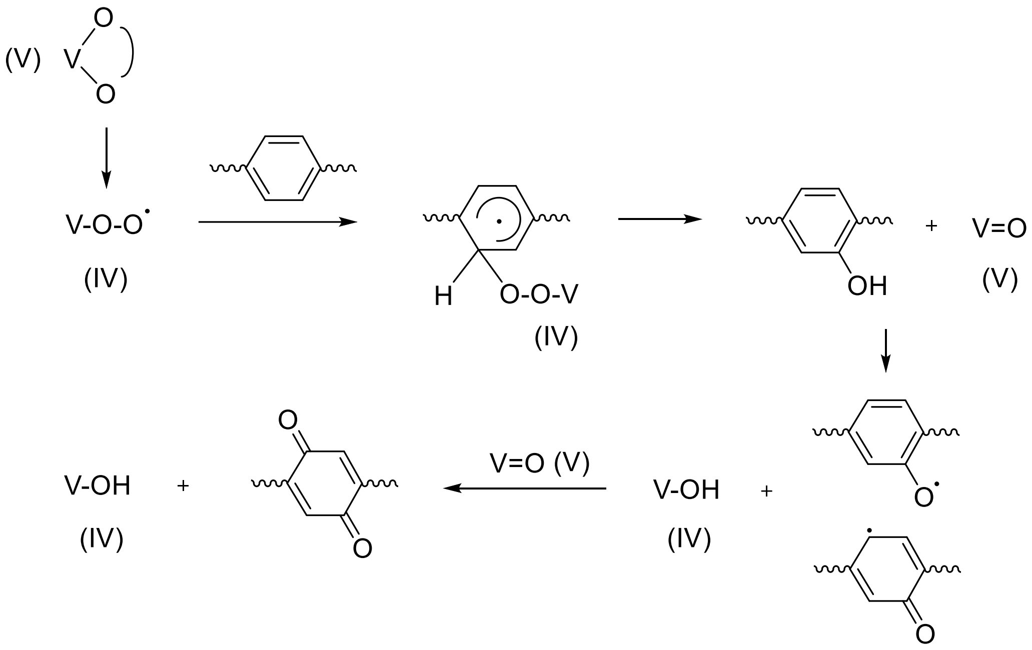

Figure 4. Suggested degradation mechanism via vanadium (V)

AEMs for VRFBs, AEMs have a fixed positively charged cation (typically quaternized ammonium) and a mobile anion which is attached to the polymer chain. Therefore, using AEMs is expected to reduce the vanadium ions permeation owing to Donnan exclusion effect [28]. The Donnan exclusion effect is used to explain how the charged ions are distributed near a permeable membrane. The positively charged cationic head groups of AEM will generate a stable electrostatic field in the membrane matrix, which creates the Donnan potential. The Donnan potential significantly affects to the membrane potential, which prevents the crossover of electroactive species with positive charge. It should be noted that the Donnan potential is highly affected by the imbibed acids, when the AEM is specially immersed in the electrolyte of a strong acid solution. In this case, the distance between AEM and electrolyte becomes narrow which will lead to weaken the repel effect among the positive charged electroactive species and the positive charged cationic head groups. Nevertheless, the Donnan effect will be still influence the transport behavior of positive charged electroactive species [29]. Excellent chemical stability of anion exchange (blend) membranes was also reported due to the either Donnan exclusion effect or cross linking via reducing the free spaces in the membrane, which limits the oxidative vanadium ions permeating through the membranes resulting in less contacts via reduced vanadium ions permeation into membrane and oxidative vanadium ions as described previously [30][31]. Therefore AEMs in VRFBs are intensively studied, for example quaternized Diels-Alder poly(phenylene) membranes, ammonium functionalized Radel membranes and quaternized poly(phthalazinone ether ketone ketone) membranes, showing improved performances in VRFBs in terms of cycling test [32][33][34].

A common and commercially available AEM for VRFBs application is polybenzimidazole (PBI) (see **Figure 5**). The nitrogen groups of imidazole in PBI are protonated in an acid medium and convert to imidazolium which can contribute the ions conducting [35]. It is known that PBI can absorb more than one acid molecule by hydrogen bonds per positively charged cationic head group compared to its halide form e.g. Cl^-, Br^- or I^-, therefore improved conductivity is expected to their halide form. Despite of additional acids absorption toward functional groups, conductivity of acid doped *meta*-PBI was much lower compared to a Nafion membrane (*m*-PBI: 15.8 mS/cm, Nafion 212: 50.7 mS/cm measured in 1M $VOSO_4$ + 4M H_2SO_4) resulting in lower energy efficiency than that of a Nafion membrane above 50 mA/cm^2 in VRFBs [30].

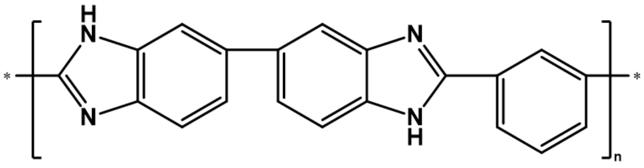

m-PBI

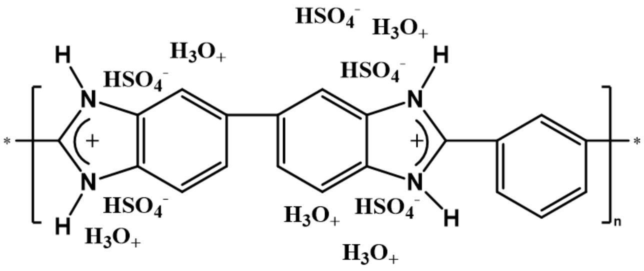

m-PBI doped in sulfuric acid

Figure 5. Structure of *m*-PBI and when it doped in sulfuric acid

Different backbone structures of PBIs (**Figure 6**) have been studied in VRFBs to improve ionic conductivity and battery performances (e.g. Bi*p*PBI, NPBI and poly[(1,4-xylylenediyl)(2-(2,4,6-trimethylphenyl)benzimidazolium 1,3-diyl bromide) [35][36][37]. Bi*p*PBI membranes showed improved conductivity about 2.7 times higher than a *meta*-PBI membrane and this membrane exhibited lower area resistance than a Nafion membrane in 4M sulfuric acid solution resulting in a better battery performance than that of a Nafion membrane in terms of energy efficiency [36]. Thin NPBI (15 µm) membrane showed comparable area resistance with a Nafion membrane exhibiting excellent energy efficiency at a relatively low current density below 100 mA/cm^2 [37]. PBI-ionene blend membranes have been studied that addition of PBI-ionene to PBI has shown the voltage efficiency increasing dramatically. However, despite the increased voltage efficiency, energy efficiency of those blend membranes was slightly lower in performance than that of a Nafion membrane [38].

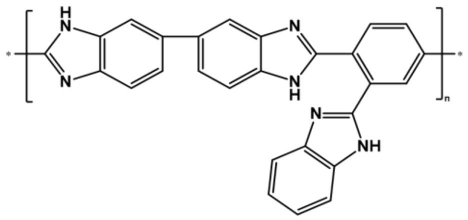

poly[2,2’-(2-benzimidazole-p-phenylene)-5,5’-bibenzimidazole] (BIpPBI)

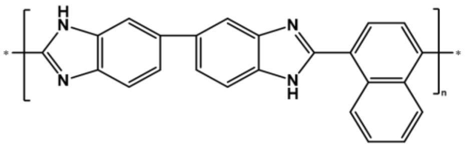

poly[2,2’-(1,4-naphthalene)-5,5’-bibenzimidazole] (NPBI)

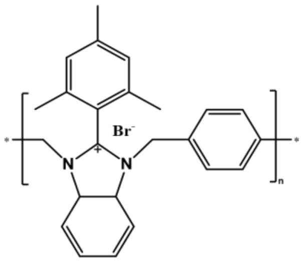

poly[(1,4-xylylenediyl)(2-(2,4,6-trimethylphenyl)benzimidazo- lium-1,3-diyl bromide)

Figure 6. Different structures of PBI used in VRFBs

Acid-base blend membranes, which comprise blending of a basic polymer with an acidic polymer forming ionical cross-links by proton transfer between acid and basic groups, showed significantly improved membrane properties in terms of mechanical, thermal and chemical stabilities and better performances than that of Nafion membranes in VRFBs [39]. Accordingly, blend membranes with sulfonated poly(ether ether ketone) and quaternized poly(ether imide) has shown improved coulombic and energy efficiencies compared to pristine sulfonated poly(ether ether ketone) in VRFBs application [40]. Likely, imidazolium-functionalized acid-base blend membranes with sulfonated poly (ether ether ketone) showed better VRFB performance in terms of self-discharging test, coulombic efficiency and energy efficiency than a Nafion membrane [41]. Those acid-base blend membranes have been intensively studied by the Kerres group: these membranes exhibit improved membrane properties in terms of mechanical, chemical and thermal stabilities compared to their homopolymer membranes (see **Figure 7**, the concept for acid-base blend membrane preparation) [42][43][44][45]. For example, for an anion exchange blend membrane (AEBM) preparation, a PBI was used as a matrix polymer to yield mechanically stable membranes. An anion exchange ionomer was used to provide anion exchange sites by a quaternization reaction with tertiary amines. A minor amount of sulfonated polymer was used to enhance the chemical and mechanical stabilities by forming ionic cross-links. Based on this anion exchange blend concept, anion exchange blend membranes were prepared and applied in vanadium redox flow battery and more details regarding synthesis and performances on VRFBs will be discussed in the following chapters.

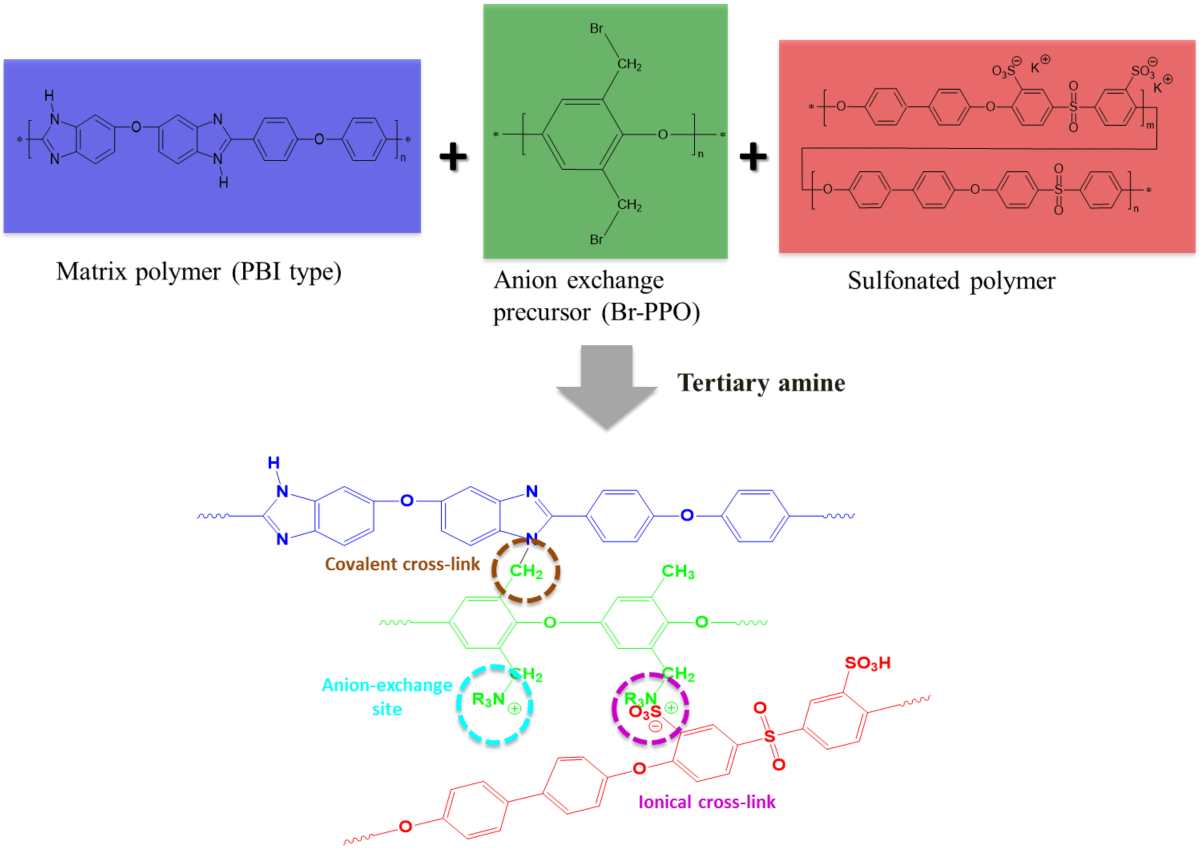

Figure 7. Concept for acid-base blend membrane preparation

Another approach to develop the anion exchange membrane for VRFBs in this study was usage of poly(pentafluorostyrene) (PPFSt). PPFSt can be modified by nucleophilic substitution on the para position of pentafluorostyrene as illustrated in **Figure 8**. A PPFSt based cation exchange membrane via either sulfonation or phosphonation has shown not only higher conductivity than a Nafion membrane but also high heat resistance stability up to e.g. 350 ^{o}C [46][47][48]. The aforementioned advantages of an anion exchange membrane in vanadium redox flow battery and high stability of PPFSt inspired us to prepare anion exchange membranes based on PPFSt. In this study, therefore, novel AEMs were synthesized by a three-step reaction sequence based on PPFSt as following. 1) grafting of 1-(2-dimethylaminoethyl)-5-mercaptotetrazole by F/S exchange on the para position, 2) methylation of the tertiary amino groups using iodomethane, 3) the blending of the anion exchange polymers with polybenzimidazole. The properties in terms of conductivity, thermal stability, dimensional stability and performances in VRFBs of synthesized AEBM were investigated. More details will be described in the following chapters.

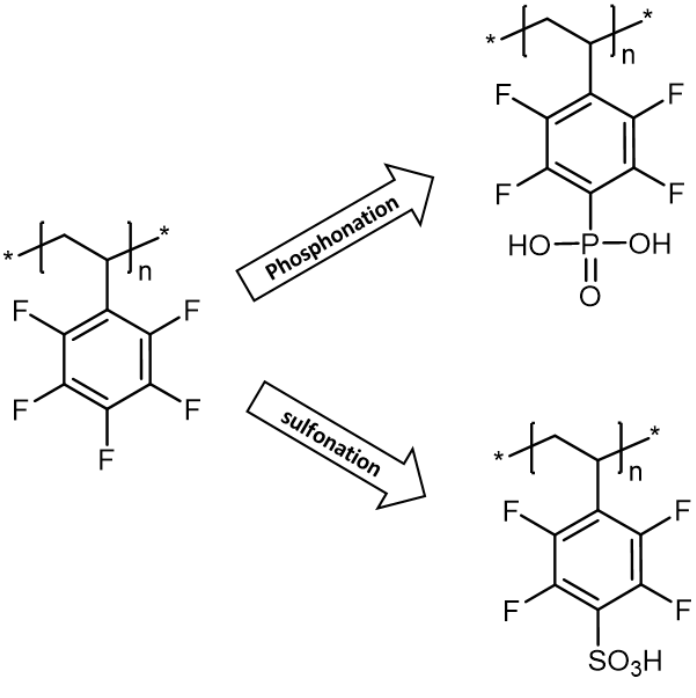

Figure 8. Modification of PPFSt to polyelectrolyte via either phosphonation or sulfonation

In this dissertation, therefore, AEBMs were prepared to be applied in VRFBs. Three papers regarding AEBMs for VRFBs have been published in journals and appended in this dissertation. The summary of each paper is presented in following chapters and the whole papers for more details can be found in next chapters.

2.3 Vanadium redox flow battery

Due to the increasing consumption of fossil fuels generating carbon dioxide, which is the main contribution to the global warming, the research for generating electric energy using renewable energy is getting more and more interest [49]. Redox flow battery (RFB) is one of the most promising candidates for energy storage systems due to its unlimited capacity, safety and flexibility of design [50]. Vanadium Redox Flow Batteries, which were first proposed by Skyllas-Kazacos and co-workers in 1985, are electrochemical energy storage devices stored in separated external tanks containing vanadium electrolytes in different oxidations states [51]. The redox reactions of vanadium ions are taking place on electrodes and can be described as below.

Cathode: $VO_2^{+} + 2H^{+} + e^{-} \underset{\text{charge}}{\overset{\text{discharge}}{\rightleftharpoons}} VO^{2+} + H_2O$

Anode: $V^{2+} \underset{\text{charge}}{\overset{\text{discharge}}{\rightleftharpoons}} V^{3+} + e^{-}$

Overall reaction: $VO_2^{+} + 2H^{+} + V^{2+} \underset{\text{charge}}{\overset{\text{discharge}}{\rightleftharpoons}} VO^{2+} + V^{3+} + H_2O$

A VRFB single cell is constructed by placing IEM between two electrodes with vanadium electrolytes circulation as shown in **Figure 9**.

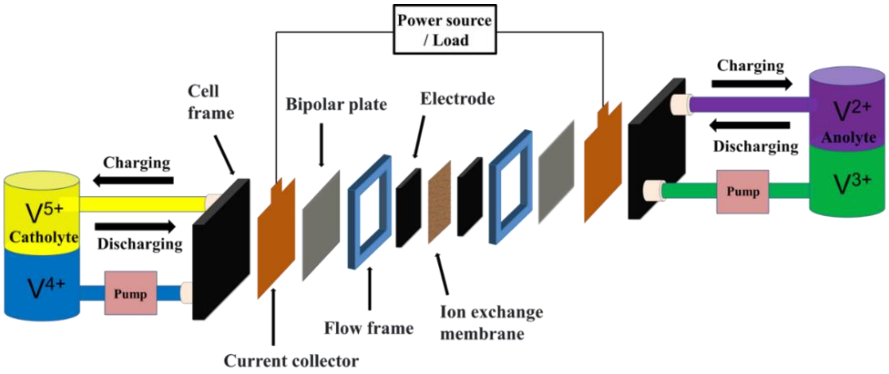

Figure 9. Configuration of a vanadium redox flow battery

Electrodes in VRFBs are providing active sites for the redox reactions of vanadium ions stored in electrolyte~~s~~ tanks. Therefore, electrodes to be used in VRFBs are required to possess properties as listed below: a) the electrodes provide only sites for the redox reactions and do not react itself, b) the electrode should be (electro)chemically stable under highly acidic condition containing strong acid, c) the electrodes have to have superior electrical conductivity to transfer fast charge reactions d) the electrodes possess good wettability with electrolytes because it contacts directly with electrolytes [50]. Various electrode~~s~~ materials have been investigated in VRFBs. As the VRFBs were first proposed by Skyllas-Kazacos and co-workers, they evaluate a range of carbon and non-carbon materials in an initial study [52]. In this study, non-carbon materials such as IrO_2 coated dimensionally stable anode electrodes or other metal electrodes were not suitable on the negative half-cell, and they have concluded that carbon-based materials are suitable in VRFBs since they can meet the requirements, as discussed above. Therefore, improved performance was achieved by surface treatments of conventional carbon-based electrodes such as oxygen functional groups formations, chemical treatments with nitric or sulfuric acid, thermal treatments or combination of thermal and chemical treatments indicating improved wettability and increasing surface area which are resulting in improved performance in VRFBs [50][53][54][55]. After that, various carbon materials such as graphene (oxide), graphene oxide nanoplatelets and multi walled carbon nano tubes have been used for VRFBs application. Graphite-graphene composite electrodes showed remarkable improvements of 30 % higher electrochemical performance in terms of reversibility and current density compared to pristine graphite electrodes in VRFBs [56].

Graphene oxide nanoplatelet, which was oxidized at 50 °C, have exhibited excellent electrocatalytic activity on the electrochemical redox reactions due to the large amount of functional groups such as C-OH and COOH formed during the oxidation step [57]. However, it turned out that those electrodes have disadvantages due to the low electrical conductivity. To improve electrical conductivity and increase the functional groups, Blanco et al. produced graphene oxide based electrodes by a thermal reduction method resulting in high electrical conductivity and enhanced vanadium redox reactions [58,59].

As discussed above, carbon materials and various graphite such as carbon felt, carbon paper, CNTs and graphene have been used and evaluated in VRFBs. In 2002, a N-doped mesoporous carbon electrode was published for the first time for VRFBs application showing highly improved redox reactions in terms of cyclic voltammetry test on both electrolytes due to the nitrogen doping resulting in enhanced electro-chemical oxidation and reduction reactions on electrodes showing that N-doped mesoporous carbon electrodes are very promising materials for VRFBs electrodes [60]. Many studies are still being continued to improve electrode materials or catalysts such as titanium/iridium (IV) oxide and Polyacrylonitrile (PAN) carbon nanofibers for use in VRFBs [61][62].

Evaluation of a VRFB performance is determined by the coulombic-, voltage- and energy-efficiencies corresponding to charging and discharging process. Coulombic efficiency (CE) is described as the ratio between charge capacity and discharge capacity. The CE losses are influenced by side reactions, electrode corrosion and diffusion of vanadium ions through the membranes (vanadium ions permeation) [63]. The voltage efficiency (VE) is affected by ohmic resistance corresponding to the ionic conductivity [63]. Overall energy efficiency (EE) is determined (calculated) by multiplication of CE and VE. To investigate the charge-discharge behavior of VRFBs, charge-discharge cycles tests of AEBMs were carried out by measuring the discharge capacities at each cycle. The upper limit charge voltage of the single cell was set to 1.6 V to avoid corrosion of the electrodes. All the battery performances tested in this dissertation were measured under the same conditions to compare the membrane effect on the VRFBs. The measurements details for VRFBs are described in the following chapters.

$$\text{CE (\%)} = \frac{Qd\ (discharging\ capacity)}{Qc\ (charging\ capacity)}$$

$$\text{VE (\%)} = \frac{Vd\ (average\ discharging\ voltage)}{Vc\ (average\ charging\ voltage)}$$

$$\text{EE (\%)} = \text{CE} \times \text{VE}$$

2.4 References

1. Hagesteijn, K.F.L.; Jiang, S.; Ladewig B.P. A review of the synthesis and characterization of anion exchange membranes. *J. Mater. Sci.* **2018**, *53*, 11131–11150.
2. Xu, T. Ion exchange membranes : State of their development and perspective. *J. Membr. Sci.* **2005**, *263*, 1–29.
3. Yanagi, H.; Fukuta, K. Anion Exchange Membrane and Ionomer for Alkaline Membrane Fuel Cells (AMFCs). *ECS Trans.* **2008**, *16*, 257–262.
4. Leng, Y.; Chen, G.; Mendoza, A.J.; Tighe, T.B.; Hickner, M.A.; Wang C.-Y. Solid-State Water Electrolysis with an Alkaline Membrane. *J. Am. Chem. Soc.* **2012**. *134*, 9054-9057.
5. Pezeshki, A.M.; Tang, Z.J.; Fujimoto, C.; Sun, C.-N.; Mench, M.M. Full Cell Study of Diels Alder Poly (phenylene) Anion and Cation Exchange Membranes in Vanadium Redox Flow Batteries. *J. Electrochem. Soc.* **2016**, *163*, A5154–A5162.
6. Kwon, T.; Lee, J.-W.; Cho, H.; Henkensmeier, D.; Kang, Y.; Hong, S.M.; Koo, C.M. Ionic polymer actuator based on anion-conducting methylated ether-linked polybenzimidazole. *Sens. Actuators B Chem.* **2015**, *214*, 43-49.
7. Lee, J.P.; Yoo, B.; Suresh, T.; Kang, M.S.; Vital, R.; Kim, K.-J. Novel silane-substituted benzimidazolium iodide as gel electrolyte for dye-sensitized solar cells. *Electrochim. Acta* **2009**, *54*, 4365–4370.
8. Kreuer. K. D. On the development of proton conducting polymer membranes for hydrogen and methanol fue cells. *J. membr. Sci.* **2001**, *185*, 29-39.
9. Wang, N.; Peng, S.; Lu, D.; Liu, S.; Liu, Y.; Huang, K. Nafion/TiO_2 hybrid membrane fabricated via hydrothermal method for vanadium redox battery. *J. Solid State Electrochem.*

2012, *16*, 1577–1584.

10. Kerres, J.A. Design Concepts for Aromatic Ionomers and Ionomer Membranes to be Applied to Fuel Cells and Electrolysis. *Polym. Rev.* **2015**, *55*, 273-306.

11. Yang, J.; Li, Q.; Jensen, J.O.; Pan, C.; Cleemann, L.N.; Bjerrum, N.J.; He, R. Phosphoric acid doped imidazolium polysulfone membranes for high temperature proton exchange membrane fuel cells. *J. Power Sources* **2012**, *205*, 114–121.

12. Cho, H.; Hur, E.; Henkensmeier, D.; Jeong, G.; Cho, E.; Kim, H.J.; Jang, J.H.; Lee, K.Y.; Hjuler, H.A.; Li, Q.; Jensen, J.O.; Cleeman, L.N. Meta-PBI/methylated PBI-OO blend membranes for acid doped HT PEMFC. *Eur. Polym. J.* **2014**, *58*, 135–143.

13. Ran, J.; Wu, L.; He, Y.; Yang, Z.; Wang, Y.; Jiang, C.; Ge, L.; Bakangura, E.; Xu, T. Ion exchange membranes: New developments and applications. *J. Memb. Sci.* **2017**, *522*, 267–291.

14. Kerres, J.A.; Krieg, H.M. Poly(Vinylbenzylchloride) Based Anion-Exchange Blend Membranes (AEBMs): Influence of PEG Additive on Conductivity and Stability. *Membranes* **2017**, *7*, 32

15. Lee, M.-S.; Kim, T.; Park, S.-H.; Kim, C.-S.; Choi, Y.-W. A highly durable cross-linked hydroxide ion conducting pore-filling membrane. *J. Mater. Chem.*, **2012**, *22*, 13928–13931.

16. Pan, Q.; Hossain, M.; Yang, Z.; Wang, Y.; Wu, L.; Xu, T. One-pot solvent-free synthesis of cross-linked anion exchange membranes for electrodialysis. *J. Membr. Sci.* **2016**, *515*, 115–124.

17. Sood, R.; Cavaliere, S.; Jones, D.J.; Rozière, J. Electrospun nanofibre composite polymer electrolyte fuel cell and electrolysis membranes. *Nano Energy* **2016**, *26*, 729–745.

18. Klose, C.; Breitwieser, M.; Vierrath, S.; Klingele, M.; Cho, H.; Büchler, A.; Kerres, J.; Thiele, S. Electrospun sulfonated poly(ether ketone) nanofibers as proton conductive reinforcement for durable Nafion composite membranes. *J. Power Sources* **2017**, *361*, 237-242.

19. Schwenzer, B.; Zhang, J.; Kim, S.; Li, L.; Liu, J.; Yang, Z. Membrane Development for Vanadium Redox Flow Batteries. *ChemSusChem* **2011**, *4*, 1388–1406.

20. Chen, D.; Wang, S.; Xiao, M.; Meng, Y. Preparation and properties of sulfonated poly(fluorenyl ether ketone) membrane for vanadium redox flow battery application. *J. Power Sources* **2010**, *195*, 2089–2095.

21. Luo, Q.; Zhang, H.; Chen, J.; Qian, P.; Zhai, Y. Modification of Nafion membrane using interfacial polymerization for vanadium redox flow battery applications. *J. Memb. Sci.* **2008**, *311*, 98–103.

22. Xi, J.; Wu, Z.; Teng, X.; Zhao, Y.; Chen, L.; Qiu, X. Self-assembled polyelectrolyte multilayer modified Nafion membrane with suppressed vanadium ion crossover for vanadium redox flow batteries. *J. Mater. Chem.* **2008**, *18*, 1232–1238.

23. Teng, X.; Zhao, Y.; Xi, J.; Wu, Z.; Qiu, X.; Chen, L. Nafion/organically modified silicate hybrids membrane for vanadium redox flow battery. *J. Power Sources* **2009**, *189*, 1240–1246.

24. Kim, S.; Tighe, T.B.; Schwenzer, B.; Yan, J.; Zhang, J.; Liu, J.; Yang, Z.; Hickner, M. A. Chemical and mechanical degradation of sulfonated poly(sulfone) membranes in vanadium redox flow batteries. *J. Appl. Electrochem.* **2011**, *41*, 1201–1213.

25. Mai, Z.; Zhang, H.; Li, X.; Bi, C.; Dai, H. Sulfonated poly(tetramethydiphenyl ether ether ketone) membranes for vanadium redox flow battery application. *J. Power Sources* **2011**, *196*, 482–487.

26. Kim, S.; Yan, J.; Schwenzer, B.; Zhang, J.; Li, L.; Liu, J.; Yang, Z.; Hickner, M. A. Cycling performance and efficiency of sulfonated poly(sulfone) membranes in vanadium redox flow batteries. *Electrochem. Commun.* **2010**, *12*, 1650–1653.

27. Chen, D.; Hickner, M.A. V^{5+} degradation of sulfonated Radel membranes for vanadium redox flow batteries. *Phys. Chem. Chem. Phys.* **2013**, *15*, 11299–11305.

28. Mohammadi, T.; Kazacos, M.S. Modification of anion-exchange membranes for vanadium redox flow battery applications. *J. Power Sources* **1996**, *63*, 179–186.

29. Zeng, L.; Zhao, T. S.; Wei, L.; Jiang, H. R.; Wu, M. C.; Anion echange membranes for aqueous acid-based redox flow batteires:Current status and challenges. *Appl. Energy* **2019,** 233, 622-643.

30. Zhou, X.L.; Zhao, T.S.; An, L.; Wei, L.; Zhang, C. The use of polybenzimidazole membranes in vanadium redox flow batteries leading to increased coulombic efficiency and cycling performance. *Electrochim. Acta* **2015**, *153*, 492–498.

31. Zeng, L.; Zhao, T.S.; Wei, L.; Zeng, Y.K.; Zhang, Z.H. Highly stable pyridinium-functionalized cross-linked anion exchange membranes for all vanadium redox flow batteries. *J. Power*

Sources **2016**, *331*, 452–461.

32. Sun, C.-N.; Tang, Z.; Belcher, C.; Zawodzinski, T.A.; Fujimoto, C. Evaluation of Diels-Alder poly(phenylene) anion exchange membranes in all-vanadium redox flow batteries. *Electrochem. Commun.* **2014**, *43*, 63–66.

33. Chen, D.; Hickner, M.A.; Agar, E.; Kumbur, E.C. Optimized Anion Exchange Membranes for Vanadium Redox Flow Batteries. *ACS Appl. Mater. Interfaces* **2013**, *5*, 7559–7566.

34. Zhang, B.; Zhang, S.; Xing, D.; Han, R.; Yin, C.; Jian, X. Quaternized poly(phthalazinone ether ketone ketone) anion exchange membrane with low permeability of vanadium ions for vanadium redox flow battery application. *J. Power Sources* **2012**, *217*, 296–302.

35. Li, Q.; Jensen, J.O.; Savinell, R.F.; Bjerrum, N.J. High temperature proton exchange membranes based on polybenzimidazoles for fuel cells. *Prog. Polym. Sci. (oxf.)* **2009**, *34*, 449–477.

36. Jang, J.-K.; Kim, T.-H.; Yoon, S.J.; Lee, J.Y.; Lee, J.-C.; Hong, Y.T. Highly proton conductive, dense polybenzimidazole membranes with low permeability to vanadium and enhanced H_2SO_4 absorption capability for use in vanadium redox flow batteries. *J. Mater. Chem. A* **2016**, *4*, 14342–14355.

37. Geng K.; Li, Y.; Xing, Y.; Wang, L.; Li, N. A novel polybenzimidazole membrane containing bulky naphthalene group for vanadium flow battery. *J Membr. Sci.* **2019**, *586*, 231–239.

38. Strużyńska-Piron, I.; Jung, M.; Maljusch, A.; Conradi, O.; Kim, S.; Jang, J.H.; Kim, H.-J.; Kwon, Y.; Nam, S.W.; Henkensmeier, D. Imidazole based ionenes, their blends with PBI-OO and applicability as membrane in a vanadium Redox flow battery. *Eur. Polym. J.* **2017**, *96*, 383–392.

39. Chromik, A.; dos Santos, A.R.; Turek, T.; Kunz, U.; Häring, T.; Kerres, J. Stability of acid-excess acid-base blend membranes in all-vanadium redox-flow batteries. *J. Membr. Sci.* **2015**, *476*, 148–155.

40. Liu, S.; Wang, L.; Li, D.; Liu, B.; Wang, J.; Song, Y. Novel amphoteric ion exchange membranes by blending sulfonated poly(ether ether ketone)/quaternized poly(ether imide) for vanadium redox flow battery applications. *J. Mater. Chem. A* **2015**, *3*, 17590–17597.

41. Yan, X.; Zhang, C.; Dai, Y.; Zheng, W.; Ruan, X.; He, G. A novel imidazolium-based

amphoteric membrane for high-performance vanadium redox flow battery. *J. Membr. Sci.* **2017**, *544*, 98–107.

42. Kerres, J.; Cui, W.U.S. Patent 6,194,474, 2001; U.S. Patent 6,300,381, 2001; EP Patent 1073690, 2004.

43. Morandi, C.G.; Peach, R.; Krieg, H.M.; Kerres, J. Novel imidazolium-functionalized anion-exchange polymer PBI blend membranes. *J. Membr. Sci.* **2015**, *476*, 256–263.

44. Morandi, C.G.; Peach, R.; Krieg, H.M.; Kerres, J. Novel morpholinium-functionalized anion-exchange PBI-polymer blends. *J. Mater. Chem. A* **2015**, *3*, 1110–1120.

45. Kerres, J.; Ullrich, A.; Häring, T. EP 1076676,2004, US 6723757, 2004.

46. Atanasov, V.; Kerres, J. Highly Phosphonated Polypentafluorostyrene. *Macromolecules* **2011**, *44*, 6416–6423.

47. Atanasov, V.; Bürger, M.; Lyonnard, S.; Porcar, L.; Kerres, J. Sulfonated poly(pentafluorostyrene): Synthesis & characterization. *Solid State Ion.* **2013**, *252*, 75–83.

48. Atanasov, V.; Gudat, D.; Ruffmann, B.; Kerres, J. Highly phosphonated polypentafluorostyrene : Characterization and blends with polybenzimidazole. *Eur. Polym. J.* **2013**. 49, 3977-3985.

49. Yang, Z.; Zhang, J.; Kintner-Meyer, M.C.W.; Lu, X.; Choi, D.; Lemmon, J.P.; Liu, J. Electrochemical Energy Storage for Green Grid. *Chem. Rev.* **2011**, *111*, 3577–3613.

50. Kim, K.J.; Park, M.-S.; Kim, Y.-J.; Kim, J.H.; Dou, S.X.; Skyllas-Kazacos, M. A technology review of electrodes and reaction mechanisms in vanadium redox flow batteries. *J. Mater. Chem. A* **2015**, *3*, 16913–16933.

51. Sum, E.; Skyllas-Kazacos, M. A study of the V(II)/V(III) redox couple for redox flow cell applications. *J. Power Sources* **1985**, *15*, 179–190.

52. Rychcik, M.; Skyllas-Kazacos, M. Evaluation of electrode materials for vanadium redox cell. *J. Power Sources* **1987**, *19*, 45–54.

53. Sun, B.; Skyllas-Kazacos, M. Chemical modification of graphite electrode materials for vanadium redox flow battery application-part II. Acid treatments. Electrochim. Acta **1992**, *37*, 2459-2495.

54. Xiao-gang, L.; Ke-long, H.; Su-qin, L.; Li-quan, C. Electrochemical behavior of diverse

vanadium ions at modified graphite felt electrode in sulphuric solution. *J. Cent. South Univ. Technol.* **2007**, *14*, 51–56.

55. Sun, B.; Skyllas-Kazacos, M.; Modification of graphite electrode materials for vanadium redox flow battery application-I. Thermal treatment. Electrochim. Acta **1992**, *37*, 1253–1260.

56. Tsai, H.-M.; Yang, S.-Y.; Ma, C.-C. M.; Xie, X. Preparation and Electrochemical Properties of Graphene- Modified Electrodes for All-Vanadium Redox Flow Batteries. *Electroanalysis* **2011**, *23*, 2139–2143.

57. Han, P.; Wang, H.; Liu, Z.; Chen, X.; Ma, W.; Yao, J.; Zhu, Y.; Cui, G. Graphene oxide nanoplatelets as excellent electrochemical active materials for VO^{2+}/VO^{+}_2 and V^{2+}/V^{3+} redox couples for a vanadium redox flow battery. *Carbon* **2011**, *49*, 693–700.

58. González, Z.; Botas, C.; Blanco, C.; Santamaría, R.; Granda, M.; Álvarez, P.; Menéndez, R. Graphite oxide-based graphene materials as positive electrodes in vanadium redox flow batteries. *J. Power Sources* **2013**, *241*, 349–354.

59. Gonzáles, Z.; Vizireanu, S.; Dinescu, G.; Blanco, C.; Santamaria, R. Carbon nanowalls thin films as nanostructured electrode materials in vanadium redox flow batteries. Nano Energy **2012**, *1*, 833–839.

60. Shao, Y.; Wang, X.; Engelhard, M.; Wang, C.; Dai, S.; Liu, J.; Yang, Z.; Lin, Y. Nitrogen-doped mesoporous carbon for energy storage in vanadium redox flow batteries. *J. Power Sources* **2010**, *195*, 4375–4379.

61. Wei, G.; Liu, J.; Zhao, H.; Yan, C. Electrospun carbon nanofibres as electrode materials toward VO^{2+}/VO_2^{+} redox couple for vanadium flow battery. *J. Power Sources* **2013**, *241*, 709–717.

62. Raguu, S.C.; Ulaganathan, M.; Lim, T.M.; Kazacos M.S. Electrochemical behaviour of titanium/iridium(IV) oxide : Tantalum pentoxide and graphite for application in vanadium redox flow battery. *J. Power Sources* **2013**, *238*, 103–108.

63. Chen, D.; Hickner, M.A.; Agar, E.; Kumbur, E.C. Optimizing membrane thickness for vanadium redox flow batteries. *J. Membr. Sci.* **2013**, *437*, 108–113.

3. Application of Novel Anion-Exchange Blend Membranes (AEBMs) to Vanadium Redox Flow Batteries

Hyeongrae Cho, Henning M. Krieg and Jochen A. Kerres

(reprinted with permission of MDPI)

Abstract

Both cation-exchange membranes and anion-exchange membranes are used as ion conducting membranes in vanadium redox flow batteries (VRFBs). Anion-exchange membranes (AEMs) are applied in vanadium redox flow batteries due to the high blocking property of vanadium ions via the Donnan exclusion effect. In this study, novel anion-exchange blend membranes (AEBMs) were prepared, characterized, and applied in VRFBs. Bromomethylated poly(2,6-dimethyl-1,4-phenylene oxide), poly[(1-(4,4′-diphenylether)-5-oxybenzimidazole)-benzimidazole] (PBI-OO) and sulfonated polyether sulfone polymer were combined to prepare 3-component AEBMs with 1,2,4,5-tetramethylimidazole (TMIm) for quaternization. 3-component AEBMs showed significantly enhanced chemical and mechanical properties compared with those of 2-component AEBMs, resulting in an improved performance in VRFBs. The compositions of the anion-exchange polymers in 3-component AEBMs were systematically varied to optimize the AEBMs for the redox-flow battery application. While the 3-component AEBMs showed comparable efficiencies with Nafion® 212 membranes, they displayed improved vanadium ions cross-over as was confirmed by open circuit voltage tests and capacity fade tests conducted in VRFBs. In addition, one of the synthesized 3-component AEBM had a superior coulombic efficiency and capacity retention in a charging–discharging test over 300 cycles at a current density of 40 mA/cm^2. It can thus be concluded that 3-component AEBMs are promising candidates for long-term operation in VRFBs.

3.1 Introduction

Vanadium redox flow batteries (VRFBs) provide a promising technology for large-scale energy storage. Vanadium redox flow batteries can be described as electrochemical devices that store energy in two separated solutions containing different redox couples. In VRFBs, vanadium ions, which are stored separately (V^{2+}/V^{3+} and V^{4+}/V^{5+}) in electrolyte reservoirs, undergo electrochemical redox reactions on the surface of electrodes [1,2]. Since ion conducting membranes are used in redox flow batteries (RFBs) as a separator between the two electrolytes, they are an integral component of VRFBs. Their role however is not only to conduct semi-permeable ions such as H^+ for cation-conducting membranes or SO_4^{2-} and HSO_4^- for anion-conducting membranes thereby maintaining charge balance, but also to prevent the cross-mixing of the two electrolytes (V^{2+}/V^{3+} and V^{4+}/V^{5+}).

For such VRFB separators, both cation-exchange membranes (CEMs) and anion-exchange membranes (AEMs) can be used. The most widely studied CEMs are based on perfluorinated polymer membranes known as Nafion® (developed by DuPont), which are commonly used in VRFBs because of their high proton conductivity and excellent chemical stability [3]. However, in VRFBs, Nafion® displays high vanadium ion permeation, resulting in fast capacity reduction in cycling tests [4]. To reduce the vanadium ions permeability, Nafion® has been modified both externally, for example by coating with polyethyleneimine [5], poly(diallyldimethylammonium chloride) (cationic layer), and poly(styrenesulfonic acid) (anionic layer) [6], or internally, for example by manufacturing composite membranes using inorganic particles [7,8]. However, in spite of these advances, Nafion® remains very expensive, limiting the large-scale commercialization of this technology [9]. For this reason, the development of alternative membranes for VRFBs has been intensively studied. For example, poly(vinylidene fluoride) (PVDF) membranes grafted onto polystyrene displayed better performances than Nafion® membranes [10]. In addition, aromatic main-chain polymers have been intensively studied due to their high chemical stability which can be traced back to their aromatic structure. One such polymer, sulfonated poly(ether ether ketone) (S-PEEK), when applied in VRFBs, has shown only a slight efficiency decrease after 80 charging–discharging cycles at 40 mA/cm^2 [11]. In contrast, sulfonated Radel®-based polymer membranes suffered from significant capacity loss after 40 charging–discharging cycles at a current density of 50 mA/cm^2, probably due to a radical attack of highly-oxidizing vanadium oxoperoxide species on the electrophilic arylene ether bond [12,13]. Therefore, partially fluorinated aryl CEMs have been developed which possess lower electron density due to pendent strong electron-attracting F moieties, which leads to better stability resulting in improved efficiencies of RFBs [14,15].

Another strategy to improve the performance of VRFBs is using acid-base blend membranes composed of a sulfonated aryl polymer and a basic polymer with aryl group-based polymers [16]. These types of blend membranes, developed by the group of Kerres over more than 15 years of research, displayed improved chemical and mechanical stability compared to membranes consisting of homopolymers [17–19]. In terms of VRFBs, preliminary investigations of the performance of acid-base blend membranes showed higher efficiencies than Nafion® [16].

Most AEMs possess positively charged functional groups such as quaternized ammonium (fixed ions) with accompanying and exchangeable anions as counter ions. Through this structure, the positively charged vanadium ions are repulsed by the membrane, which is known as the Donnan exclusion effect, resulting in extremely low vanadium ions cross-over [20]. Low vanadium permeation is the reason for studying AEMs for VRFBs. For example, quaternized Diels–Alder poly(phenylene) membranes showed slower capacity fade than Nafion® [21]. Similarly, a quaternized ammonium functionalized poly(fluorenyl ether) AEM exhibited very low vanadium permeation and achieved 100% coulombic efficiency [22]. In another study, quaternized poly (phthalazinone ether ketone ketone) membranes were prepared and investigated for VRFB suitability showing almost 100% coulombic efficiency at a charging–discharging test for 80 cycles measured at a current density of 80 mA/cm^2 [23]. Recently, polysulfone-based cross-linked AEMs were applied in VRFBs also showing coulombic efficiencies of 100% after 100 cycles at 50 mA/cm^2 indicating excellent blocking of vanadium ions [24]. Ren et al. [25] investigated blend membranes of quaternized polysulfone/polyvinylidene fluoride (PVDF) showing improved mechanical properties and performance in VRFBs due to blending. Various studies have investigated the use of amphoteric membranes via acid-base blending for VRFBs [26,27]. Again these blend membranes showed high coulombic efficiencies where the capacity retention for long-time cycling from one of the ImPSf/SPEEK blend membranes was 69% at the 50th cycle measured at a current density of 80 mA/cm^2 while blend membranes prepared from sulfonated poly(ether ether ketone) and quaternized poly(ether imide) reached 64% at the 100th cycle measured at a current density of 50 mA/cm^2.

As mentioned previously, blend membranes according to the literature showed improved VRFB performance compared to homopolymer membranes. Previously, results obtained from 2-component blend membranes were published indicating improved performance as aforementioned. In this study, 3-component polymer containing anion-exchange blend membranes (AEBMs) were prepared and characterized in terms of the physical properties, chemical stability, and performance in VRFBs. For the 3-component blend membranes, bromomethylated poly(2,6-dimethyl-1,4-phenylene oxide) (Br-PPO) was used as an anion-exchange precursor with 1,2,4,5-tetramethylimidazole (TMIm), and poly[(1-(4,4′-diphenylether)-5-oxybenzimidazole)-benzimidazole] (PBI-OO) being used as a matrix polymer to improve the mechanical stability. A small amount of a sulfonated polymer (9 to 15% in blend membranes) was added as a third polymer component for ionical cross-linking. The 3-component anion-exchange blend membranes showed significantly improved VRFB performance regarding vanadium ion cross-over when compared to 2-component blend membranes containing only PPO-Br and PBI-OO. One of the 3-component anion-exchange blend membranes did not show any changes in coulombic efficiency during 300 cycles maintaining almost 100%. At the 300th cycle performed at the current density of 40 mA/cm^2, 77% of capacity had remained. The anion-exchange blend membrane showed significantly longer stability during the open circuit voltage (OCV) test due to the lower vanadium ions cross-over when compared to commercial membranes. Accordingly, the anion-exchange blend membranes would be promising candidates for long-term operation in VRFB applications.

3.2 Materials and Methods

Materials

All chemicals were used without further purification. Poly(2,6-dimethyl-1,4-phenylene oxide) (PPO) was purchased from Sigma Aldrich (Munich, Germany), and bromination was conducted in the same way as described previously [28]. Poly[(1-(4,4′-diphenylether)-5-oxybenzimidazole)-benzimidazole] (PBI-OO) was purchased from FuMA-Tech GmbH (Bietigheim-Bissingen, Germany). Sulfonated polymer was synthesized as previously reported in the literature [29]. 1,2,4,5-tetramethylimidazole was purchased from TCI chemicals. *N*,*N*-Dimethylacetamide (DMAc) and methanol were obtained from VWR International GmbH (Bruchsal, Germany). Sulfuric acid, potassium hydroxide, 0.1 N standard hydrochloric acid, and sodium hydroxide were purchased from Carl Roth GmbH (Karlsruhe, Germany). Vanadium electrolyte was provided by RIVA GmbH Batteries. The structures used in this study are presented in Figure 1.

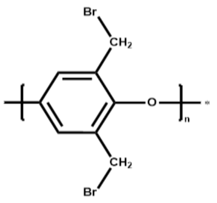

Bromomethylated PPO

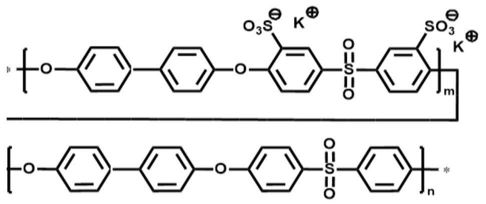

Sulfonated polymer

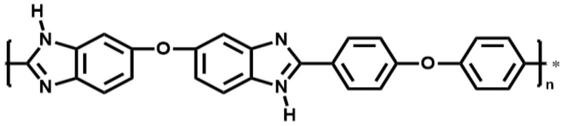

PBI-OO

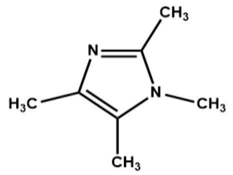

1,2,4,5-tetramethyl-1*H*-imidazole (TMIm)

Figure 1. Structures of polymers and TMIm used in this study.

Membranes Preparation

Details of the preparation of the anion-exchange blend membranes are shown in Figure 2. Each polymer solution was prepared separately as a 10 wt % solution in DMAc. Polymer solutions were mixed together, then TMIm was added into the polymer mixture solution directly in the desired quantities and homogenized. The blend solution was then casted onto a glass plate, followed by solvent evaporation in a convection oven (pre-heated at 40 °C) at 60 °C for 24 h. After drying, the formed membrane was separated from the glass plate by immersion in water. Then membranes were immersed in 1 M sulfuric acid for 1 day at room temperature with one replacement of the sulfuric acid solution during this period. The membranes were repeatedly washed with deionized water at room temperature for 1 day to remove all excess sulfuric acid before being stored in plastic zipper bags before further use.

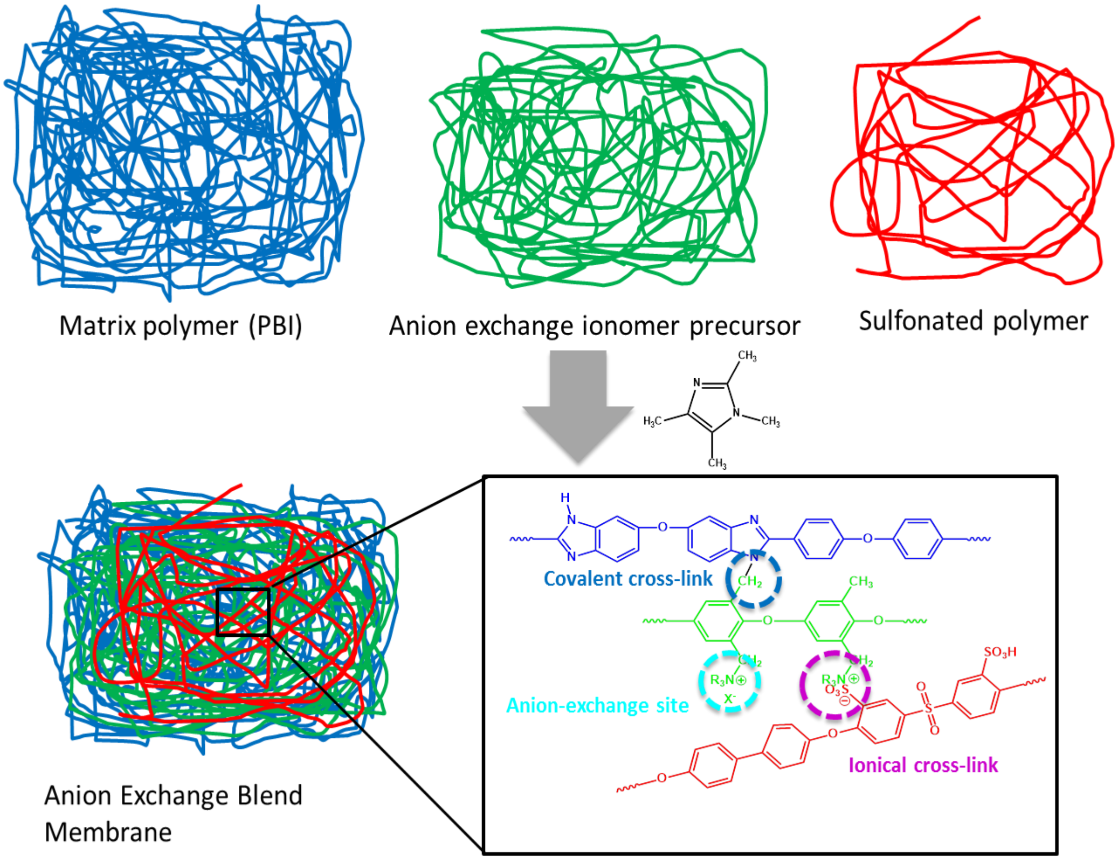

Figure 2. Preparation of anion-exchange blend membranes.

Membrane Characterization

Ion Exchange Capacity

The membranes were immersed in a 1 M KOH solution for 1 day at 90 °C for ion exchange to hydroxide form. After ion exchange, the membranes were washed with water several times to remove excess KOH. Subsequently, the membranes were immersed in a 60 mL saturated sodium chloride solution to exchange the anion-exchange groups to chloride and stirred for 1 day. Subsequently, 3 mL of a standard 0.1 N hydrochloric acid was added to the saturated sodium chloride solution and stored overnight. The next day, the membranes were washed with 25 mL deionized water and this water was added to the 60 mL saturated sodium chloride solution. The back titration was conducted with a 0.1 N sodium hydroxide solution. Finally, the membrane was repeatedly washed with water and dried at 60 °C. The total IEC was calculated using the following equation.

$$\text{IEC} = (C_{\text{HCl}} \times V_{\text{HCl}} - C_{\text{NaOH}} \times V_{\text{NaOH}})/m_{\text{dry}} \tag{1}$$

where IEC is the ion exchange capacity (OH form, mmol/g), C_{HCl} is the concentration of a hydrochloric acid solution, V_{HCl} is the used volume of a hydrochloric acid solution, C_{NaOH} is the concentration of a sodium hydroxide solution, V_{NaOH} is the added volume of a sodium hydroxide solution, and m_{dry} is the dry weight of the membrane.

Conductivity

A Zahner–elektrik IM6 impedance spectrometer (Kronach, Germany) was used for measuring impedance under ambient atmosphere. The impedance was recorded at room temperature in a 1 M sulfuric acid solution with a frequency range of 200 KHz to 8 MHz in the potentiostatic mode (amplitude 10 mV). The membrane resistance was obtained from the intercept in the real X-axis. The conductivity was determined using the follow equation.

$$\sigma = 1/R_{sp} = d/R \times A \tag{2}$$

where σ is the conductivity (mS/cm), R_{sp} is the resistivity (Ω cm), d is the thickness of membrane (cm), R is the ohmic resistance (Ω), and A is the electrode area (cm^2)

Water Uptake (WU) and Swelling Ratio (SR)

The water uptake and swelling ratio were determined by comparing the membrane weight, length, width, and thickness of a dry and a wetted membrane. A wet membrane sample was cut and the weight, length, width, and thickness was measured after removal of residual water on the surface by blotting with a tissue paper. After drying the membrane at 90 °C for 1 day, the weight, length, width, and thickness were again measured. The water uptake and swelling ratio were calculated using the following equations.

$$\text{WU (\%)} = (\text{Wet weight} - \text{Dry weight})/\text{Dry weight} \times 100 \qquad (3)$$

$$\text{SR}_\text{L}\text{ (\%)} = (\text{Wet length} - \text{Dry length})/\text{Dry length} \times 100 \qquad (4)$$

$$\text{SR}_\text{W}\text{ (\%)} = (\text{Wet width} - \text{Dry width})/\text{Dry width} \times 100 \qquad (5)$$

$$\text{SR}_\text{T}\text{ (\%)} = (\text{Wet thickness} - \text{Dry thickness})/\text{Dry thickness} \times 100 \qquad (6)$$

Fourier-Transform Infrared Spectroscopy (FT-IR)

FT-IR spectra of the membranes were recorded comprising 64 scans in the wave number range from 4000 to 400 cm^{-1} using a Nicolet iS5 (Thermofisher Scientific, Karlsruhe, Germany) and a diamond attenuated total reflectance (ATR) module.

Gel Content by Extraction

To determine the degree of dissolution of the membrane in an organic solvent, the weight loss was calculated by measuring the weight difference of the membranes before and after DMAc extraction. The dry membrane was kept in DMAc for 4 days at 90 °C and the following 3 days in methanol. The weight loss was determined using the following equation.

$$\text{Gel (\%)} = (\text{Weight after}/\text{Weight before}) \times 100 \qquad (7)$$

Thermal Stability

To investigate the thermal stability of the membrane, thermal gravimetric analysis (TGA) was done using a dried membrane (dried at 90 °C in convection oven) at a heating rate of 20 °C per minute under O_2/N_2 atmosphere (65–70% oxygen) with a NETZSCH TGA, model STA 499C (Selb, Germany).

Chemical Stability

The chemical stability of the membrane was determined using an electrolyte solution (1.6 M $VOSO_4$ in 30% H_2SO_4). A dry membrane was soaked in this solution at room temperature for 12 days. Subsequently, the membrane was washed repeatedly with water for 1 day before being dried at 90 °C in an oven. The weight loss (WL) of the membrane was determined using the following equation.

$$\text{WL (\%)} = [(\text{Weight before} - \text{Weight after})/\text{weight before}] \times 100 \qquad (8)$$

Vanadium Redox Flow Battery (VRFB) Test

A VRFB single cell was manufactured as shown in Figure 3. The anion-exchange blend membrane with an active area of 28 cm^2 was placed between two carbon felts. Copper plates were used as a current collector. The single cell was assembled between two end plates, and the screws were fastened with a torque of 3.5 Nm. Polyethylene tubes were utilized to supply the electrolytes. Twenty mL of 1.6 M $VOSO_4$ in 30% H_2SO_4 was filled in tubes of both sides as electrolytes, without pumps and tanks. The cell was first charged to 1.6 V at 40 mA/cm^2 and discharged to 1.0 V at the same current density, then charged and discharged at different current densities. The open circuit voltage (OCV) was recorded after charging the cell to 1.6 V. A long-term charging–discharging cycles test was conducted with a current density of 40 mA/cm^2. The coulombic efficiency (CE), voltage efficiency (VE), and energy efficiency (EE) for the process were calculated as follows.

$$CE\ (\%) = t_d/t_c \times 100 \tag{9}$$

$$VE\ (\%) = V_d/V_c \times 100 \tag{10}$$

$$EE\ (\%) = CE \times VE \times 100 \tag{11}$$

where t_d is the discharging time, t_c is the charging time, V_d is the average discharging voltage, and V_c is the average charging voltage.

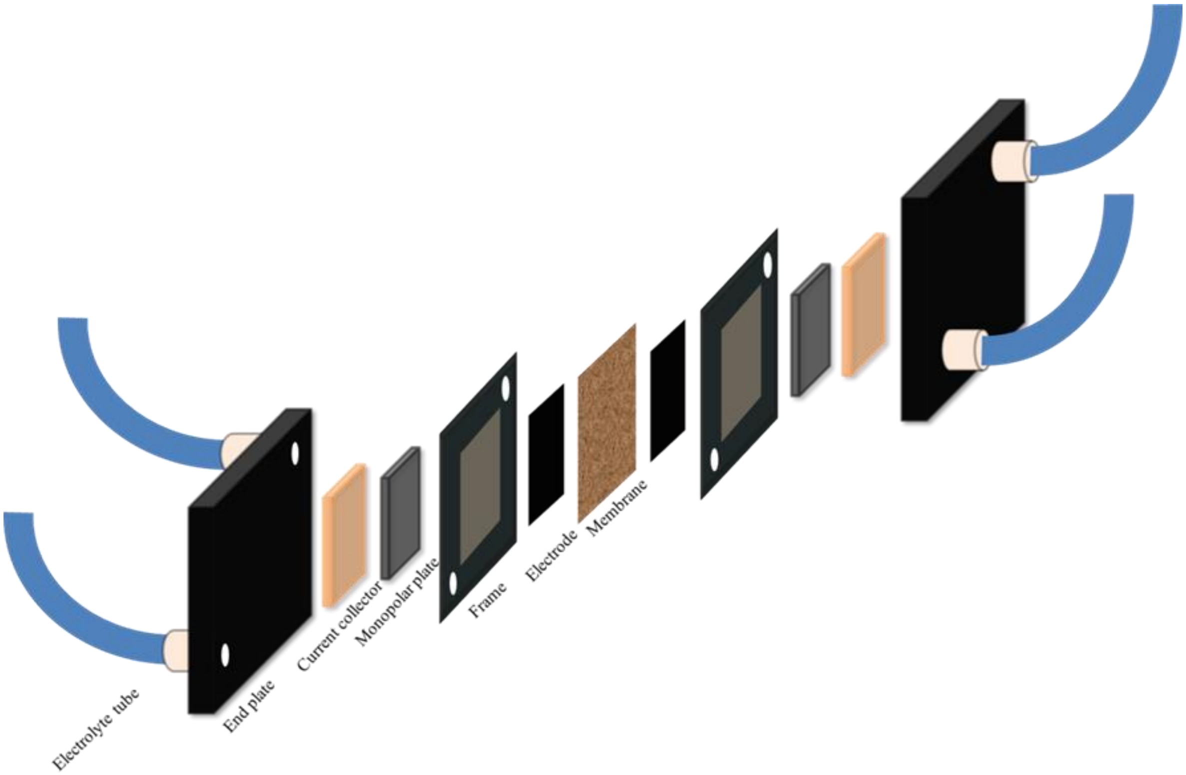

Figure 3. The configuration of vanadium redox flow battery single cell.

3.3 Results and Discussion

Preparation and Properties of Anion-Exchange Blend Membranes

Anion-exchange blend membranes composed of two or three polymeric components which had been quaternized with TMIm were prepared. Details of the membranes and their compositions are listed in Table 1. PBI-OO was used as a matrix polymer since polybenzimidazoles are known to possess high mechanical and thermal stabilities [30]. The mechanical stability was further enhanced in the blend system by the covalent cross-linking with Br-PPO [31,32], as shown in Figure 2. Br-PPO was used as an anion-exchange precursor, and the anion-exchange polymer was formed by quaternization of the bromomethyl groups of Br-PPO with TMIm. A sulfonated polymer was used as an ionical cross-linker (sulfonate anions with tetramethylimidazolium cations).

Table 1. The compositions of the anion-exchange blend membranes.

Entry	Br-PPO**/wt %	PBI-OO***/wt %	S-Polymer****/wt %	TMIm***** (Equivalent)
BM-TMIm* 1	52	35	13	3
BM-TMIm 1-1	52	35	13	1
BM-TMIm 2	60	26	15	1
BM-TMIm 4	45	45	11	1
BM-TMIm 5	36	55	9	1
BM-TMIm 6	60	40	0	1

* Abbreviations : BM-TMIm : blend membranes with 1,2,4,5-tetramethylimidazole, ** Br-PPO : Bromomethylated poly(2,6-dimethyl-1,4-phenylene oxide), *** PBI-OO : poly[(1-(4,4′-diphenylether)-5-oxybenzimidazole)-benzimidazole], **** S-Polymer : sulfonated polymer, ***** TMIm : 1,2,4,5-tetramethylimidazole. For structures of polymers, see Figure 1.

Initially the anion-exchange blend membranes were made using an excess of TMIm (BM-TMIm 1), but the membranes showed turbidity after solvent evaporation. Moreover, they were mechanically unstable when wet due to high water uptake (Figure S1). Thus, the amount of TMIm was reduced to the same equivalent of Br-PPO (except for BM-TMIm 1—see Table 1) resulting in transparent membranes after solvent evaporation and mechanical stability of the water-swollen membranes. Anion-exchange blend membranes were prepared with different ratios between the PBI-OO and Br-PPO. It was subsequently observed that BM-TMIm 2 (Br-PPO:PBI-OO = 7:3 by wt %) was a turbid membrane when dry and mechanically not very stable. Transparent and mechanically stable blend membranes were obtained by reducing the anion-exchange polymer (i.e., Br-PPO amounts). It turned out that blend membranes containing high amounts (more than 52%) of TMIm-quaternized PPO yielded turbid membranes after solvent evaporation, being mechanically instable when wet. It should be noted that the blend membrane composed of Br-PPO and PBI-OO (6:4 by weight percent) without TMIm showed very low conductivity (0.41 mS/cm in 1 M sulfuric acid) and no performance in the VRFBs test, thus, blend membranes in this study, mostly from quaternized groups originated from the quaternization reaction of Br-PPO with TMIm.

A structural analyses of the three individual polymers (Br-PPO, S-polymer, PBI-OO) used as well as on one membrane (BM-TMIm 1) were performed using FT-IR (ATR mode) as presented in Figure 4. According to the literature, the peaks of the imidazolium-quaternized PPO were found at 1573, 752, and 3400 cm^{-1} [33]. These peaks are found in blend membranes (Figure S2). However, in the blend membranes these peaks overlap with other polymer peaks and were hence not clearly recognizable. The stretching vibration peaks of the CH_2Cl group in poly(vinylbenzyl chloride) were found at 675, 709, and 1267 cm^{-1} [34]. Thus, the strong peak at 1302 cm^{-1} in Br-PPO in Figure 4 can be assigned as a stretching vibration of the CH_2Br group, which is not found in the blend membranes, indicating that no bromomethyl groups were left in the blend membranes after quaternization.

A summary of the properties of the membranes is listed in Table 2. All synthesized anion-exchange blend membranes in this study showed comparable IECs with other published results [35]. It is known that the conductivity of anion-exchange membranes is much lower than proton conductivity of cation-exchange membranes in aqueous solution [22]. Both BM-TMIm 1 and BM-TMIm 2 showed higher ionic conductivities (149 and 144 mS/cm, respectively) than Nafion® (98.5 mS/cm) in acidic media (1 M sulfuric acid), which can be ascribed to the high uptake of sulfuric acid contributing to ionic conductivity. This confirms that conductivities can be achieved that are comparable to cation-exchange membranes. Therefore, the disadvantage of the low conductivity of AEMs can be overcome by adjusting the IECs and electrolyte uptakes when applied in VRFBs, since contribution of conductivity in AEMs is sulfate anions and protons. But in the PEMs, some of the anionic sites are occupied by low mobility vanadium anions [36]. With increasing Br-PPO content in the blend membranes, the conductivity increased while the dimensional stability decreased due to the increased water uptake. The addition of the sulfonated polymer resulted in decreased conductivities but enhanced dimensional stability and higher gel content (see data of BM-TMIm 1-1 and BM-TMIm 6 in Table 2). Thus swelling properties of the anion-exchange blend membranes can be controlled by varying the anion-exchange polymer percent and/or addition of a sulfonated polymer, where a tradeoff has to be sought between the swelling degree and the ionic conductivity.

Table 2. The properties of anion-exchange blend membranes.

Entry	IECs (OH Form)	Conductivities (mS/cm)	Gel (%)	Dimensional Stability				T onset (°C)	Thickness (μm, Wet in 1 M H_2SO_4)
				WU (%)	SR_L (%)	SR_W (%)	SR_T (%)		
BM-TMIm 1	2.71	149	95	71	31	29	16	281	89
BM-TMIm 1-1	3.26	40.9	95	47	19	18	15	314	71
BM-TMIm 2	3.04	144	94	105	n. a. **	n. a. **	n. a. **	320	92
BM-TMIm 4	3.41	21.0	94	31	12	12	9	306	57
BM-TMIm 5	2.93	13.7	92	33	12	11	8	306	66
BM-TMIm 6	3.39	65.2	92	58	21	20	15	303	63
FAP 450 *	2.18	35.2	- ***	19	9	8	9	304	58
Nafion® 212	0.88 (H form)	98.5	-	8	7	9	3	299	53

*FAP 450 : anion-exchange membrane produced by Fuma-Tech ** not applicable due to mechanical failure, *** extremely swelling in DMAc.

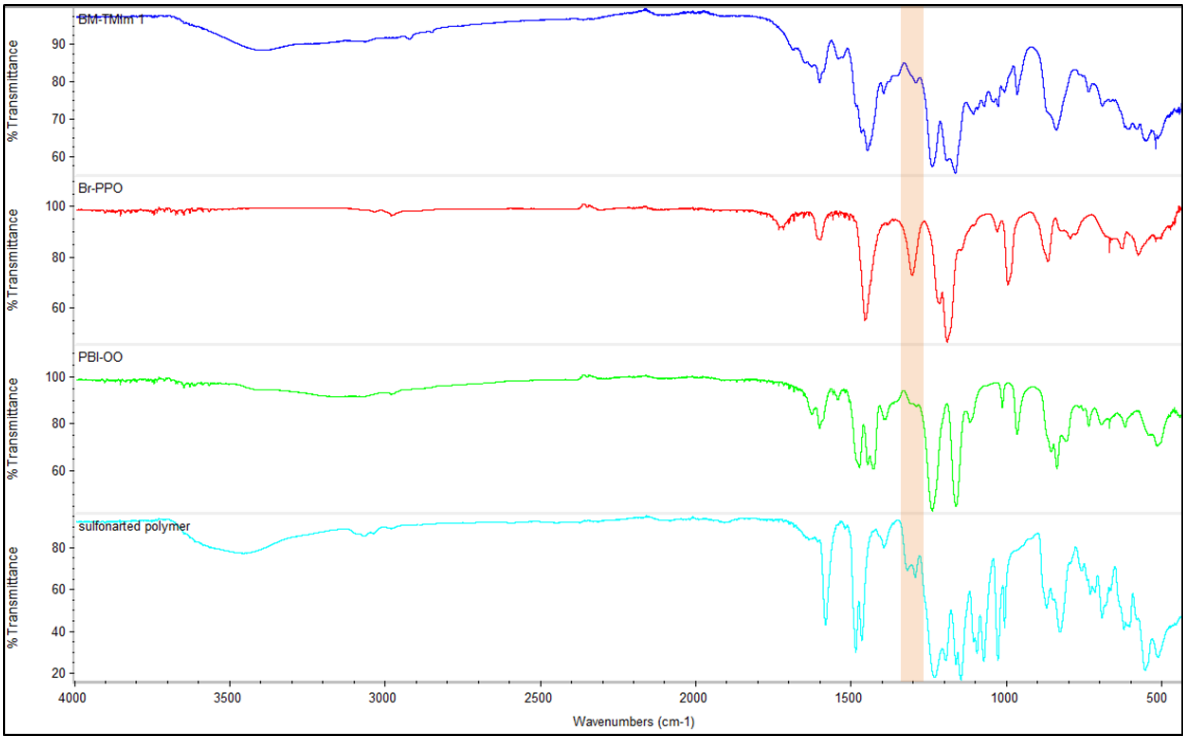

Figure 4. Fourier-Transform Infrared (FT-IR) spectrum of blend-forming polymers and of one anion-exchange blend membrane as an example (BM-TMIm 1).

The thermal stability of the blend membranes as determined using thermal gravimetric analysis (TGA) is shown in Figure 5. The first weight loss step (50–150 °C) is attributed to the water evaporation absorbed in the membranes. The second step starts at 300 °C, which is due to the loss of quaternized imidazolium groups and splitting-off of the sulfonate groups of the sulfonated blend component [37]. Thus, thermal stabilities of 2-component (BM-TMIm 6, 303 °C, loss of quaternized imidazolium) and 3-component (BM-TMIm 1-1, 314 °C, loss of quaternized imidazolium and sulfonated group) blend membranes showed similar thermal stabilities. It is clear from the TGA traces that all the anion-exchange blend membranes had excellent thermal stabilities.

By comparing the weight variation of membranes after immersion in electrolyte solution, the relative chemical stability can be evaluated [38]. According to the literature, the proposed degradation pathway for membranes is based on aromatic backbone degradation caused by vanadium peroxo radicals resulting in chain-scission and weight loss by leaching out the degraded polymer chains of the blend components [13]. For the chemical stability test, the membranes were immersed in an electrolyte solution (1.6 M $VOSO_4$ in 30% H_2SO_4) at room temperature for 12 days. The weight losses before and after the test are shown in Figure 6. All the blend membranes showed weight losses in the range of 5% to 8% which is higher than the weight loss of Nafion® which had an outstanding chemical stability due to its perfluorinated alkyl backbone. The weight loss of the commercial anion-exchange membrane FAP 450 lies in the same range as these of the AEBMs. It can be seen that the 3-component blend membranes (e.g., BM-TMIm 1-1, 5.2%) showed less weight loss than the 2-component blend membrane (BM-TMIm 6, 7.8%). These two membranes are comparable as they were prepared with the same amount of Br-PPO and PBI-OO, with only the sulfonated polymer added in BM-TMIm 1-1 confirming that the additional sulfonated polymer enhanced the chemical stability and mechanical stability.

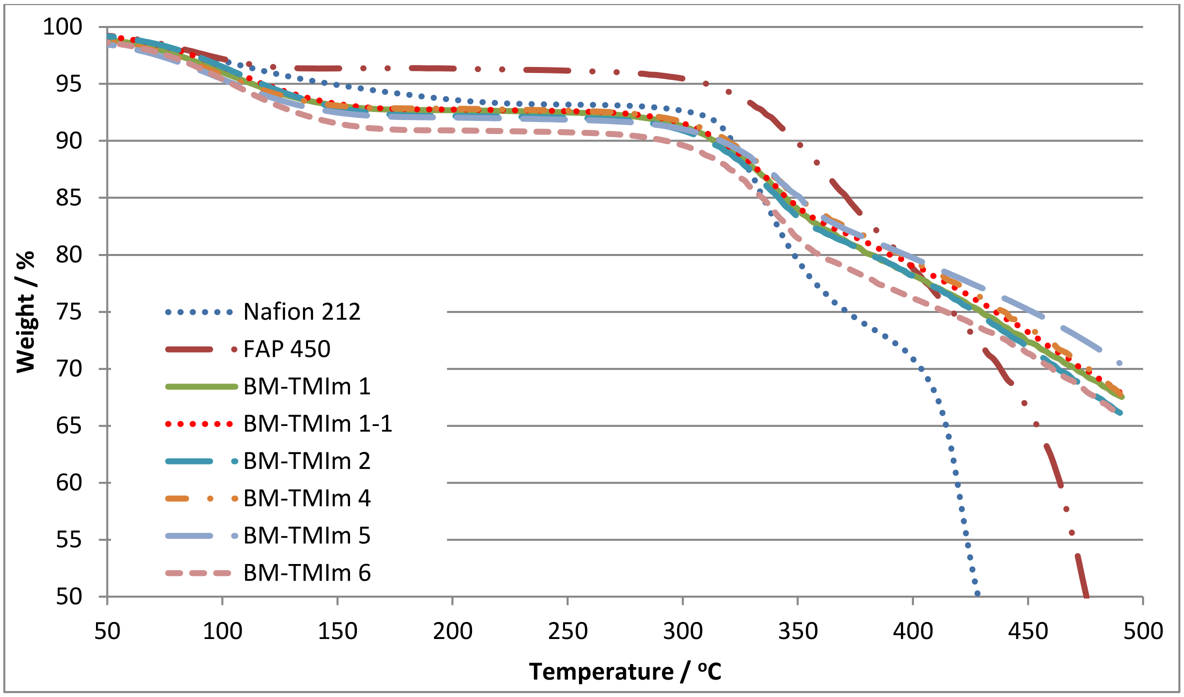

Figure 5. Thermal gravimetric analysis (TGA) traces of membranes in comparison to FAP 450 (anion-exchange membrane produced by Fuma-Tech) and to Nafion® 212.

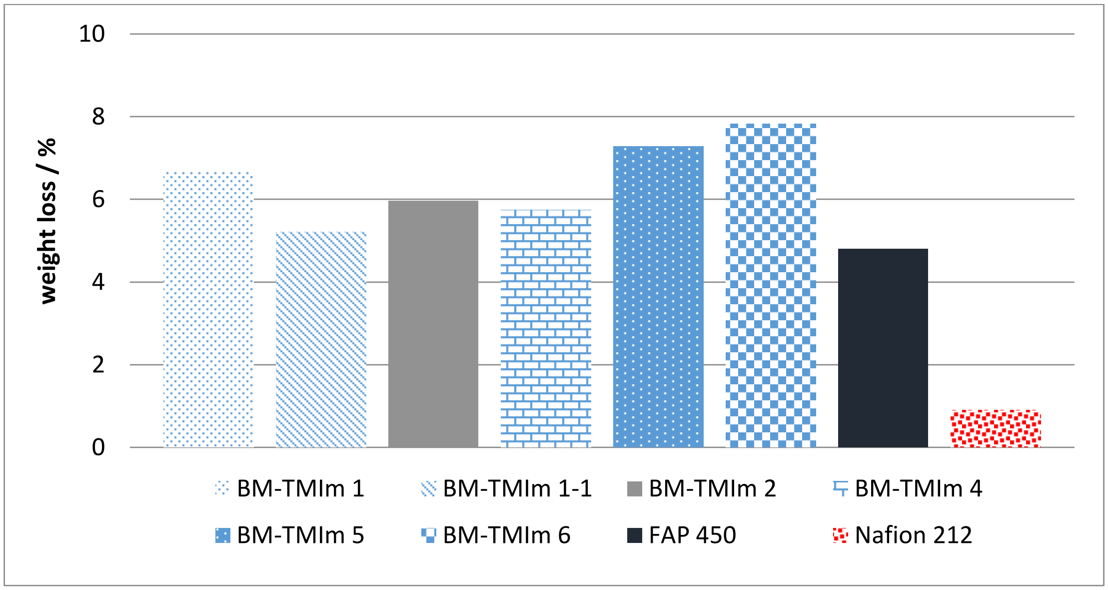

Figure 6. Weight losses after soaking in electrolyte solution at room temperature for 12 days.

Vanadium Redox Flow Battery Performance

The upper limit charge voltage of the single cell was set to 1.6 V to avoid corrosion of the electrodes [39]. The performance of the different membranes was recorded using a single VRFB cell. Due to mechanical membrane failure during single cell preparation (broken, BM-TMIm 1) and a very fast cross-over of electrolyte (BM-TMIm 2) in the VRFB caused by high water uptake and therefore low dimensional stabilities of blend membranes, the performance of BM-TMIm 1 and BM-TMIm 2 were not further measured in battery tests. Figure 7a–c shows the respective CE, VE, and EE of the VRFB as a function of the current density. In general, the CE of VRFBs is influenced by vanadium ions permeation, possible side reactions, and electrode corrosion [40]. Since the VRFB setup was identical for all single cell performance measurements in this study, the side reactions and electrode corrosion should be similar for all battery measurements. Therefore, the main contribution to the CE is the vanadium ions cross-over.

All anion-exchange blend membranes have shown higher CEs than Nafion® due to the Donnan exclusion effect mentioned previously. The 3-component AEBMs had a higher CE than the 2-component AEBMs in VRFBs indicating less vanadium ions cross-over via enhanced dimensional stability. These membranes also showed an increased CE as a function of current density due to the decreased time allowed for vanadium permeation. Hence the 3-component AEBMs had improved vanadium ions blocking properties than the 2-component AEBMs. The VE of all membranes decreased with increasing current density due to the increasing over voltage at the electrodes [41]. The VE is affected by the ohmic resistance which corresponds to the ionic conductivity [40]. Nafion®, as expected, showed the highest VE of all the tested membranes in VRFBs due to its high cation conductivity and BM-TMIm 5 showed lowest VE due to the lowest conductivity among the tested membranes. However, it can be seen that the differences of the VEs between BM-TMIm 1-1 or BM-TMIm 4 and Nafion® were small despite the higher conductivity of Nafion® 212, compared to that of most of the blend membranes. Moreover, VEs of BM-TMIm 1-1 and BM-TMIm 4 showed almost the same value despite the higher conductivity of BM-TMIm 1-1, compared to that of BM-TMIm 4. These results suggest that the ionic conductivity in VRFBs is not a critical parameter. The overall energy efficiencies (EE) of AEBMs showed higher values than that of FAP 450 and comparable values to Nafion® irrespective of the current densities. The EE of BM-TMIm 4 was slightly higher than that of Nafion® below a current density of 50 mA/cm^2, which allows the conclusion that this membrane should be operated in a VRFB at moderate current densities.

Open circuit voltage measurements of VRFBs are often used as an indirect method to investigate the vanadium ions cross-over [27]. Hence, a self-discharge test was run by measuring the OCV as a function of time (Figure 8). It is clear that complete cross-over of vanadium ions through the membranes cannot be avoided because of the diffusion of vanadium ions through the membranes caused by different concentrations of vanadium ion oxidation states between the two electrolytes [42]. In all cases, a sudden OCV drop was observed which can be explained by the disappearance of VO_2^+ in the positive electrolyte originating from vanadium ions cross-over. Firstly, the single cell was charged to 1.6 V with a current density of 40 mA/cm^2 followed immediately by the self-discharge test. While most membranes, including the commercial membranes, showed a sudden drop before 40 h, BM-TMIm 4 had a drop off only after 184.3 h correlating with results of coulombic efficiency originating from the reduced vanadium ions cross-over. It seems that self-discharge is influenced by water uptakes. Higher water uptakes mean higher electrolyte uptake resulting in faster vanadium ions diffusion through the electrolyte. The water uptakes of blend membranes are found to be in the order of BM-TMIm 6 (58%) > BM-TMIm 1-1 (47%) > BM-TMIm 4 (31%) and self-discharge times were 5.3, 38.3, 184.3 h, respectively, as shown in Figure 8. Thus, it can be concluded that the AEMs should possess proper water uptakes for VRFB application (it should be noted that a low water uptake leads to a low conductivity).

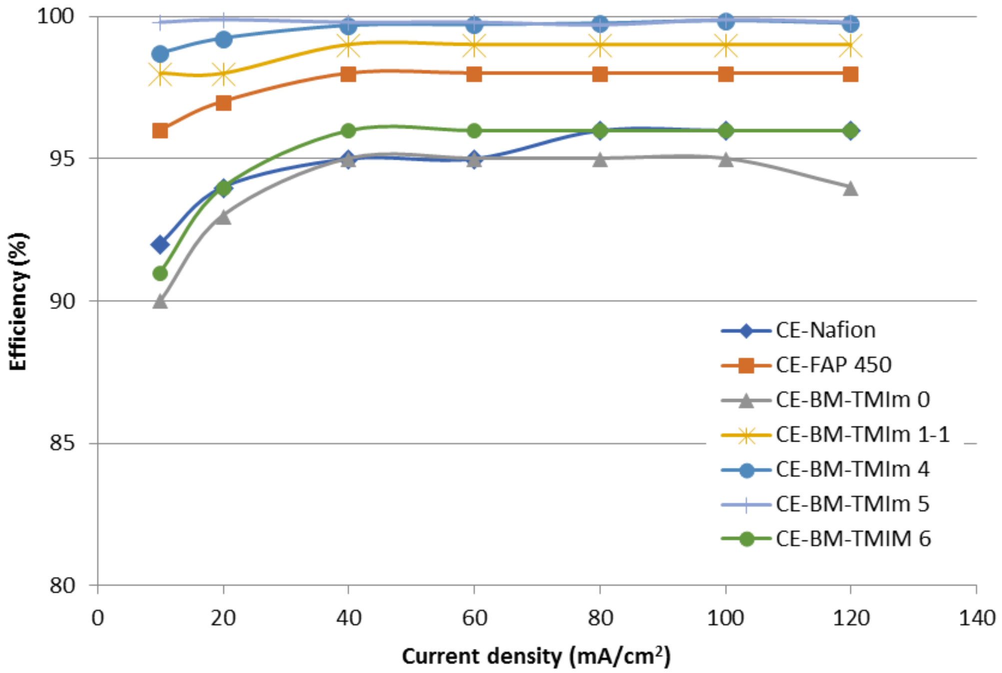
Efficiency (%)
100
95
90
85
80
Current density (mA/cm²)
0
20
40
60
80
100
120
140
CE-Nafion
CE-FAP 450
CE-BM-TMIm 0
CE-BM-TMIm 1-1
CE-BM-TMIm 4
CE-BM-TMIm 5
CE-BM-TMIM 6

(a)

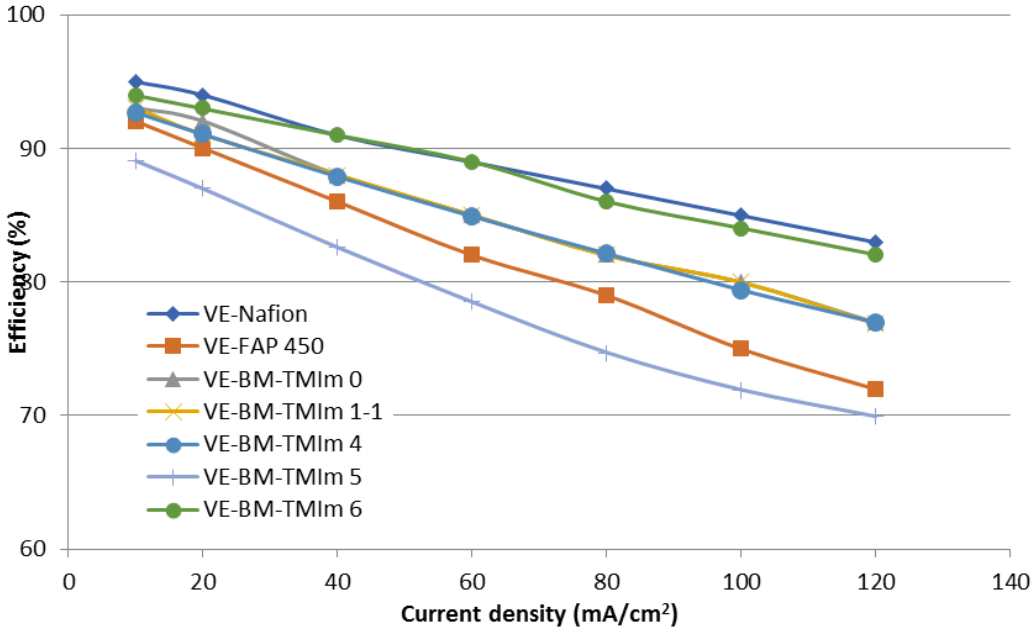
Efficiency (%)
100
90
80
70
60
Current density (mA/cm²)
0
20
40
60
80
100
120
140
VE-Nafion
VE-FAP 450
VE-BM-TMIm 0
VE-BM-TMIm 1-1
VE-BM-TMIm 4
VE-BM-TMIm 5
VE-BM-TMIm 6

(b)

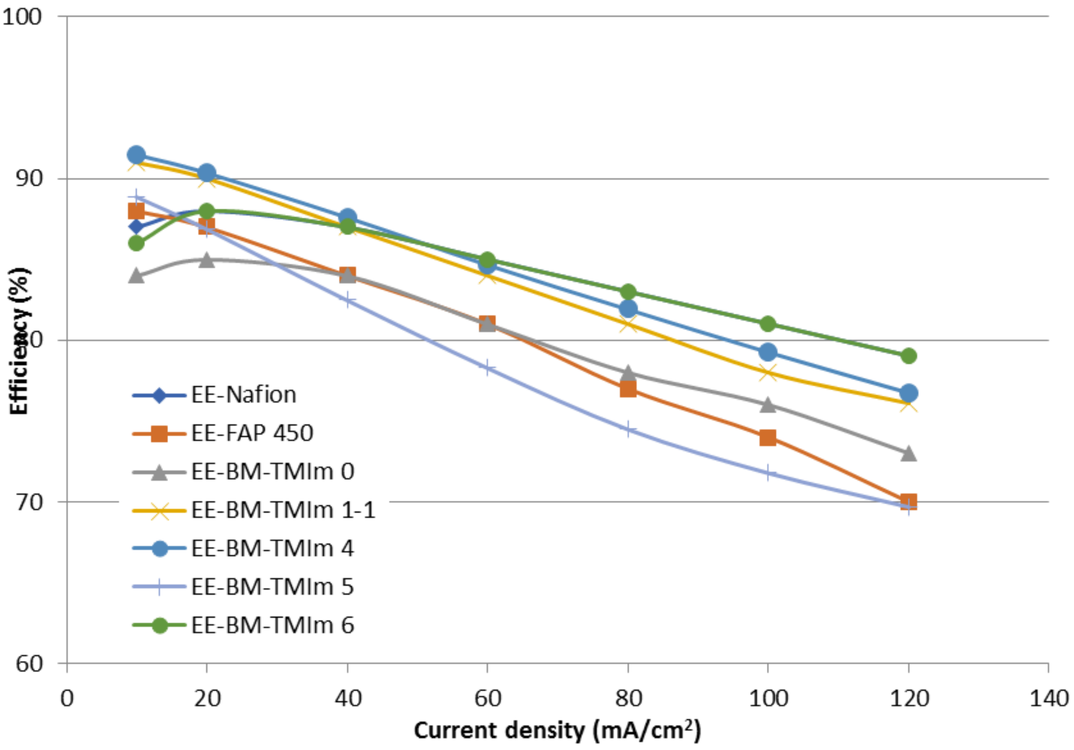

(**c**)

Figure 7. Coulombic efficiency (CE) (**a**); voltage efficiency (VE) (**b**); and energy efficiency (EE) (**c**) of different membranes in VRFBs at various current densities.

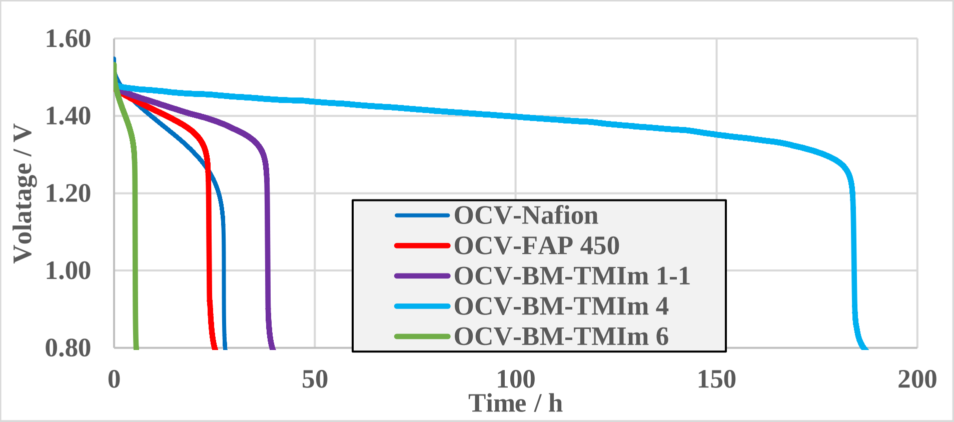

Figure 8. The self-discharge of the VRFBs with different membranes.

To compare the VRFB performance, charging–discharging cycles tests of the two anion-exchange blend membranes BM-TMIm 1-1 and BM-TMIm 6 were conducted (Figure 9). These two were selected to compare the performances of VRFB between 2-component and 3-component blend membranes. The 2-component blend membrane (BM-TMIm 6) almost completely lost its capacity (13% remaining at 100th cycle), while the 3-component blend membrane BM-TMIm 1-1 had a residual capacity of 72% after the same number of cycles. This test is correlating with the self-discharge results depicted in Figure 8. It can be concluded that 3-component blend membranes displayed a significantly reduced vanadium ions cross-over in the VRFB when compared to the 2-component blend membrane. It is clear that the ionical cross-linking via the sulfonated polymer not only enhanced the blocking of vanadium ions but also increased the dimensional stability.

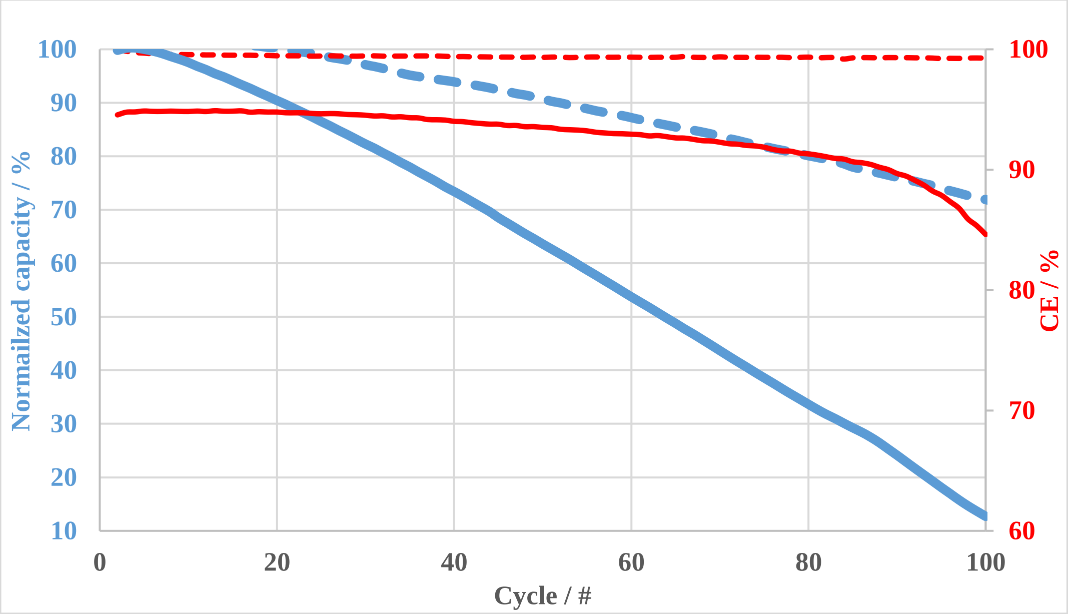

Figure 9. Charging–discharging cycles tests of blend membranes BM-TMIm 1-1 and BM-TMIm 6.

Because BM-TMIm 4 possessed the longest self-discharge time of all the tested membranes in this study, a long-term charging–discharging cycles test was conducted with this blend membrane (Figure 10). It turned out that the coulombic efficiency remained almost 100% (99.6–99.5%) over 300 cycles. According to Figures 9 and 10, the BM-TMIm 4 membrane showed less capacity decay than BM-TMIm 1-1. This result suggests that by adjusting anion-exchange polymer proportion in the blend membrane, improved performance in VRFBs can be achieved. According to Figure 10, the capacity retention of BM-TMIm 4 measured at a current density of 40 mA/cm^2 was 95, 86, and 77% at the 100th, 200th, and 300th cycle, respectively. Compared with values from other VRFB studies of membranes in the literature, it is obvious that the anion-exchange blend membranes in this study showed improved capacity retention, e.g., when using the imidazole-based amphoteric membrane ImPSf/SPEEK 17% the capacity retention was 69% at the 50th cycle with a current density of 80 mA/cm^2 [26], and the capacity retention of an acid-base blend membrane of S/Q-15 was 64% at the 100th cycle at a current density of 50 mA/cm^2 [27]. The outstanding capacity retention of the anion-exchange blend membrane presented in this study suggests that this membrane type is a promising candidate for vanadium redox flow battery application if the proportion of the components in the blend membrane and the cross-linking density (covalent and/or ionical) is carefully adjusted.

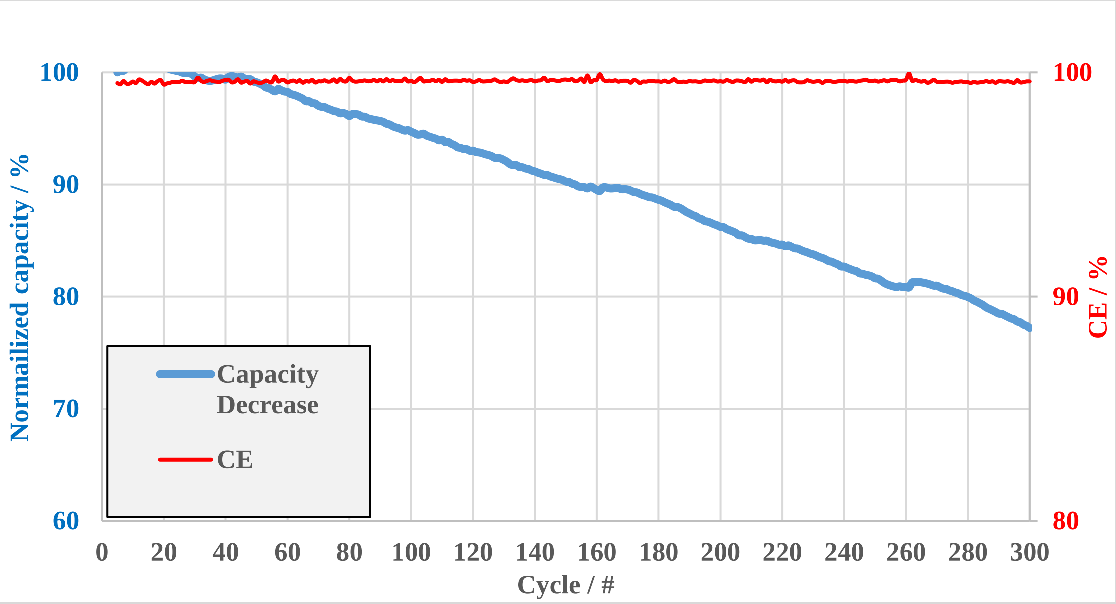

Figure 10. Long-term charging–discharging cycles test with BM-TMIm 4 membrane.

3.4 Conclusions

A series of anion-exchange blend membranes (AEBMs) having similar thicknesses (wet in 1 M H_2SO_4, applied in VRFBs) were fabricated and characterized ex-situ and in-situ in a vanadium redox-flow battery setup. The 3-component AEBMs were composed of bromomethylated PPO, PBI-OO, and a sulfonated polyethersulfone polymer, where the bromomethyl groups of the PPO blend component were quaternized with TMIm. The third component in the blend membranes, the sulfonated polymer, enhanced the chemical stability and dimensional stability of the blend membranes and reduced the vanadium ions cross-over, resulting in improved redox flow battery performance. One of the prepared 3-component blend membranes (BM-TMIm 4) showed an excellent coulombic efficiency of almost 100% after 300 charging–discharging cycles with a significant capacity retention of 77% of the initial value after 300 cycles at a current density of 40 mA/cm^2. Therefore, it can be concluded that the investigated 3-component AEBMs are promising candidates for long-term operation as an energy storage system in VRFBs if the proportion and type of the different components in the blend is carefully adjusted. In ongoing research on VRFB membranes, BM-TMIm 5 is showing very long self-discharge time as elucidated in our lab and will be reporting soon along with further types of anion-exchange blend membranes where the type and/or proportion of the different components in the anion-exchange blend membranes, including the type of the halomethylated precursor, the type of the tertiary amine for quaternization, the type of the matrix polymer, and the type of the sulfonated or phosphonated ionically cross-linking polymer, will be varied.

3.5 Supporting Materials

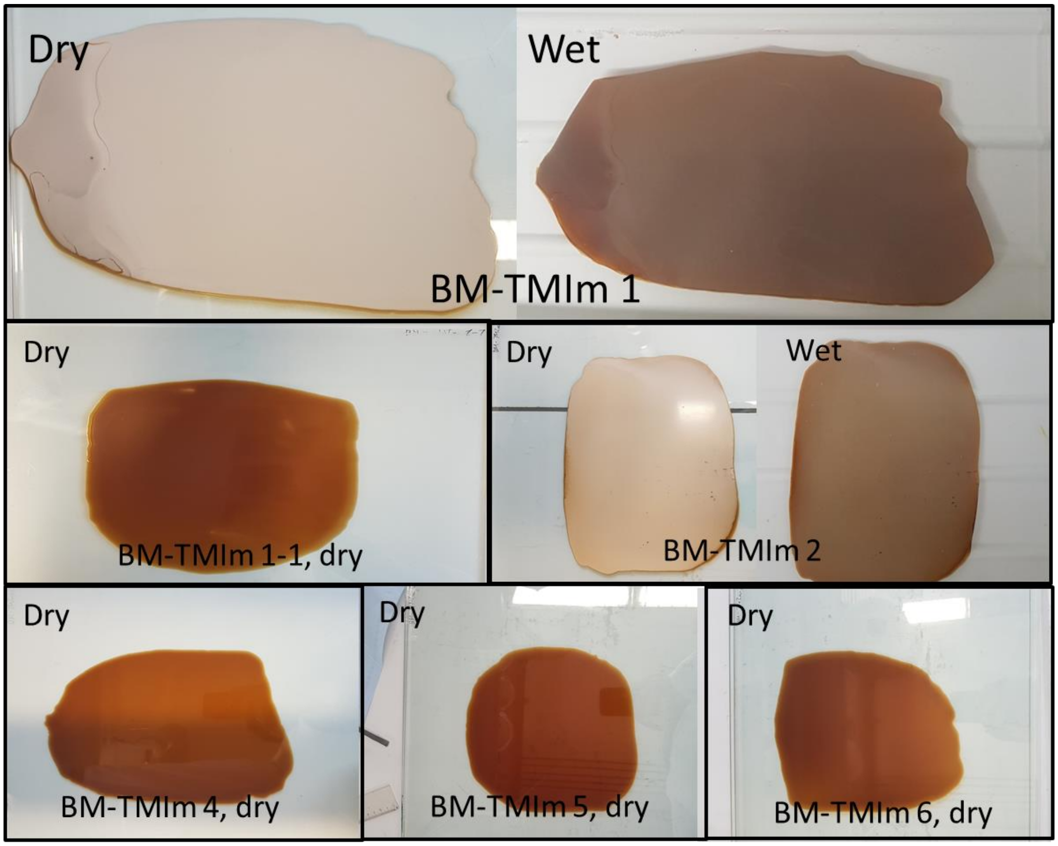

Figure S1. Anion exchange blend membranes tested in this study.

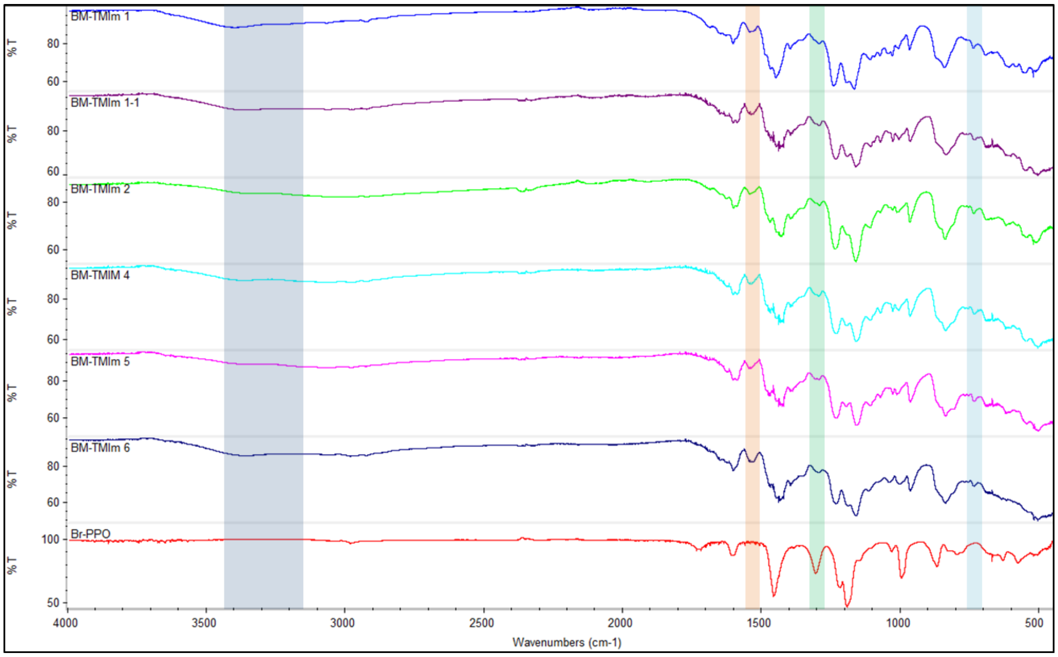

Figure S2. Comparison of FT-IR spectrum of AEBMs with Br-PPO.

3.6 Acknowledgments

We gratefully acknowledge the valuable help of Inna Kharitonova and Galina Schumsky in performing the membrane characterization experiments and Marcus Mehlhorn for redox flow battery performance measurements.

3.7 References

1. Kim, K.J.; Park, M.-S.; Kim, Y.-J.; Kim, J.H.; Dou, S.X.; Skyllas-Kazacos, M. A technology review of electrodes and reaction mechanisms in vanadium redox flow batteries. *J. Mater. Chem. A* **2015**, *3*, 16913–16933.
2. Rychcik, M.; Robins, R.G.; Fane, A.G. THE New All-Vanadium Redox Flow Cell. *J. Electrochem. Soc.* **1986**, *133*, 1057–1058.
3. Schwenzer, B.; Zhang, J.; Kim, S.; Li, L.; Liu, J.; Yang, Z. Membrane development for vanadium redox flow batteries. *ChemSusChem* **2011**, *4*, 1388–1406.
4. Chen, D.; Wang, S.; Xiao, M.; Meng, Y. Preparation and properties of sulfonated poly(fluorenyl ether ketone) membrane for vanadium redox flow battery application. *J. Power Sources* **2010**, *195*, 2089–2095.

5. Luo, Q.; Zhang, H.; Chen, J.; Qian, P.; Zhai, Y. Modification of Nafion membrane using interfacial polymerization for vanadium redox flow battery applications. *J. Memb. Sci.* **2008**, *311*, 98–103.
6. Xi, J.; Wu, Z.; Teng, X.; Zhao, Y.; Chen, L.; Qiu, X. Self-assembled polyelectrolyte multilayer modified Nafion membrane with suppressed vanadium ion crossover for vanadium redox flow batteries. *J. Mater. Chem.* **2008**, *18*, 1232–1238.
7. Teng, X.; Zhao, Y.; Xi, J.; Wu, Z.; Qiu, X.; Chen, L. Nafion/organically modified silicate hybrids membrane for vanadium redox flow battery. *J. Power Sources* **2009**, *189*, 1240–1246.
8. Wang, N.; Peng, S.; Lu, D.; Liu, S.; Liu, Y.; Huang, K. Nafion/TiO_2 hybrid membrane fabricated via hydrothermal method for vanadium redox battery. *J. Solid State Electrochem.* **2012**, *16*, 1577–1584.
9. Kim, S.; Tighe, T.B.; Schwenzer, B.; Yan, J.; Zhang, J.; Liu, J.; Yang, Z.; Hickner, M.A. Chemical and mechanical degradation of sulfonated poly(sulfone) membranes in vanadium redox flow batteries. *J. Appl. Electrochem.* **2011**, *41*, 1201–1213.
10. Luo, X.; Lu, Z.; Xi, J.; Wu, Z.; Zhu, W.; Chen, L.; Qiu, X. Influences of permeation of vanadium ions through PVDF-g-PSSA membranes on performances of vanadium redox flow batteries. *J. Phys. Chem. B* **2005**, *109*, 20310–20314.
11. Mai, Z.; Zhang, H.; Li, X.; Bi, C.; Dai, H. Sulfonated poly(tetramethydiphenyl ether ether ketone) membranes for vanadium redox flow battery application. *J. Power Sources* **2011**, *196*, 482–487.
12. Kim, S.; Yan, J.; Schwenzer, B.; Zhang, J.; Li, L.; Liu, J.; Yang, Z.; Hickner, M.A. Cycling performance and efficiency of sulfonated poly(sulfone) membranes in vanadium redox flow batteries. *Electrochem. Commun.* **2010**, *12*, 1650–1653.
13. Chen, D.; Hickner, M.A. V^{5+} degradation of sulfonated Radel membranes for vanadium redox flow batteries. *Phys. Chem. Chem. Phys.* **2013**, *15*, 11299–11305.
14. Chen, D.; Kim, S.; Li, L.; Yang, G.; Hickner, M.A. Stable fluorinated sulfonated poly(arylene ether) membranes for vanadium redox flow batteries. *RSC Adv.* **2012**, *2*, 8087–8094.
15. Chen, D.; Hickner, M.A.; Wang, S.; Pan, J.; Xiao, M.; Meng, Y. Directly fluorinated

polyaromatic composite membranes for vanadium redox flow batteries. *J. Memb. Sci.* **2012**, *415–416*, 139–144.

16. Chromik, A.; dos Santos, A.R.; Turek, T.; Kunz, U.; Häring, T.; Kerres, J. Stability of acid-excess acid-base blend membranes in all-vanadium redox-flow batteries. *J. Memb. Sci.* **2015**, *476*, 148–155.
17. Kerres, J.; Cui, W.U.S. Acid-base polymer blends and their application in membrane processes. US Patent 6194474, 2004.
18. Kerres, J.; Ullrich, A.; Häring, T. Engineering ionomer blends and engineering ionomer blend membranes. European Patent 1076676, 2004
19. Kerres, J.; Zaidi, S.M.J.; Matsuura, T. Blend concepts for fuel cell membranes. In *Polymer Membranes for Fuel Cells*; Springer: Boston, MA, USA, 2008; pp. 185–221.
20. Mohammadi, T.; Skyllas Kazacos, M. Modification of anion-exchange membranes for vanadium redox flow battery applications. *J. Power Sources* **1996**, *63*, 179–186.
21. Sun, C.N.; Tang, Z.; Belcher, C.; Zawodzinski, T.A.; Fujimoto, C. Evaluation of Diels-Alder poly(phenylene) anion exchange membranes in all-vanadium redox flow batteries. *Electrochem. Commun.* **2014**, *43*, 63–66.
22. Chen, D.; Hickner, M.A.; Agar, E.; Kumbur, E.C. Selective anion exchange membranes for high coulombic efficiency vanadium redox flow batteries. *Electrochem. Commun.* **2013**, *26*, 37–40.
23. Zhang, B.; Zhang, S.; Xing, D.; Han, R.; Yin, C.; Jian, X. Quaternized poly(phthalazinone ether ketone ketone) anion exchange membrane with low permeability of vanadium ions for vanadium redox flow battery application. *J. Power Sources* **2012**, *217*, 296–302.
24. Cha, M.S.; Jeong, H.Y.; Shin, H.Y.; Hong, S.H.; Kim, T.H.; Oh, S.G.; Lee, J.Y.; Hong, Y.T. Crosslinked anion exchange membranes with primary diamine-based crosslinkers for vanadium redox flow battery application. *J. Power Sources* **2017**, *363*, 78–86.
25. Ren, J.; Dong, Y.; Dai, J.; Hu, H.; Zhu, Y.; Teng, X. A novel chloromethylated/quaternized poly(sulfone)/poly(vinylidene fluoride) anion exchange membrane with ultra-low vanadium permeability for all vanadium redox flow battery. *J. Memb. Sci.* **2017**, *544*, 186–194.

26. Yan, X.; Zhang, C.; Dai, Y.; Zheng, W.; Ruan, X.; He, G. A novel imidazolium-based amphoteric membrane for high-performance vanadium redox flow battery. *J. Memb. Sci.* **2017**, *544*, 98–107.
27. Liu, S.; Wang, L.; Li, D.; Liu, B.; Wang, J.; Song, Y. Novel amphoteric ion exchange membranes by blending sulfonated poly(ether ether ketone)/quaternized poly(ether imide) for vanadium redox flow battery applications. *J. Mater. Chem. A* **2015**, *3*, 17590–17597.
28. Katzfuß, A.; Gogel, V.; Jörissen, L.; Kerres, J. The application of covalently cross-linked BrPPO as AEM in alkaline DMFC. *J. Memb. Sci.* **2013**, *425–426*, 131–140.
29. Chromik, A.; Kerres, J.A. Degradation studies on acid-base blends for both LT and intermediate T fuel cells. *Solid State Ionics* **2013**, *252*, 140–151.
30. Li, Q.; Jensen, J.O.; Savinell, R.F.; Bjerrum, N.J. High temperature proton exchange membranes based on polybenzimidazoles for fuel cells. *Prog. Polym. Sci.* **2009**, *34*, 449–477.
31. Morandi, C.G.; Peach, R.; Krieg, H.M.; Kerres, J. Novel imidazolium-functionalized anion-exchange polymer PBI blend membranes. *J. Memb. Sci.* **2015**, *476*, 256–263.
32. Morandi, C.G.; Peach, R.; Krieg, H.M.; Kerres, J. Novel morpholinium-functionalized anion-exchange PBI–polymer blends. *J. Mater. Chem. A* **2015**, *3*, 1110–1120.
33. Ran, J.; Wu, L.; Varcoe, J.R.; Ong, A.L.; Poynton, S.D.; Xu, T. Development of imidazolium-type alkaline anion exchange membranes for fuel cell application. *J. Memb. Sci.* **2012**, *415–416*, 242–249.
34. Lu, W.; Shao, Z.G.; Zhang, G.; Zhao, Y.; Yi, B. Crosslinked poly(vinylbenzyl chloride) with a macromolecular crosslinker for anion exchange membrane fuel cells. *J. Power Sources* **2014**, *248*, 905–914.
35. Merle, G.; Wessling, M.; Nijmeijer, K. Anion exchange membranes for alkaline fuel cells: A review. *J. Memb. Sci.* **2011**, *377*, 1–35.
36. Chen, D.; Hickner, M.A.; Agar, E.; Kumbur, E.C. Optimized anion exchange membranes for vanadium redox flow batteries. *ACS Appl. Mater. Interfaces* **2013**, *5*, 7559–7566.
37. Kerres, J.; Ullrich, A.; Hein, M.; Gogel, V.; Friedrich, K.A.; Jörissen, L. Cross-linked polyaryl

blend membranes for polymer electrolyte fuel cells. *Fuel Cells* **2004**, *4*, 105–112.

38. Tian, B.; Yan, C.W.; Wang, F.H. Modification and evaluation of membranes for vanadium redox battery applications. *J. Appl. Electrochem.* **2004**, *34*, 1205–1210.
39. Liu, H.; Xu, Q.; Yan, C.; Qiao, Y. Corrosion behavior of a positive graphite electrode in vanadium redox flow battery. *Electrochim. Acta* **2011**, *56*, 8783–8790.
40. Chen, D.; Hickner, M.A.; Agar, E.; Kumbur, E.C. Optimizing membrane thickness for vanadium redox flow batteries. *J. Memb. Sci.* **2013**, *437*, 108–113.
41. Cunha, Á.; Martins, J.; Rodrigues, N.; Brito, F.P. Vanadium redox flow batteries: A technology review. *Int. J. Energy Res.* **2015**, *39*, 889–918.
42. Sun, C.; Chen, J.; Zhang, H.; Han, X.; Luo, Q. Investigations on transfer of water and vanadium ions across Nafion membrane in an operating vanadium redox flow battery. *J. Power Sources* **2010**, *195*, 890–897.

4. Performances of Anion-Exchange Blend membranes (AEBMs) on Vanadium Redox Flow Batteries (VRFBs)

Hyeongrae Cho, Henning M. Krieg and Jochen A. Kerres

(reprinted with permission of MDPI)

Abstract

Anion exchange blend membranes (AEBMs) were prepared for use in Vanadium Redox Flow Batteries (VRFBs). These AEBMs consisted of 3 polymer components. Firstly, PBI-OO (nonfluorinated PBI) or F6-PBI (partially fluorinated PBI) were used as a matrix polymer. The second polymer, a bromomethylated PPO, was quaternized with 1,2,4,5-tetramethylimidazole (TMIm) which provided the anion exchange sites. Thirdly, a partially fluorinated polyether or a non-fluorinated poly(ether sulfone) was used as an ionical cross-linker. While the AEBMs were prepared with different combinations of the blend polymers, the same weight ratios of the three components were used. The AEBMs showed similar membrane properties such as ion exchange capacity, dimensional stability and thermal stability. For the VRFB application, comparable or better energy efficiencies were obtained when using the AEBMs compared to the commercial membranes included in this study, i.e. Nafion (cation exchange membrane) and FAP 450 (anion exchange membrane). One of the blend membranes showed no capacity decay during a charge-discharge cycles test for 550 cycles run at 40 mA/cm^2 indicating superior performance compared to the commercial membranes tested.

4.1 Introduction

Due to the environmental impact of using fossil fuels and their resources, producing carbon dioxide which is considered the main contributor to global warming, the use of renewable sources for generating electric energy is attracting increasing scientific interest [1].

Developing alternative sources however not only entails the development of energy generating but also energy storage capacity. Among the energy storage systems which are currently available, the redox flow battery (RFB) is thought of as one of the most promising candidates because of its storage capacity only being dependent on size of the electrolyte tanks, design flexibility and safety [2]. Among the suggested RFBs currently available, the all vanadium redox flow battery (VRFB) which was first proposed and developed by Skyllas-Kazacos and co-workers in 1985 [3], is the most extensively studied, advanced, and only commercially available and widely distributed RFB to date [4]. In VRFBs, ions of vanadium (V) with different oxidation states are used as both electrolytes (V (+2) / V (+3) as the negative electrolyte and V (+4) / V (+5) as the positive electrolyte). This avoids the problem of cross-contamination even though crossover can take place resulting in self-discharge [5]. In addition to the general advantages of RFBs, VRFBs have the additional advantages of room temperature operation, relatively rapid response times and long cycle times [6]. In VRFBs, the membrane is one of the more important components acting as a separator between the two electrolytes used, where it not only prevents the crossover of the electrolytes between the positive and negative half cells, but also allows the permeation of charge balancing ions such as H^+, SO_4^{2-} and HSO_4^- to complete the electrical circuit. Accordingly, such membranes should have high ionic conductivity and chemical stability during operation at an affordable price especially when considering larger scale commercial applications [7]. Both cation exchange membranes (CEMs) and anion exchange membranes (AEMs) can be used in VRFBs. For AEMs, the positively charged cationic fixed ions repel the positively charged vanadium ions, which is known as the Donnan repelling effect, resulting in a reduction of the vanadium ion crossover [8]. A general disadvantage is that AEMs generally have lower conductivities than CEMs [9]. However, upon immersion of AEMs in the electrolyte solutions, additional sulfuric acid can be absorbed leading to improved conductivities [10]. As a result, AEMs are intensively studied in terms of their suitability in VRFBs. Recent studies, where for example quaternized Diels-Alder poly(phenylene) membranes were developed and tested, showed a higher capacity retention during a cycling test than Nafion [11]. In another study, a quaternary ammonium functionalized Radel (QA-Radel) membrane with an ion exchange capacity of 2.0 mmol/g displayed better coulombic efficiency and capacity retention than Nafion when used in a VRFB [12]. Similarly, quaternized poly(phthalazinone ether ketone ketone) membranes when used in VRFBs showed an almost 100 % coulombic efficiency measured by a charge-discharge cycle test for 100 cycles at a current density of 80 mA/cm^2 [13]. Recently, polysulfone-based crosslinked AEMs with a diamine-based crosslinker were developed and applied in VRFBs [14]. One of those membranes showed a coulombic efficiency of 100 % during 100 charge-discharge cycles measured at a current density of 50 mA/cm^2.

Using acid-base blending to prepare membranes has led to improved membrane properties such as mechanical, thermal and chemical stability as well as their performances in VRFBs [15]. Accordingly, an amphoteric blend membrane consisting of sulfonated poly(ether ether ketone) and quaternized poly(ether imide) showed higher coulombic and energy efficiencies without significant declines, compared to a pristine sulfonated poly(ether ether ketone) as well as Nafion membranes for 100 cycles measured at 50 mA/cm^2 [16]. Similarly, acid-base blend membranes from imidazolium-functionalized polysulfone blended with sulfonated poly(ether ether ketone) exhibited an improved performance than a Nafion membrane in terms of coulombic and energy efficiencies as well as during a self-discharge test [17]. These studies have clearly shown that acid-base blend membranes have the potential to improve further on existing VRFB performance. When using acid-base blending, literature has shown that 3-component blend membranes perform better in VRFBs than 2-component blend membranes [18]. Accordingly, in this study, anion exchange blend membranes (AEBMs) composed of 3 blend components were prepared and characterized in a VRFB.

It is known that the binding energy of a C-F bond is higher than that of a C-H bond [19]. As a result, partially fluorinated polymer blend membranes in VRFB operation have a higher chemical stability in terms of molecular weight changes during change/discharge cycles [15]. To confirm this, 3-component AEBMs were prepared and applied to VRFBs using different combinations of blend polymers. In this study, two polybenzimidazoles (nonfluorinated PBI-OO or partially fluorinated F_6-PBI) were used as the matrix polymer to provide mechanical strength. Bromomethylated PPO was used as the anion-exchange precursor that was quaternized with 1,2,4,5-tetramethylimidazole (TMIm). Finally, two sulfonated polymers (a partially fluorinated polyether or a non-fluorinated poly (ether sulfone)) were investigated as ionic macromolecular crosslinkers. Finally, the efficiency of the partially fluorinated and non-fluorinated AEBMs was determined in a VRFB.

4.2 Materials and Methods

Materials

All chemicals were used as received without further purification. Poly(2,6-dimethyl-1,4-phenylene oxide) (PPO) was purchased from Sigma Aldrich, and Bromination of PPO was conducted as described in literature [20]. Poly[(1-(4,4′-diphenylether)-5-oxybenzimidazole)-benzimidazole] (PBI-OO) was obtained from FuMA-Tech GmbH, Germany. Fluorinated PBI (F6-PBI) was purchased from Yanjin Technology, China. The sulfonated polymers were prepared as previously described in the literature [21]. 1,2,4,5-Tetramethylimidazole (TMIm) was purchased from TCI Chemicals. *N*,*N*-Dimethylacetamide (DMAc) and methanol were purchased from VWR International GmbH, Germany. Potassium carbonate was purchased from ABCR GmbH, Germany. Sulfuric acid, potassium hydroxide, 0.1 N standard hydrochloric acid, sodium chloride and sodium hydroxide were purchased from Carl Roth GmbH, Germany. The vanadium electrolyte solution (1.6 M vanadium in 30% sulfuric acid : 50% VO^{2+} and 50% V^{3+}), was provided by RIVA GmbH Batteries. The structures of the polymers components used in this study are presented in Figure 1. Reference membranes Nafion®212 (N212) and Fumasep®FAP-450 (FAP 450) were supplied by Ion Power GmbH and Fumatech GmbH respectively.

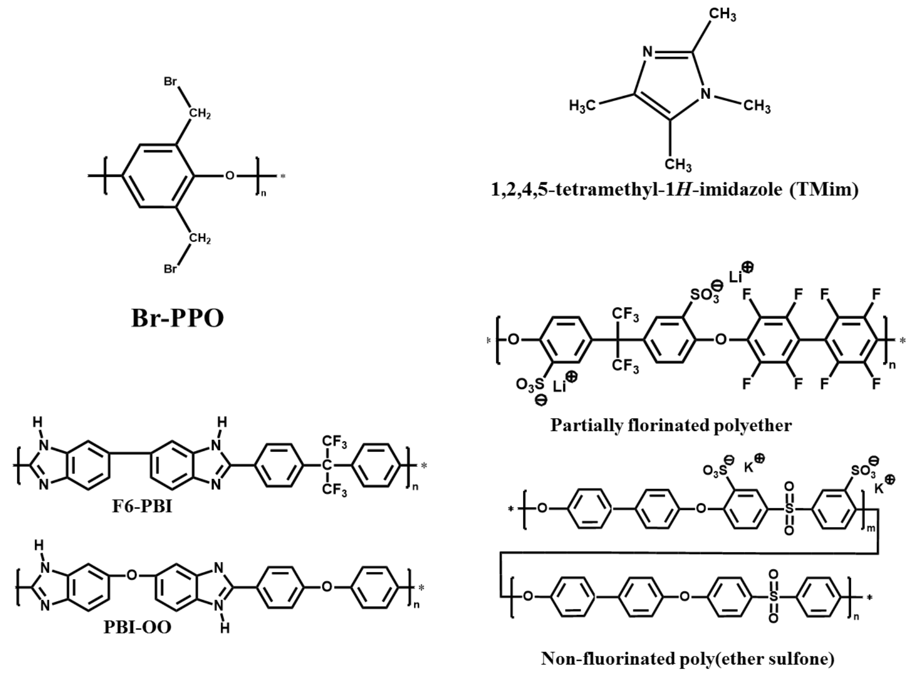

Figure 1. Structures of polymers and TMIm used in this study.

Membranes preparation

A diagrammatic depiction of how the anion-exchange blend membranes were prepared, is shown in Figure 2. Initially, each polymer solution except for F_6-PBI (F6-PBI : 5 wt% in DMAc) was prepared separately as a 10 wt % solution in DMAc. After mixing the polymer solutions in specific ratios, TMIm (same equivalent to the Br-PPO) was directly added to the polymer solution and homogenized. When using F_6-PBI during membrane preparation, additional DMAc was added due to the high viscosity of the 5% F_6-PBI solution. The blend polymer solution was then cast onto a glass plate, followed by solvent evaporation in a convection oven (pre-heated at 40 °C) at 60 °C for 24 hours. After solvent evaporation, the membrane was removed from the glass plate by soaking in water. Subsequently, the membranes were soaked in 1 M sulfuric acid for 24 hours at an ambient temperature with one replacement of the 1 M sulfuric acid solution during this period. The membranes were washed with deionized water several times at room temperature to remove all excess sulfuric acid and kept in plastic zipper bags.

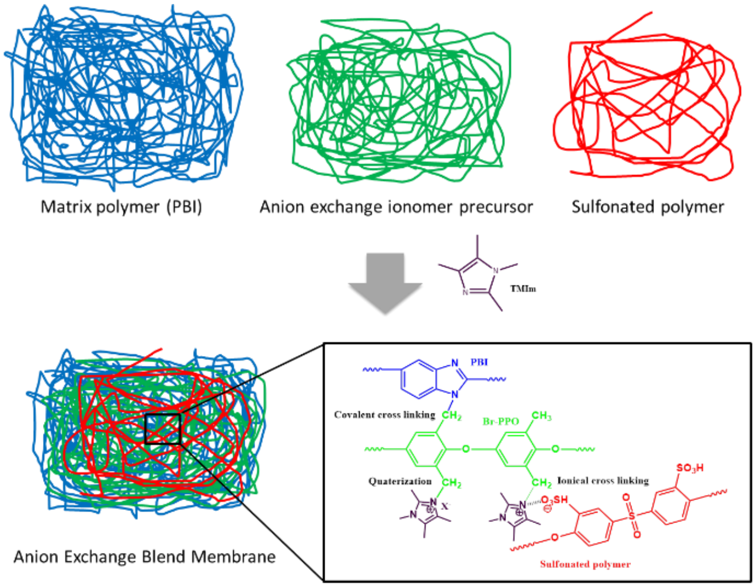

Figure 2. A diagrammatic depiction of the preparation of the anion-exchange blend membranes.

Membranes characterization

Ion Exchange Capacity (IEC)

The membranes were immersed in a 1 M KOH solution for 1 day at 90 °C to convert the bromide to the hydroxide form. After ion exchange, the membranes were washed with water intensively to remove excess KOH on the membrane surface. Subsequently, the membranes were soaked in a 60 mL saturated NaCl solution in order to convert the hydroxide to chloride for 1 day. Subsequently, 3 mL of a standard 0.1 N HCl solution was added to the saturated sodium chloride solution and kept overnight. Then, the membranes were washed with 25 mL distilled water and this water was transferred to the saturated sodium chloride solution. The back titration was carried out with a 0.1 N NaOH solution. Finally, the membranes were thoroughly washed with water and dried at 60 °C. The total IEC was calculated by using equation (1).

$$\mathbf{IEC} = \frac{\mathbf{CHCl \times VHCl - CNaOH \times VNaOH}}{\mathbf{mdry}} \quad (1)$$

where IEC is the ion exchange capacity (OH form, mmol/g), C_{HCl} is the concentration of a HCl solution (mmol/ml), V_{HCl} is the used volume of a HCl solution (ml), C_{NaOH} is the concentration of a NaOH solution (mmol/ml), V_{NaOH} is the added volume of a NaOH (ml), and m_{dry} is the weight of the membrane after drying (g).

Conductivity

Conductivity was determined by impedance spectrometer with A Zahner–elektrik IM6 under ambient atmosphere. The impedance was investigated in the frequency range of 200 KHz to 8 MHz at room temperature in a 1 M sulfuric acid solution (amplitude 10 mV). The resistance of membrane was obtained from the intercept of the impedance with the real X-axis. The conductivity was calculated by the following equation.

$$\boldsymbol{\sigma} = \frac{\mathbf{1}}{\mathbf{Rsp}} = \frac{\boldsymbol{d}}{\mathbf{R \times A}} \quad (2)$$

where σ is the conductivity (mS/cm), R_{sp} is the resistivity (Ω cm), d is the thickness of membrane (cm), R is the ohmic resistance (Ω), and A is the electrode area (cm^2).

Water Uptake (WU) and Swelling Ratio (SR)

The dimensional stability such as water uptake and swelling ratio was characterized by comparing the weight, length, width, and thickness of a dry and a wetted membrane. An approximately 4 × 1 cm^2 of wet membrane sample was cut and the weight, length, width, and thickness was measured using a balance and a digital vernier caliper after removal of residual water by wiping out the surface with a tissue paper. After drying the membrane at 90 °C for 1 day, the weight, length, width, and thickness were measured again. The water uptake (WU) and swelling ratios (SR - length, width and thickness) were calculated using equations 3 - 6. Four measurements were taken per membrane from which an average value was obtained.

$$\mathrm{WU}\ (\%)\ = \frac{(\text{Wet weight} - \text{Dry weight})}{\text{Dry weight}} \times\ 100 \quad (3)$$

$$\mathrm{SRL}\ (\%)\ = \frac{(\text{Wet length} - \text{Dry length}))}{\text{Dry length}} \times\ 100 \quad (4)$$

$$\mathrm{SRW}\ (\%)\ = \frac{(\text{Wet width} - \text{Dry width})}{\text{Dry width}} \times\ 100 \quad (5)$$

$$\mathrm{SRT}\ (\%) = \frac{(\text{Wet thickness} - \text{Dry thickness})}{\text{Dry thickness}} \times\ 100 \quad (6)$$

Fourier-Transform Infrared Spectroscopy (FT-IR)

FT-IR spectra of the membranes were recorded by using a Nicolet iS5 and a diamond attenuated total reflectance (ATR) module with 64 scans in the wave number range from 4000 to 400 cm^{-1} under an ambient atmospheric environment.

Gel Content by Extraction

In order to determine the gel content of the membrane, the weight loss was calculated by measuring the weight difference of the dry membranes before and after DMAc extraction. The dry membrane was stored in DMAc for 4 days at 90 °C and the following 3 days in methanol. The weight loss was calculated by using the follow equation.

$$\mathbf{Gel}\ (\%)\ = \frac{\textbf{Dry weight after}}{\textbf{Dry weight before}} \times\ \mathbf{100}\ (7)$$

Thermal Stability

Thermal stability of the membrane was analysed using a NETZSCH TGA, model STA 499C. Thermal gravimetric analysis (TGA) was performed with a dried membrane (dried at 90 °C in convection oven for 1day before TGA measurement) with a heating rate of 20 °C per minute under an O_2 / N_2 atmosphere (65–70% oxygen).

Weight gain measured in 30 % sulfuric acid

To determine the weight gain of AEBMs, the dry membranes (sulphated form) were immersed in a 30 % sulfuric acid solution at room temperature. The wet weight of the blend membranes was measured after 120 hours of doping in the 30 % sulfuric acid. The weight gain was calculated using the following equation.

$$\textbf{Weight gain}\ (\%) \quad = \frac{(\textbf{wet weight} - \textbf{dry weight})}{\textbf{dry weight}} \times \ \mathbf{100}\ (8)$$

Vanadium Redox Flow Battery (VRFB) single cell Test

A VRFB single cell was assembled as descried in the literature [18]. The anion exchange blend membrane was sandwiched by two carbon felts with an active area of 28 cm^2 and copper plates as a current collector. The single cell was assembled between two end plates with the screws as a torque of 3.5 Nm. 20 ml of electrolytes (1.6 M vanadium (50% VO^{2+}, 50% V^{3+}) in 30 % H_2SO_4) were fed into polyethylene tubes on both sides and allowed to flow through the VRFB without using pumps and tanks. The cell was first charged to 1.6 V and discharged to 1.0 V with the current density of 40 mA/cm^2, then charged at 40 mA/cm^2 and discharged at different current densities (six charge and discharge cycles at each current density) for efficiencies evaluation. The open circuit voltage (OCV) was monitored after it was charged to 1.6 V. A long-term charging–discharging cycling test was performed with a same charging and discharging current density of 40 mA/cm^2. Capacity retention as a function of cycles was calculated by the remaining capacity percent from the beginning capacity. The coulombic efficiency (CE), voltage efficiency (VE), and energy efficiency (EE) for the charging and discharging process were calculated as follows.

$$\mathbf{CE}\ (\%) \quad = \frac{\mathbf{td}}{\mathbf{tc}} \times\ \mathbf{100}\ (9)$$

$$\mathbf{VE}\ (\%) \quad = \frac{\mathbf{Vd}}{\mathbf{Vc}} \times\ \mathbf{100}\ (10)$$

$$\mathbf{EE}\ (\%) \quad = \mathbf{CE} \times \mathbf{VE} \times\ \mathbf{100}\ (11)$$

where t_d and t_c is the discharging and charging time respectively (s), while V_d and V_c is the average discharging and charging voltage (V) respectively.

4.3 Results and Discussion

Membranes preparation

Details of the composition of the AEBMs that were prepared as well as the obtained wet thicknesses are listed in Table 1. PBIs were used as a matrix polymer due to their high thermal and mechanical stabilities [22] enhancing the mechanical stability by forming covalent bonds with the halomethylated polymer. The sulfonated polymers were used as ionical cross-linkers between the sulfonated anions and the imidazolium cations which has previously been shown to enhance the chemical stability of blend membranes [23,24]. Br-PPO was used as the precursor for the quaternization with TMim. The same weight ratios of different combinations of the polymers were used. The variation in the thickness of the blend membranes was probably due to the high viscosity of the fluorinated F_6-PBI polymer solutions resulting in the addition of extra solvent, thereby decreasing the concentration of the polymer mixture solution. This resulted in thinner membranes, specifically for the F_6-PBI based partially fluorinated polymers-containing blend membranes.

Table 1. Membranes preparation details.

Membrane	Mass of Br-PPO (g)	Mass (g) and type of PBI	Mass (g) and type of S-polymer	Wet thickness (µm)
BM-TMIm 4 NN	1	1 (PBI-OO)	0.24 (Non-fluorinated polymer)	56 ± 0.96
BM-TMIm 4 NF	1	1 (PBI-OO)	0.24 (Fluorinated polymer)	43 ± 5.25
BM-TMIm 4 FN	1	1 (F6-PBI)	0.24 (Non-fluorinated polymer)	37 ± 0.82
BM-TMIm 4 FF	1	1 (F6-PBI)	0.24 (Fluorinated polymer)	34 ± 0.58
FAP 450	-	-	-	58
Nafion 212	-	-	-	53

To confirm the possible binding of the bromomethyl groups from Br-PPO to the TMIm or PBI, a structural analysis was performed by FT-IR (Figure 3). The strong peak observed at 1302 cm^{-1} can be assigned to a stretching vibration of the CH_2-Br groups of Br-PPO, which was not observed in the polymers of any of the blend membranes indicating that all CH_2-Br groups have completely reacted either with TMIm for quaternization or PBI for formation of covalent bonds [18].

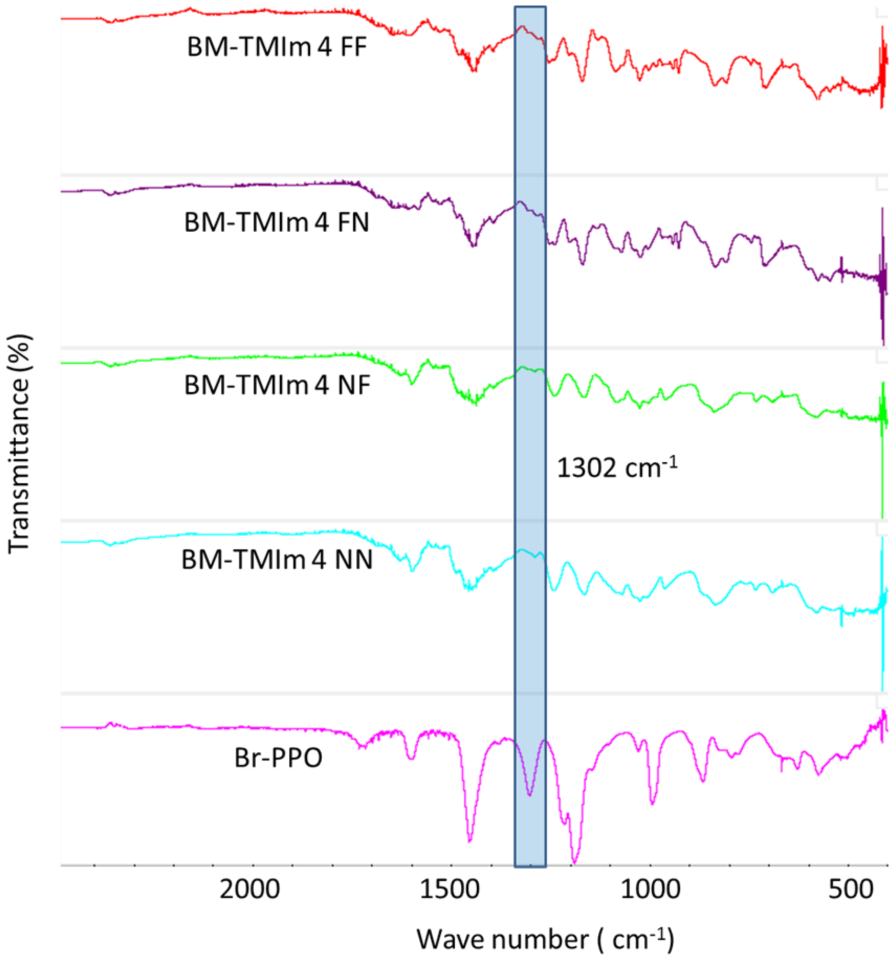

Figure 3. FT-IR spectrum of anion exchange blend membranes and Br-PPO.

Membranes properties

Various membrane properties of the synthesized AEBMs are summarized in Table 2. Since the same amounts of anion-exchange groups was present in each blend membrane, all the synthesized AEBMs had similar IECs ranging from 2.37 to 2.75 mmol/g. All membranes further also possessed dimensional stabilities that were comparable to those presented in literature [9]. It is known that the anion exchange sites (positively charged) absorb more acid (as HSO_4^- and SO_4^{2-}) when immersed in the electrolytes, which contributes to the ionic conductivity [25]. Therefore higher conductivities of AEMs can be expected than the pure form of AEMs under the acidic conditions in which VRFBs are operated. The conductivities of the AEBMs from this study measured in 1 M sulfuric acid were in the range of 21-27 mS/cm, which was lower than that of Nafion. However, according to the literature, comparable conductivities of AEBMs can be achieved by adjusting the anion exchange polymer ratio [18].

Table 2. Membrane characterization data

Membrane	IECs (mmol / g)	Conductivity (mS / cm)	WU (%)	SR_L (%)	SR_T (%)	SR_W (%)	Extraction (%)	T onset (° C)
BM-TMIm 4 NN	2.75	21.3 ± 0.8	22 ± 2.0	11 ± 0.3	6 ± 2	11 ± 0.3	93	280
BM-TMIm 4 NF	2.55	25.4 ± 0.8	14 ± 0.9	9 ± 0.7	8 ± 0.7	10 ± 1.0	93	284
BM-TMIm 4 FN	2.58	24.9 ± 0.7	17 ± 1.1	9 ± 0.8	7 ± 0.7	9 ± 1.1	92	278
BM-TMIm 4 FF	2.37	26.6 ± 1.3	13 ± 0.8	8 ± 0.8	4 ± 1.1	7 ± 1.2	92	265
FAP 450	2.18	35.2 ± 7.3	14 ± 3.2	8 ± 0.7	3 ± 1.4	8 ± 1.5	-	305
Nafion 212	0.88 (H+)	98.5 ± 5.0	13 ± 1.2	11 ± 0.6	8 ± 1.5	13 ± 2.2	-	300

To investigate the thermal stability of AEBMs, thermal gravimetric analysis (TGA) was conducted (Figure 4). The first weight loss step (up to 200 ^{o}C) is attributed to water evaporation. The second weight loss step starting at approximately 300 ^{o}C can be assigned to the splitting-off of the imidazolium groups as well as sulfonated groups from the sulfonated blend component [26]. All AEBMs showed excellent thermal stabilities measured under harsh oxidative conditions (65-70% oxygen). The weight loss measured via solvent extraction showed similar values, compared to our previously published results where more than 90 % of the initial membrane weight remained after extraction, indicating successful covalent cross-linking [20].

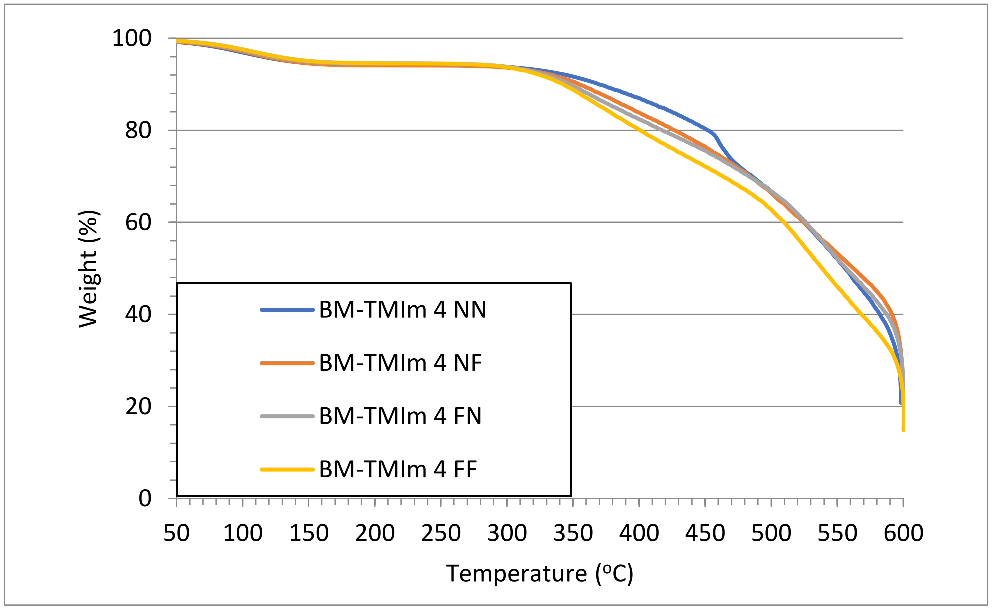

Figure 4. Weight loss as a function of temperature measured by TGA.

The acid uptakes measured in 30% sulfuric acid as a function of immersion time for the blend membranes are shown in Figure 5. All blend membrane showed similar weight gains in a sulfuric acid solution of around 60 % after 25 hours which then remained near constant for the residual doping time (120 hours). Due to the similar IECs of the AEBMs, the weight gain values were expected to be similar for all the investigated AEBMs. From these results complete doping of all the AEBMs can be concluded.

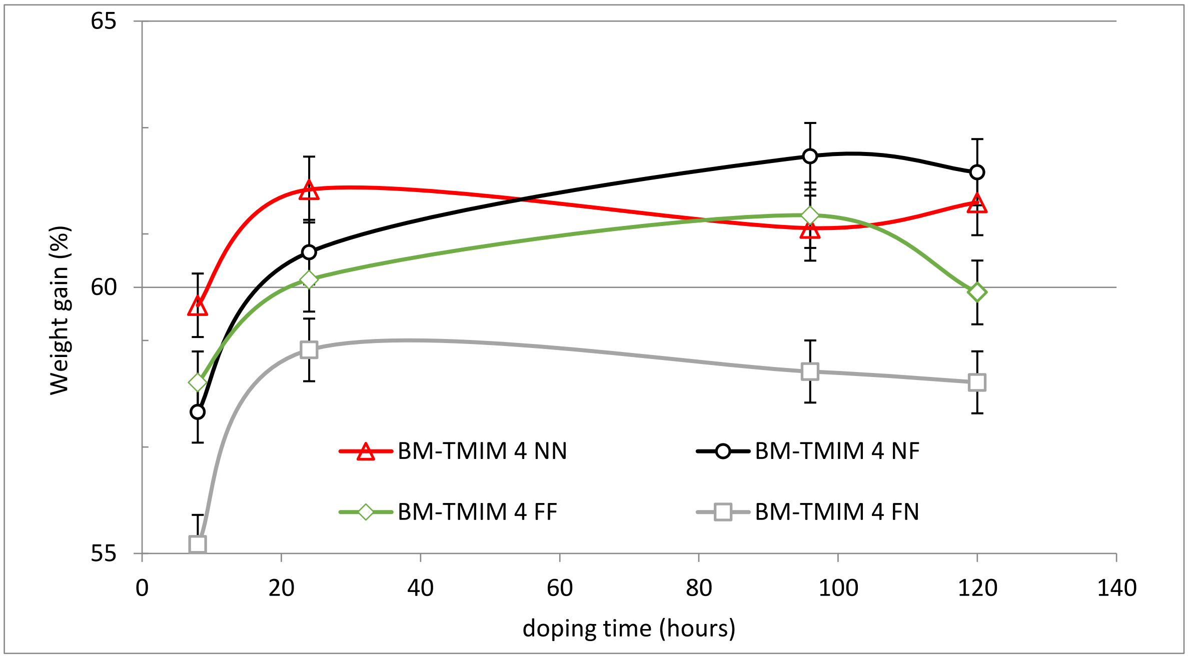

Figure 5. Acid uptake of blend membranes doped in a 30% sulfuric acid solution as a function of time.

For aromatic backbone based cation exchange membranes, sulfonated Radel chemical degradation was reported via vanadium peroxo radical attack resulting in chain scissions [27]. However, for cross-linked bromomethylated PPO-based AEMs, high chemical stability in vanadium electrolyte solution was reported [28]. Similarly, sulfonic acid doped PBI AEMs showed remarkable stability over 120 days in a 1 M vanadium solution in sulfuric acid at room temperature [29]. The superior chemical stability of AEMs has been attributed to the Donnan repelling effect, leading to limited permeation of vanadium ions into the membranes. In view thereof, a high chemical stability during operation in VRFBs is in principle expected for AEMs. However, in the case of PBI-OO, the electron-rich phenyl ring is prone to sulfonation showing increased peaks intensity in FT-IR spectra in a few days which was doped in 3M sulfuric acid

[31,32]. As a result, sulfuric acid can be lost via ionical cross-linking as suggested in Figure S1. Thus, FT-IR spectra of F6-PBI membranes was investigated as a function of sulfuric acid doping time in 30% sulfuric acid solution. F6-PBI membrane was doped in sulfuric acid for specific time and de-doped in carbonate solution and membranes were dried. The FT-IR spectra of F6-PBI membranes are shown in Figure S2. No significant changes of spectrum were observed for 9 days doping suggesting that F6-PBI as a matrix polymer is suitable for VRFB.

Vanadium redox flow battery performance

A single cell was used to determine the performance of the AEBMs in a vanadium redox flow battery. The single cell was first charged to 1.6 V to avoid electrode corrosion [32]. Subsequently it was allowed to discharge. Figure 6 a, b and c show the respective CE, VE and EE of the AEBMs, Nafion and FAP 450 membranes as a function of the current density. CE (Figure 6 a) is generally affected by the crossover of vanadium ions, side reactions, electrode corrosion as well as by membrane thickness [33]. Since all single cell performances were measured under the same conditions, side reactions and electrode corrosion should be similar for all VRFB experiments. Therefore, the vanadium ion crossover should have the biggest influence on the CE. As expected, all AEBMs showed better CE than Nafion due to the Donnan exclusion effect discussed previously. The CE increased as a function of current density due to the decreased time required for vanadium permeation during charge-discharge at higher current densities [10]. Considering the membrane thickness, the thicker membrane (BM-TMIm 4 NN) showed slightly higher CEs than other AEBMs because of the longer time required for vanadium permeation.

It is known that the VE (Figure 6 b) is affected by the membrane's ohmic resistance corresponding to its conductivity [33]. Nafion showed higher VEs than the AEBMs due to its high conductivity. It can be seen that the VE decreased with increasing current density due to increasing ohmic losses. For AEBMs, even though they have similar conductivities, the thinner membranes (BM-TMIm 4 FF) showed a higher VE than the thicker membranes due to the higher area resistance of the thicker membranes. The AEBMs possessed similar conductivities. Thus thicker membranes have a higher area resistance resulting in lower VEs as was expected [34]. The EE (overall efficiency - Figure 6 c) of BM-TMIm 4 FN, BM-TMIm 4 FF and BM-TMIm 4 NF was slightly higher than that of the Nafion membrane due to the higher CEs (VEs were similar) at all current densities. These results confirm that the manufactured AEBMs are promising candidates for VRFBs.

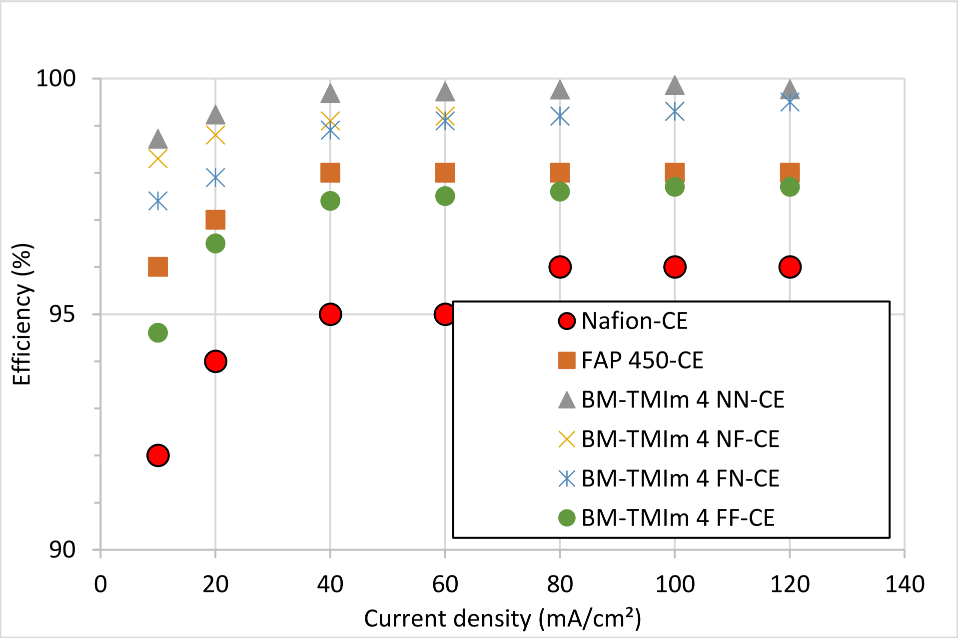

(a) Coulombic efficiencies.

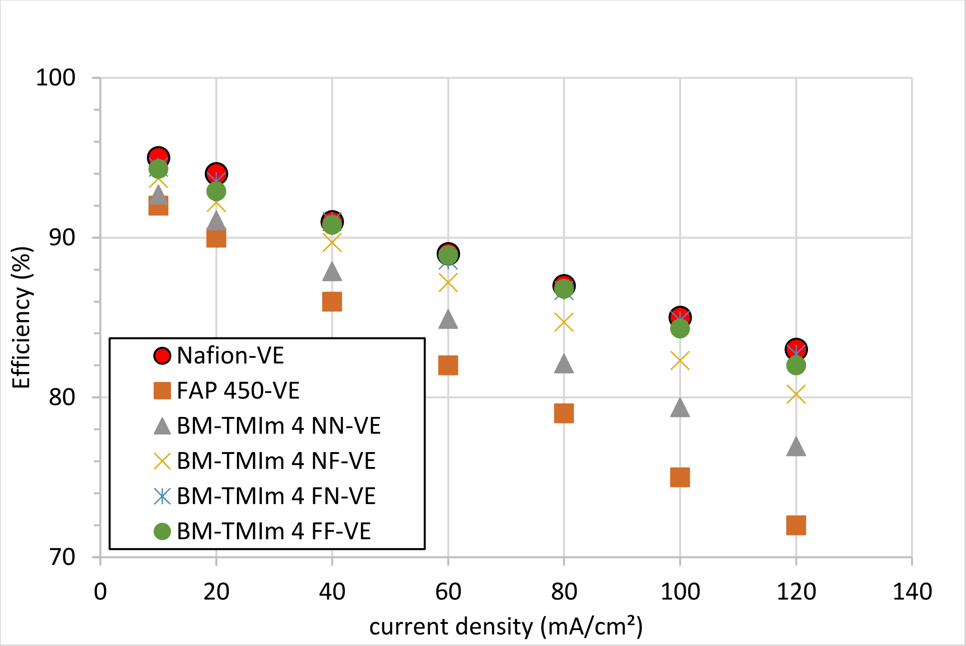

(b) Voltage efficiencies.

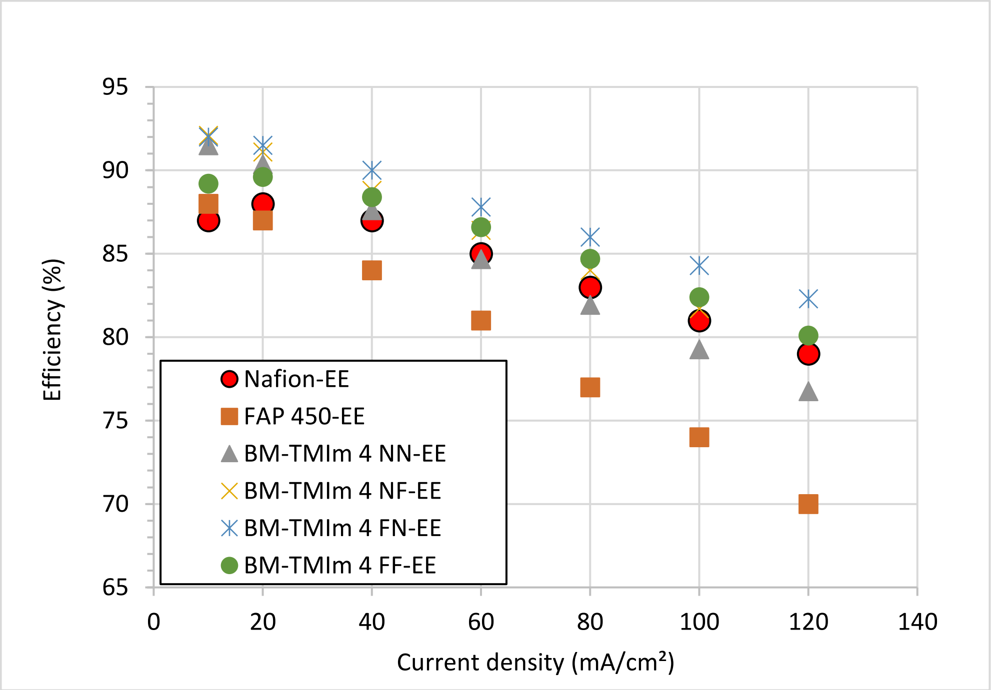

(c) Energy efficiencies.

Figure 6. CE (a), VE (b) and EE (c) of studied membranes.

Open circuit voltage (OCV) measurements of VRFBs are considered an indirect way to confirm the rate of the vanadium ion crossover [16]. The OCV of VRFBs was monitored as a function of time after the cell had been charged to 1.6 V (Figure 7). The OCV values gradually decreased as a function of time, followed by a sudden OCV drop with the disappearance of VO$_2^+$ from the positive electrolyte due to vanadium crossover [35]. According to Figure 7, the thinner membrane (BM-TMim 4 FF) showed similar self-discharge times (31 hours) as the Nafion membrane (27 hours). The self-discharge time of blend membranes increased with increased membrane thickness indicating the correlation between the OCV time and the membrane thickness as would have been expected in view of the influence of membrane thickness on the transport rate of vanadium ions. The thicker membrane (BM-TMIm 4 NN) showed the longest self-discharge time of 184 hours. All AEBMs showed longer self-discharge time than commercial membranes even though they are thinner, confirming the Donnan exclusion effect. It should be noted that not all AEMs show longer self-discharge times. If a membrane has poor dimensional stability, the self-discharge time of the membranes shorten [18], confirming that AEMs should be prepared carefully considering their IECs, water uptake values and dimensional stabilities.

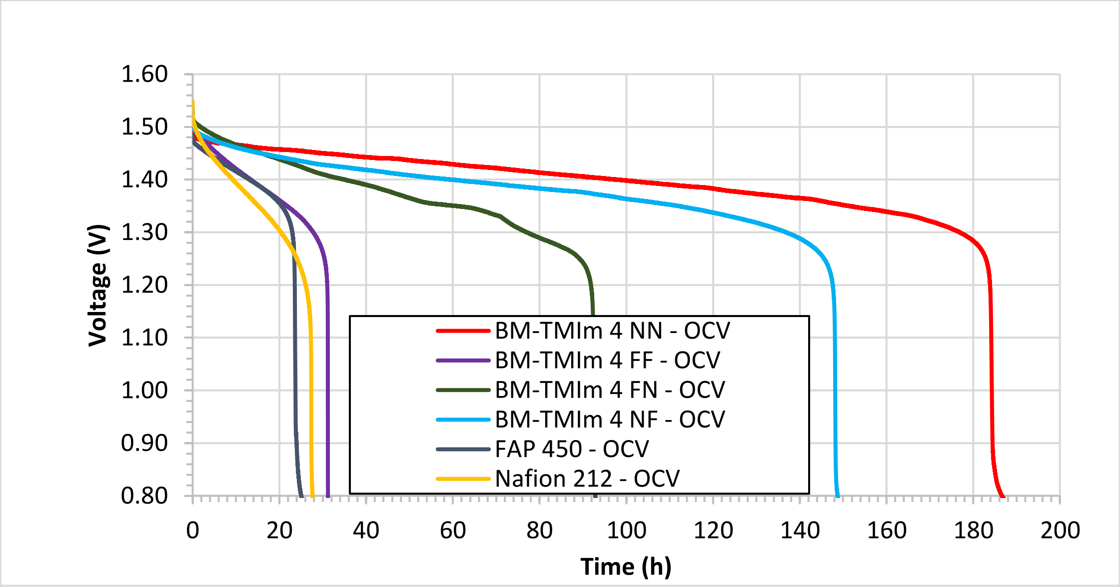

Figure 7. Open circuit voltage (OCV) measurements (self-discharge time) of AEBMs and commercial membranes.

To investigate the charge-discharge behavior of VRFBs, charge-discharge cycles tests of AEBMs were conducted at a current density of 40 mA/cm^2. The results are shown in Figure 8. Commercial membranes showed fast capacity decay showing respectively 10 % and 41 % capacity retention for Nafion 212 and FAP 450 after 100 cycles. While the BM-TMIm 4 NN membrane, which had a similar thickness to the commercial membranes, showed a 77 % capacity retention after 300 cycles, confirming a high cycling performance. BM-TMIm 4 FF was the most stable membrane with no capacity decay after 550 cycles. According to literature, thicker membranes need higher potentials to achieve the same current density than thinner membranes [34]. This additional potential probably allows vanadium ions to surpass the interface of the membrane and electrode allowing vanadium ions to enter the membrane, resulting in a relatively faster vanadium crossover and capacity decay. Thus, BM-TMIm 4 FF showed excellent capacity retention during the charge-discharge cycles test despite its low thickness. These results once again confirm the suitability of the novel AEBMs presented in this study for VRFB applications.

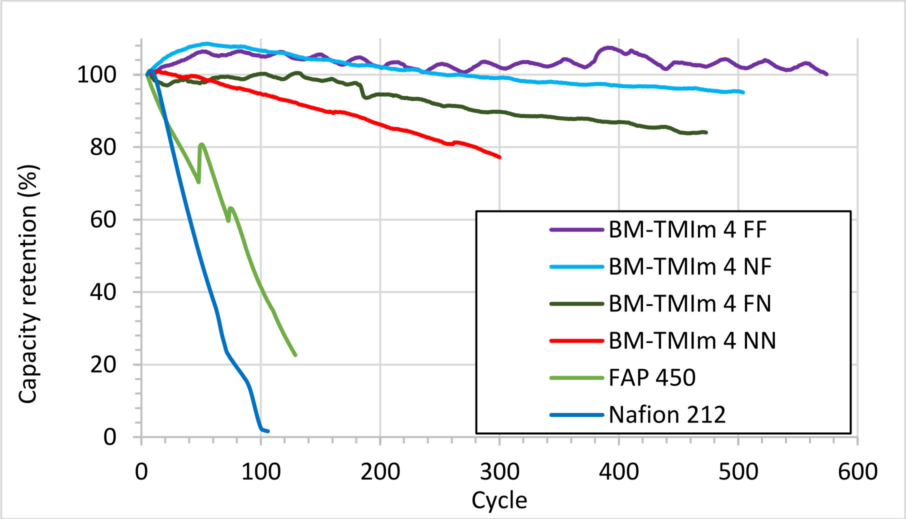

Figure 8. Charge-discharge cycles test run at 40 mA / cm^2.

4.4 Conclusion

Novel anion exchange blend membranes (AEBMs) were prepared and studied in VRFBs. The blend membranes were synthesized with bromomethylated PPO which was quaternized with TMIm. The PBI polymers (non-fluorinated or partially fluorinated) functioned as a matrix polymer for mechanical property enhancement of the AEBMs. The sulfonated polymer (non-fluorinated or partially fluorinated) was used to form ionical cross-links with the 1,2,4,5-tetramethylimidazolium cations of the AEM blend component. All synthesized AEBMs showed similar membrane properties such as IEC, conductivity, thermal stability and dimensional stability. The partially fluorinated polymer-containing blend membranes were chemically stable, as was expected. For the vanadium redox flow battery application, AEMs are known for their high chemical stability due to the Donnan exclusion effect hindering the vanadium ion from entering the membranes thereby limiting the degradation caused by vanadium radical attack. While one problem seemed to be the sulfonation of PBI, resulting in a loss of sulfuric acid during ionical cross-linking, however, F_6-PBI as a matrix polymer indicated suitable for VRFB application in acidic conditions showing no structural changes confirmed by FT-IR spectrum. All AEBMs performed better than the commercial membranes (Nafion (a CEM) and FAP 450 (an AEM)) in terms of CE, VE and EE as well as charge-discharge cycles test when used in a VRFB. One of the investigated blend membranes (BM-TMIm4 FF) had excellent capacity retention with no capacity loss during 550 charge-discharge cycles performed at 40 mA/cm^2. Thus one can conclude that, if the matrix polymer is chosen properly (it has to be thin and stable in acidic environments), the AEBMs are expected to show excellent performance in VRFBs specially, in terms of long term cycling tests. Further studies will focus on the increase of the chemical stabilities of the AEBMs by suitable selection of blend components, particularly for use of anion-exchange blend components having increased chemical stability resulting from both an increase of chemical stability of the polymer backbone and of the cationic group, compared to TMIm-quaternized PPO. A further focus will be to investigate the dependence of the VRFB performance on the thickness of the AEBM.

4.5 Supplementary Materials

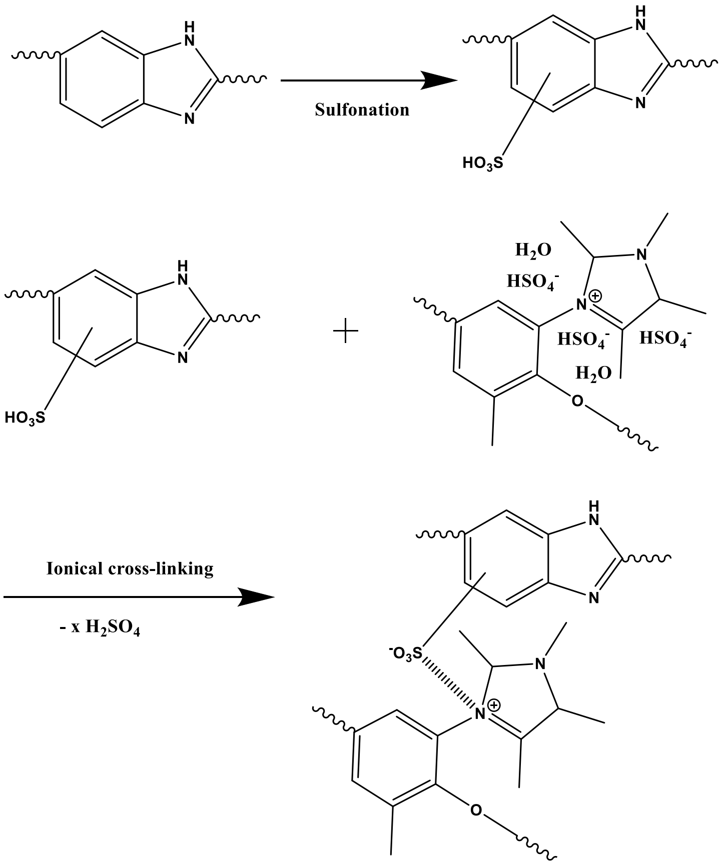

Figure S1. Possible loss of H_2SO_4 during the sulfonation of PBI based blend membranes.

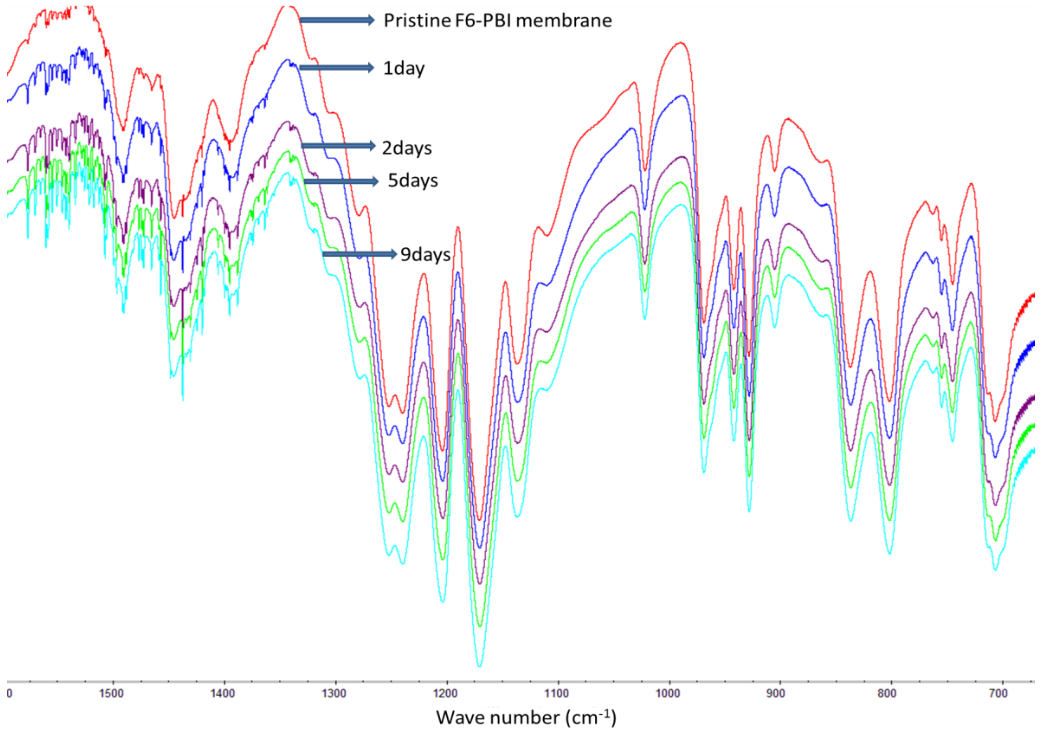

Figure S2. FT-IR spectrum of F6-PBI membrane as a function of sulfuric acid doping time (30% sulfuric acid at room temperature).

4.6 Acknowledgement

The authors gratefully acknowledge the valuable assistance of Inna Kharitonova and Galina Schumsky in performing the membrane characterization measurements.

4.7 References

1. Yang, Z.; Zhang, J.; Kintner-Meyer, M.C.W.; Lu, X.; Choi, D.; Lemmon, J.P.; Liu, J. Electrochemical energy storage for green grid. *Chem. Rev.* **2011**, *111*, 3577–3613.
2. Kim, K.J.; Park, M.-S.; Kim, Y.-J.; Kim, J.H.; Dou, S.X.; Skyllas-Kazacos, M. A technology review of electrodes and reaction mechanisms in vanadium redox flow batteries. *J.*

Mater. Chem. A **2015**, *3*, 16913–16933.

3. E. Sum, M.S.-K. A study of the V(II)/V(III) redox couple for redox flow cell applications. *J. Power Sources* **1985**, *15*, 179–190.
4. Choi, C.; Kim, S.; Kim, R.; Choi, Y.; Kim, S.; Jung, H. young; Yang, J.H.; Kim, H.T. A review of vanadium electrolytes for vanadium redox flow batteries. *Renew. Sustain. Energy Rev.* **2017**, *69*, 263–274.
5. Weber, A.Z.; Mench, M.M.; Meyers, J.P.; Ross, P.N.; Gostick, J.T.; Liu, Q. Redox flow batteries: A review. *J. Appl. Electrochem.* **2011**, *41*, 1137–1164.
6. Ashraf Gandomi, Y.; Aaron, D.S.; Mench, M.M. Coupled Membrane Transport Parameters for Ionic Species in All-Vanadium Redox Flow Batteries. *Electrochim. Acta* **2016**, *218*, 174–190.
7. Prifti, H.; Parasuraman, A.; Winardi, S.; Lim, T.M.; Skyllas-Kazacos, M. Membranes for redox flow battery applications. *Membranes* **2012**, *2*, 275–306.
8. Mohammadi, T.; Skyllas Kazacos, M. Modification of anion-exchange membranes for vanadium redox flow battery applications. *J. Power Sources* **1996**, *63*, 179–186.
9. Merle, G.; Wessling, M.; Nijmeijer, K. Anion exchange membranes for alkaline fuel cells: A review. *J. Membr. Sci.* **2011**, *377*, 1–35.
10. Chen, D.; Hickner, M.A.; Agar, E.; Kumbur, E.C. Selective anion exchange membranes for high coulombic efficiency vanadium redox flow batteries. *Electrochem. Commun.* **2013**, *26*, 37–40.
11. Sun, C.N.; Tang, Z.; Belcher, C.; Zawodzinski, T.A.; Fujimoto, C. Evaluation of Diels-Alder poly(phenylene) anion exchange membranes in all-vanadium redox flow batteries. *Electrochem. Commun.* **2014**, *43*, 63–66.
12. Chen, D.; Hickner, M.A.; Agar, E.; Kumbur, E.C. Optimized Anion Exchange Membranes for Vanadium Redox Flow Batteries. *ACS Appl. Mater. Interfaces* **2013**, *5*, 7559–7566.
13. Zhang, B.; Zhang, S.; Xing, D.; Han, R.; Yin, C.; Jian, X. Quaternized poly(phthalazinone ether ketone ketone) anion exchange membrane with low permeability of vanadium ions for vanadium redox flow battery application. *J. Power Sources* **2012**, *217*, 296–302.
14. Cha, M.S.; Jeong, H.Y.; Shin, H.Y.; Hong, S.H.; Kim, T.H.; Oh, S.G.; Lee, J.Y.; Hong, Y.T.

Crosslinked anion exchange membranes with primary diamine-based crosslinkers for vanadium redox flow battery application. *J. Power Sources* **2017**, *363*, 78–86.

15. Chromik, A.; dos Santos, A.R.; Turek, T.; Kunz, U.; Häring, T.; Kerres, J. Stability of acid-excess acid-base blend membranes in all-vanadium redox-flow batteries. *J. Membr. Sci.* **2015**, *476*, 148–155.
16. Liu, S.; Wang, L.; Li, D.; Liu, B.; Wang, J.; Song, Y. Novel amphoteric ion exchange membranes by blending sulfonated poly(ether ether ketone)/quaternized poly(ether imide) for vanadium redox flow battery applications. *J. Mater. Chem. A* **2015**, *3*, 17590–17597.
17. Yan, X.; Zhang, C.; Dai, Y.; Zheng, W.; Ruan, X.; He, G. A novel imidazolium-based amphoteric membrane for high-performance vanadium redox flow battery. *J. Membr. Sci.* **2017**, *544*, 98–107.
18. Cho, H.; Krieg, H.M.; Kerres, J.A. Application of Novel Anion-Exchange Blend Membranes (AEBMs) to Vanadium Redox Flow Batteries. *Membranes* **2018**, *8*.33.
19. Gorman, C.B.; Vest, R.W.; Palovich, T.U.; Serron, S. Preparation of poly(cyanoacetylene) using late-transition-metal catalysts. *Macromolecules* **1999**, *32*, 4157–4165.
20. Katzfuß, A.; Gogel, V.; Jörissen, L.; Kerres, J. The application of covalently cross-linked BrPPO as AEM in alkaline DMFC. *J. Membr. Sci.* **2013**, *425–426*, 131–140.
21. Chromik, A.; Kerres, J.A. Degradation studies on acid-base blends for both LT and intermediate T fuel cells. *Solid State Ion.* **2013**, *252*, 140–151.
22. Li, Q.; Jensen, J.O.; Savinell, R.F.; Bjerrum, N.J. High temperature proton exchange membranes based on polybenzimidazoles for fuel cells. *Prog. Polym. Sci. (Oxf.)* **2009**, *34*, 449–477.
23. Morandi, C.G.; Peach, R.; Krieg, H.M.; Kerres, J. Novel imidazolium-functionalized anion-exchange polymer PBI blend membranes. *J. Membr. Sci.* **2015**, *476*, 256–263.
24. Morandi, C.G.; Peach, R.; Krieg, H.M.; Kerres, J. Novel morpholinium-functionalized anion-exchange PBI-polymer blends. *J. Mater. Chem. A* **2015**, *3*, 1110–1120.
25. Ye, R.; Henkensmeier, D.; Yoon, S.J.; Huang, Z.; Kim, D.K.; Chang, Z.; Kim, S.; Chen, R. Redox Flow Batteries for Energy Storage: A Technology Review. *J. Electrochem. Energy*

Convers. Storage **2017**, *15*, 010801.

26. Kerres, J.; Ullrich, A.; Hein, M.; Gogel, V.; Friedrich, K.A.; Jörissen, L. Cross-Linked Polyaryl Blend Membranes for Polymer Electrolyte Fuel Cells. *Fuel Cells* **2004**, *4*, 105–112.
27. Chen, D.; Hickner, M.A. V5+ degradation of sulfonated Radel membranes for vanadium redox flow batteries. *Phys. Chem. Chem. Phys.* **2013**, *15*, 11299–11305.
28. Zeng, L.; Zhao, T.S.; Wei, L.; Zeng, Y.K.; Zhang, Z.H. Highly stable pyridinium-functionalized cross-linked anion exchange membranes for all vanadium redox flow batteries. *J. Power Sources* **2016**, *331*, 452–461.
29. Zhou, X.L.; Zhao, T.S.; An, L.; Wei, L.; Zhang, C. The use of polybenzimidazole membranes in vanadium redox flow batteries leading to increased coulombic efficiency and cycling performance. *Electrochim. Acta* **2015**, *153*, 492–498.
30. Strużyńska-Piron, I.; Jung, M.; Maljusch, A.; Conradi, O.; Kim, S.; Jang, J.H.; Kim, H.J.; Kwon, Y.; Nam, S.W.; Henkensmeier, D. Imidazole based ionenes, their blends with PBI-OO and applicability as membrane in a vanadium Redox flow battery. *Eur. Polym. J.* **2017**, *96*, 383–392.
31. Peron, J.; Ruiz, E.; Jones, D.J.; Rozière, J. Solution sulfonation of a novel polybenzimidazole. A proton electrolyte for fuel cell application. *J. Membr. Sci.* **2008**, *314*, 247–256.
32. Liu, H.; Xu, Q.; Yan, C.; Qiao, Y. Corrosion behavior of a positive graphite electrode in vanadium redox flow battery. *Electrochim. Acta* **2011**, *56*, 8783–8790.
33. Chen, D.; Hickner, M.A.; Agar, E.; Kumbur, E.C. Optimizing membrane thickness for vanadium redox flow batteries. *J. Membr. Sci.* **2013**, *437*, 108–113.
34. Noh, C.; Jung, M.; Henkensmeier, D.; Nam, S.W.; Kwon, Y. Vanadium Redox Flow Batteries Using meta -Polybenzimidazole-Based Membranes of Different Thicknesses. *Acs Appl. Mater. Interfaces* **2017**, *9*, 36799–36809.
35. Sun, C.; Chen, J.; Zhang, H.; Han, X.; Luo, Q. Investigations on transfer of water and vanadium ions across Nafion membrane in an operating vanadium redox flow battery. *J. Power Sources* **2010**, *195*, 890–897.

5. Novel Anion Exchange Membrane Based on Poly(pentafluorostyrene) Substituted with Mercaptotetrazole Pendant Groups and Its Blend with Polybenzimidazole for Vanadium Redox Flow Battery Application

Hyeongrae Cho, Vladimir Atanasov, Henning M. Krieg and Jochen A. Kerres

(reprinted with permission of MDPI)

Abstract

In order to evaluate the performance of the anion exchange membranes in a vanadium redox flow battery, a novel anion exchange polymer was synthesized via a 3 steps process. First, 1-(2-dimethylaminoethyl)-5-mercaptotetrazole was grafted onto poly(pentafluorostyrene) by nucleophilic F/S exchange. In the second step, the tertiary amino groups were quaternized by using iodomethane to provide anion exchange sites. Finally, the synthesized polymer was blended with polybenzimidazole to be applied in vanadium redox flow battery. The blend membranes exhibited better single cell battery performance in terms of efficiencies, open circuit voltage test and charge-discharge cycling test than that of a Nafion 212 membrane. The battery performance results of synthesized blend membranes suggest that those novel anion exchange membranes are promising candidates for vanadium redox flow battery.

5.1 Introduction

Vanadium Redox Flow Batteries (VRFBs) are electrochemical energy storage systems producing electricity from chemical redox reactions. Significant contributions to the development of the VRFB technology have been made at the University of New South Wales by Maria Skyllas-Kazacos's group [1]. VRFBs are among the most promising energy storage systems for renewable power generation due to their high energy efficiency, flexible design, unlimited capacity and satisfactory safety [2].

As an important component of the VRFBs, an ion exchange membrane separates the two electrolytes to prevent cross-mixing of the positive and negative electrolyte, while allowing the transport of ion species such as H^+ when a cation-exchange membrane (CEM) is used as the separator material, or HSO_4^- or SO_4^{2-} when the two electrolyte compartments are separated by an anion-exchange membrane (AEM) to maintain charge balance [3]. As the CEM, Nafion® type membranes developed by DuPont have been widely employed for VRFBs due to their high ionic conductivity and superior chemical stability, however, it turned out that Nafion® type membranes suffer from high vanadium ion cross-over resulting in fast capacity fade when used in VRFBs [4,5].

In the last decade, the interest of using AEMs in various applications, such as alkaline anion exchange membrane fuel cells [6], alkaline anion exchange membrane water electrolysis [7], ionic polymer membrane actuators [8], dye-sensitized solar cells [9], CO_2 pumps [10] and redox flow batteries [11] has strongly increased. In a recent review paper, the number of journal articles published in the field of anion exchange membranes has been analyzed by using Web of Science (SCI-EXPENDED) showing a steady growth since 2007 [12]. The significant advantage of AEMs when applied in a VRFB is that their positively charged fixed ion groups (commonly quaternary ammonium) exclude positively charged strongly oxidizing vanadium ions from the membrane interior due to the Donnan exclusion effect leading to extremely low vanadium ions cross-over [11].

Additionally, modified poly(pentafluorostyrene) (PPFSt) was applied in proton exchange membrane fuel cells as sulfonated [13] or phosphonated [14] CEMs exhibiting outstanding oxidative and thermal stabilities which were better than that of their non-fluorinated styrene polymer analogues due to the higher bond strength of the C-F bonds compared to those of C-H bonds [15]. The outstanding stability of PPFSt-based CEMs inspired us to find a route to prepare a PPFSt-based anion exchange polymer along with the advantages of AEMs. Introducing spacer units between the polymer backbone and the side chains in an AEM, was thought to lead to an enhanced ion-conductivity which might be facilitated by an improved phase separation between the hydrophobic polymer backbone and the cation-carrying side chains [16]. Tetrazole tethered polymers showed an improved conductivity compared to that of tetramethylammonium-based quaternized poly(phenylene oxide) AEMs, which is thought to be caused by the long-range hydrogen bond network formation by the tetrazole moiety contributing to the ion conductivity [17].

In this study, we synthesized AEMs based on poly(pentafluorostyrene) (PPFSt) by a three-step process: 1) grafting of 1-(2-dimethylaminoethyl)-5-mercaptotetrazole, 2) methylation (quaternization) of the tertiary amino groups, 3) blending of the anion-exchange polymer with polybenzimidazole. Due to inability to prepare a free-standing membrane from the functionalized polymer, it was blended in the third step with the partially fluorinated and highly stable polybenzimidazole (F6-PBI) for enhancing the film forming properties and mechanical strength of the AEMs [18,19]. In our earlier study it has already been shown that polybenzimidazoles as blend components have a positive impact on the mechanically stability and toughness of the cation-exchange redox-flow battery separator blend membranes [20]. The properties of the blend membranes such as conductivity, thermal stability, dimensional stability and VRFB performance are described. Synthesized blend membranes in this study showed better VRFBs performances than that of Nafion membrane. To the best of our knowledge, AEMs based on PPFSt have not been reported yet.

5.2 Materials and Methods

Materials

PPFSt was prepared as described in our earlier study [13]. F6-PBI was purchased from Yanjin Technology, Shenzhen, China. Sulfuric acid, methyl ethyl ketone, potassium hydroxide, 0.1 N standard hydrochloric acid and sodium chloride were purchased from Carl Roth GmbH, Karlsruhe, Germany. N-methyl-2-pyrrolidone (NMP) and diethyl ether were obtained from Sigma-Aldrich, Munich, Germany. N,N-dimethylacetamide was purchased from Acros Organics, Darmstadt, Germany. Sulfuric acid was purchased from VWR International, Bruchsal, Germany. 1-(2-dimethylaminoethyl)-5-mercaptotetrazole (DMAEMTZ) and triethylamine were purchased from TCI Chemicals, Eschborn, Germany. Iodomethane was purchased from Merck, Darmstadt, Germany. The vanadium electrolyte solution (1.6 M vanadium in 30 % sulfuric acid: 50% VO^{2+} and 50% V^{3+}) was supplied by RIVA GmbH Batteries, Backnang, Germany. Nafion®212 (Nafion) was purchased from Ion Power GmbH, Munich, Germany.

PPFSt synthesis

PPFSt was obtained via emulsion polymerization of pentafluorostyrene as described in the literature as mentioned in the materials section (M_n: 52 kDa, M_w: 124 KDa, PDI: 2.4: determined by GPC in THF at 30 °C with standard polystyrene) [13].

^{19}F NMR (400MHz, THF-d_8, δ): -144 (t, 2F), -157 (s, 1F), -163 (s, 2F).

1-(2-Dimethylaminoethyl)-5-mercaptotetrazole grafting onto PPFSt (PPFSt-MTZ)

A flask, which was equipped with magnetic stirrer, condenser, an argon in- and outlet, was charged with PPFSt (1 g, 5.152 mmol) in 40 mL of methyl ethyl ketone (MEK). After the complete dissolution of PPFSt, 20 mL of dry NMP were added. Subsequently, triethylamine (7.82 g, 77.28 mmol) and 1-(2-dimethylaminoethyl)-5-mercaptotetrazole (4.55 g, 25.76 mmol) were added. The mixture was stirred at 95 °C for 3 days. After cooling to room temperature, the reaction solution was dropwise precipitated in water. The polymer precipitate was filtered off and washed several times using excess of deionized water. The final polymer was dried overnight in vacuum at 60 °C and 1.21 g of product was obtained.

^{1}H NMR (400MHz, THF-d_8, δ): 4.43 (s, 2H), 2.61 (s, 2H), 2.16 (s, 7H).

^{19}F NMR (400MHz, THF-d_8, δ): -134 (s), -142 (s), -156 (s), -163 (s).

Quaternization of PPFSt-MTZ (M-PPFSt-MTZ)

For the quaterization of PPFSt-MTZ, 0.5 g PPFSt-MTZ was dissolved in 20 mL NMP. A high excess of iodomethane (0.89 mL, 2000% excess) was added to the reaction medium using a syringe and stirred at room temperature for 4 days to achieve full conversion. Subsequently, the reaction solution was added dropwise to diethylether where the polymer precipitated. The precipitation was filtered and washed twice with diethylether and dried overnight under vacuum at 60 °C. 0.56 g of a yellowish powder were obtained.

^{1}H NMR (400MHz, DMSO-d$_6$, δ): 5.06 (s, 2H), 4.08 (s, 2H), 3.28 (s, 8.5H + water).

Membrane preparation

F_6-PBI was dissolved at 80 °C in NMP as a 5 wt. % solution. The M-PPFSt-MTZ was dissolved in NMP, also as a 5 wt. % solution. After complete dissolution of the polymers in the solvent, the two polymer solutions were mixed at room temperature. Subsequently, the mixed solution was cast into a petri-dish or onto a glass plate and placed in an oven at 80 °C for 16 h to evaporate the solvent. The dried membrane was peeled off from the glass supports by immersion in deionized water at room temperature. The resulting membrane was soaked in 1 M sulfuric acid for 24 h, which was replaced once with fresh sulfuric acid during this period, before immersing the membranes in DI water for 24 h to remove excess sulfuric acid from the membrane surfaces.

Ion exchange capacity (IEC)

IEC was measured as described in the literature [18]. IEC was calculated by the back-titration method. Accordingly, the membrane sample was immersed in a 1 M KOH solution at 90 °C for 1 day to allow full ion exchange to occur. After intense washing with DI water, the membrane was immersed in a saturated sodium chloride solution for 1 day. Then 3 mL of standard 0.1 N hydrochloric acid was added and the mixture stirred for 1 day. The resulting solution was titrated with standard 0.1 N sodium hydroxide solution. The membrane was again washed intensely with deionized water and dried overnight at 90 °C. The dry weight of the membrane was then determined. The IEC was calculated using the following equation (eq. 1).

$$\mathbf{IEC} = \frac{C_{HCl} \times V_{HCl} - C_{NaOH} \times V_{NaOH}}{m_{dry}} \tag{1}$$

where IEC is the ion exchange capacity (OH form, mmol/g), C_{HCl} is the concentration of the hydrochloric acid solution (mmol/mL), V_{HCl} is the volume of the hydrochloric acid solution used (mL), C_{NaOH} is the concentration of the sodium hydroxide solution (mmol/mL), V_{NaOH} is the added volume of the sodium hydroxide solution (mL), and m_{dry} is the dry weight of the membrane (g).

Conductivity

Membrane resistances were measured by electrochemical impedance spectroscopy using a Zahner elektrik IM6 device (Zahner-elektrik GmbH, Kronach, Germany) in 1 M sulfuric acid at room temperature. The resistance was investigated in a frequency range of 200 KHz - 8 MHz by intercepting the impedance with the real x-axis. Four samples per membrane were measured. The conductivity was calculated using the following equation (eq. 2).

$$\boldsymbol{\sigma} = \frac{1}{R_{sp}} = \frac{d}{\mathbf{R} \times \mathbf{A}} \tag{2}$$

where σ is the conductivity (S/cm), R_{sp} is the resistivity (Ω cm), d is the thickness of membrane (cm), R is the ohmic resistance (Ω), and A is the electrode area (cm^2).

Swelling ratio (%) and water uptake (%)

The swelling ratio was characterized by dimensional expansions of length, width and thickness (SRL, SRW and SRT respectively), which was measured by determining the difference between the wet and dry state of the membrane (eq. 3–5). Similarly, the relative water uptake (WU) was determined by determining the weight difference of the wet and dry membrane (eq. 6). In each case five membrane samples were used from which an average was obtained.

$$\mathrm{SRL}\ (\%) = \frac{(\text{Wet length} - \text{Dry length}))}{\text{Dry length}} \times 100 \qquad (3)$$

$$\mathrm{SRW}\ (\%) = \frac{(\text{Wet width} - \text{Dry width})}{\text{Dry width}} \times 100 \qquad (4)$$

$$\mathrm{SRT}\ (\%) = \frac{(\text{Wet thickness} - \text{Dry thickness})}{\text{Dry thickness}} \times 100 \qquad (5)$$

$$\mathrm{WU}\ (\%) = \frac{(\text{Wet weight} - \text{Dry weight})}{\text{Dry weight}} \times 100 \qquad (6)$$

Thermal stability

The thermal stability of the polymers was investigated using a Netzsch STA 449 F3 (Netzsch, Selb, Germany). The temperature was increased with a heating rate of 20 °C/min from 30 °C to 600 °C under an O_2/N_2 atmosphere (O_2: 56 mL/min, N_2: 24 mL/min). Decomposed gases coming out during the thermal gravimetric analysis (TGA) were analyzed by FT-IR coupled to TGA.

Vanadium redox flow battery performance

To evaluate the vanadium redox flow battery performance, a single cell was built as described in literature [21]. The membrane was placed between two electrodes (active area: 28 cm^2, SIGRACELL® GDF 4.6 EA, SGL Carbon GmbH, Bonn, Germany,) which were thermally treated at 450 ^{o}C for 5 hours after immersing in 1M sulfuric acid for 1 day. Copper plates were used for loading and as current collectors. The cell was assembled with screws by applying a torque of 3.5 Nm. 20 mL of a vanadium electrolyte (1.6 M vanadium in 30 % sulfuric acid: 50 % VO^{2+} and 50% V^{3+}) was used on both the anode and cathode sides. All the measurements were performed in a stationary mode i.e. without electrolytes flowing through the cell. The cell was initially charged to 1.6 V and discharged to 1.0 V. The cell was charged with 40 mA/cm^2 and discharged with different current densities to obtain the coulombic efficiency (CE), voltage efficiency (VE) and energy efficiency (EE). The open circuit voltage (OCV, self-discharge test) was monitored as a function of time after charging the cell to 1.6 V. A long term charging-discharging cycling test was performed with a current density of 40 mA/cm^2 for both charging and discharging. All experiments of the vanadium redox flow battery were conducted under ambient temperature. The CE, VE and EE were calculated as follows.

$$\mathrm{CE}\ (\%) = \frac{\text{discharge capacity}}{\text{Charge capacity}} \times 100 \tag{9}$$

$$\mathrm{VE}\ (\%) = \frac{\text{average discharge capacity}}{\text{average charge capacity}} \times 100 \tag{10}$$

$$\mathrm{EE}\ (\%) = \mathrm{CE}\ \times \mathrm{VE} \tag{11}$$

5.3 Results and Discussion

Synthesis of M-PPFSt-MTZ

The M-PPFSt-MTZ was synthesized according to the reaction scheme described in Figure 1. First, grafting of 1-(2-dimethylaminoethyl)-5-mercaptotetrazole onto PPFSt was conducted according to the literature where mercaptoalcohols were grafted onto the PPFSt by nucleophilic displacement of the 4-F of the pentafluorophenyl moiety with the thiolate [22]. According to the literature, when using MEK as a solvent for the reaction of PPFSt with mercaptoalcohols, an almost 100% degree of substitution (DOS) was achieved at 50 °C after 50 h. Therefore, PPFSt-MTZ was initially synthesized in MEK. However, when 1-(2-dimethylaminoethyl)-5-mercaptotetrazole was added to the reaction solution, it did not fully dissolve. Thus, additional 20 mL of dry NMP was added to the reaction vessel resulting in complete dissolution. Then the reaction mixture was heated to 95 °C for 3 days (See Table S1 in supporting information for optimization of reaction). As shown in Figure 2, ^{19}F NMR spectra of the polymers were recorded. The new peak at -134 ppm on the ^{19}F NMR spectra, that can be attributed to the grafting of the 1-(2-dimethylaminoethyl)-5-mercaptotetrazole, was used to calculate the DOS according to the literature [22]. For this specific synthesis, the calculated DOS was 41%. For the DOS calculation, see Figure S1 of the supporting information.

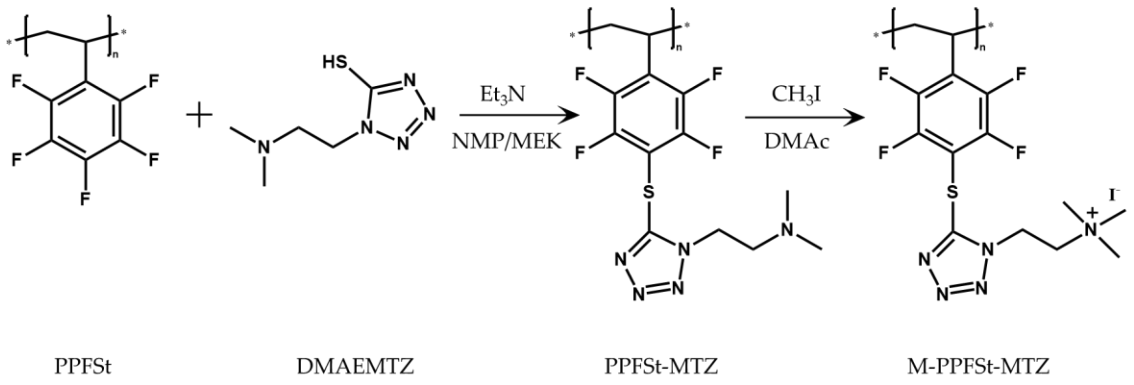

Figure 1. Anion exchange polymer preparation.

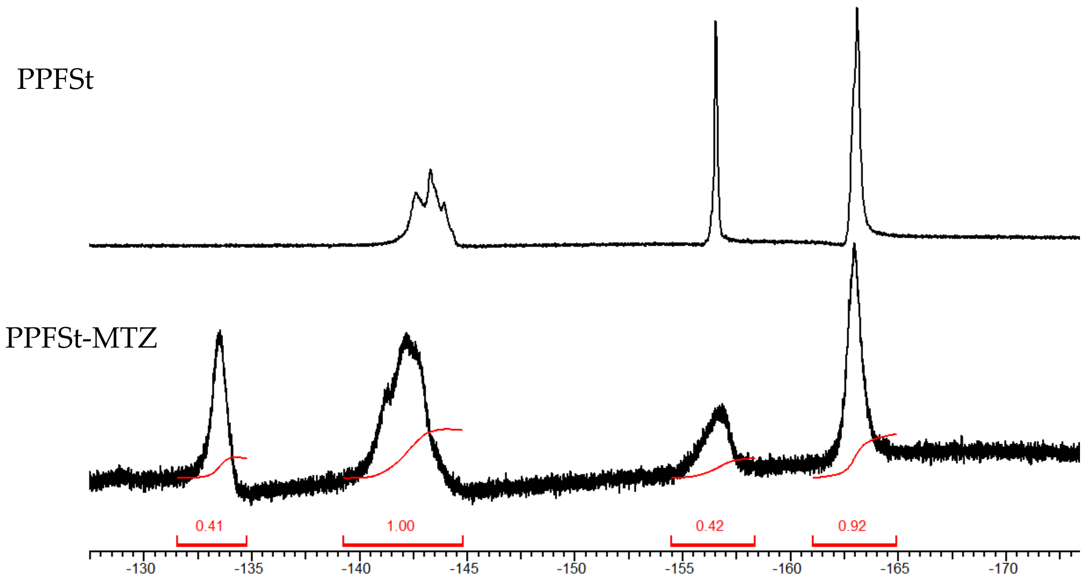

Figure 2. ^{19}F-NMR spectra of PPFSt and PPFSt-MTZ (chemical shift, ppm).

For the quaternization of PPFSt-MTZ, the tertiary amine groups were methylated using iodomethane (see Figure 1). Methylation of tertiary amines with large excess of iodomethane for complete quaternization has been widely used for anion exchange membrane preparation [23–26]. The ^{1}H NMR spectra of both PPFSt-MTZ and M-PPFSt-MTZ are shown in Figure 3. The CH_3 signal of PPFSt-MTZ on nitrogen was observed at 2.16 ppm. After methylation, the CH_3 signal had shifted completely to 3.28 ppm due to the de-shielding from the quaternized nitrogen indicating complete quaternization by iodomethane.

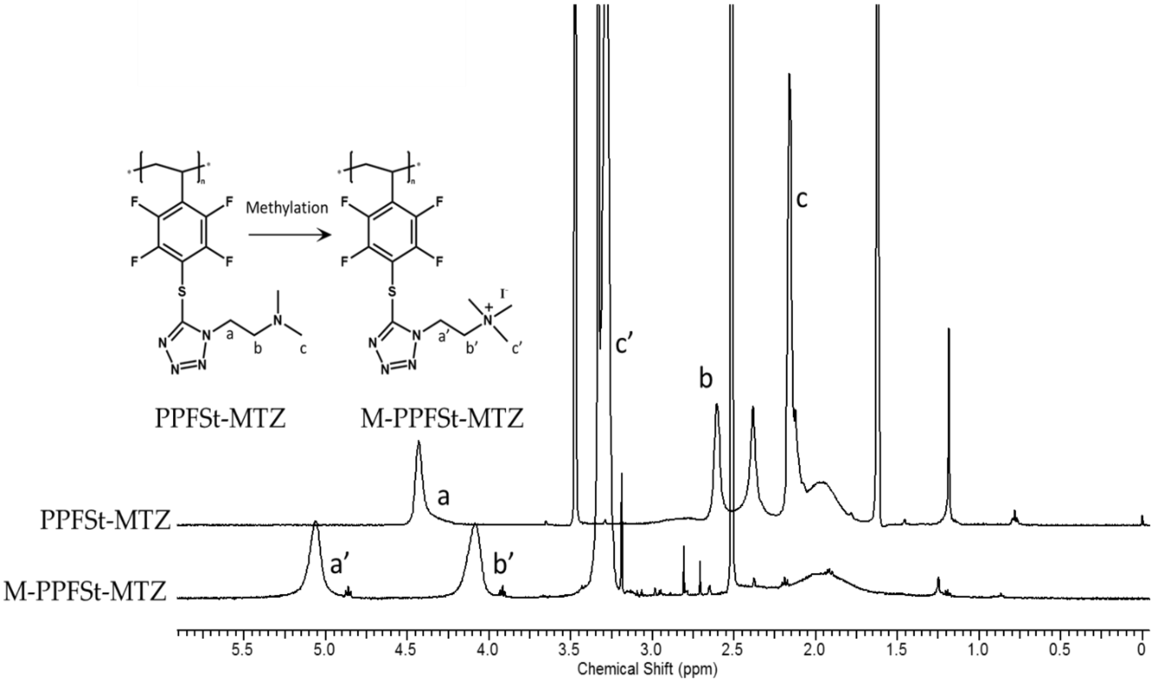

Figure 3. ^{1}H-NMR spectra of PPFSt-MTZ and M-PPFSt-MTZ.

Membranes preparation and characterization

The details of the preparation and the properties of the blend membranes are presented in Table 1. Firstly, blend membranes were prepared by using 90 wt. % and 80 wt. % of M-PPFSt-MTZ (M-PPFSt-MTZ-Me 1 and M-PPFSt-MTZ-Me 2 respectively) and 10, 20 wt. % of F6-PBI respectively. However, the membranes were found to be mechanically unstable after solvent evaporation and broke into pieces (see Figure S2 and Table S2 in the supporting information), probably due to the strong intermolecular hydrogen bonding and dipole-dipole association of the highly functionalized with charged functional groups PPFSt. In the literature, the similar polymer bearing tetrazole as a functional group has been reported to form mechanically stable membranes at low functionalization degree [17]. Therefore it is thought that the mechanical stability of membranes can be improved by decreasing the degree of functionalization or increasing the molecular weight of PPFSt [27,28]. This issue will be addressed in future work. Another approach to improve mechanical stability entails the addition of a polymer with possessing good film-forming properties and stability. Thus, blend membranes were prepared by blending M-PPFSt-MTZ with polybenzimidazole (F6-PBI) containing 70 wt. % and 60 wt. % of M-PPFSt-MTZ in the blend membrane (M-PPFSt-MTZ-Me 3 and M-PPFSt-MTZ-Me 4 respectively, see Table 1). This gave us access to mechanically stable blend membranes based on the newly obtained M-PPFSt-MTZ.

Table 1. Properties of blend membranes and Nafion212.

Membranes	M-PPFSt-MTZ/ F6-PBI (by weight)	IEC (mmol/g)	Conductivity (mS/cm)	Water uptake (%)	Dimensional stability (%)		
					Length	Width	Thickness
M-PPFSt-MTZ-Me 1	9 / 1	-	-	-	-	-	-
M-PPFSt-MTZ-Me 2	8 / 2	-	-	-	-	-	-
M-PPFSt-MTZ-Me 3	7 / 3	1.60	19.1 ± 1.64	12 ± 1.9	8 ± 0.6	5 ± 0.7	4 ± 1.2
M-PPFSt-MTZ-Me 4	6 / 4	1.15	13.5 ± 0.68	10 ± 2.2	7 ± 0.7	7 ± 0.7	4 ± 1.2
N 212	n.a	0.88	98.5 ± 4.95	13 ± 1.2	11 ± 0.6	8 ± 1.5	13 ± 2.2

$^{-}$ Membranes mechanically unstable after solvent evaporation, $^{n.a}$ not applicable

The IECs of the blend membranes were relatively lower (up to 1.6 mmol/g) as compared to other published results due to the low DOS [29,30]. Accordingly, the blend membranes showed low chloride conductivities of 0.043 and 0.038 mS/cm for M-PPFSt-Me 3 and M-PPFSt-Me 4 respectively measured in 1 M sodium chloride solution. However, when the anion exchange membranes were acidified using sulfuric acid or phosphoric acid, they absorbed more sulfate or bisulfate ions per anion exchange group via hydrogen bridges resulting in higher conductivities than in their pure form. In 1 M sulfuric acid conductivities of 19.1 ± 1,64 mS/cm for M-PPFSt-MTZ-Me 3 and 13.5 ± 0,68 mS/cm for M-PPFSt-MTZ-Me 4 were measured. It is known, as shown in Figure 4, that the imidazole moiety of PBI is protonated in an acidic medium with hydrogen sulfate counter ions significantly contributing to ion conductivity [31]. Thus, the conductivity of pure F6-PBI membrane was also investigated, which was 6.22 ± 0.27 mS/cm in 1 M sulfuric acid. It is thus clear that, the conductivity was increased by blending compared to the conductivity of the pure F6-PBI membrane indicating that the increase in conductivity originated from the anion exchange groups of the novel anion-exchange polymer synthesized in this study. Water uptake of membranes is one of the important parameters, as higher water uptake of membranes normally results in excessive swelling leading to a poor dimensional stability. Water uptake of the M-PPFSt-MTZ-Me 3 membrane was higher than that of M-PPFSt-MTZ-Me 4 membrane due to the somewhat higher IEC. The blend membranes in this study showed comparable dimensional stability compared to literature values being lower than 10% [32].

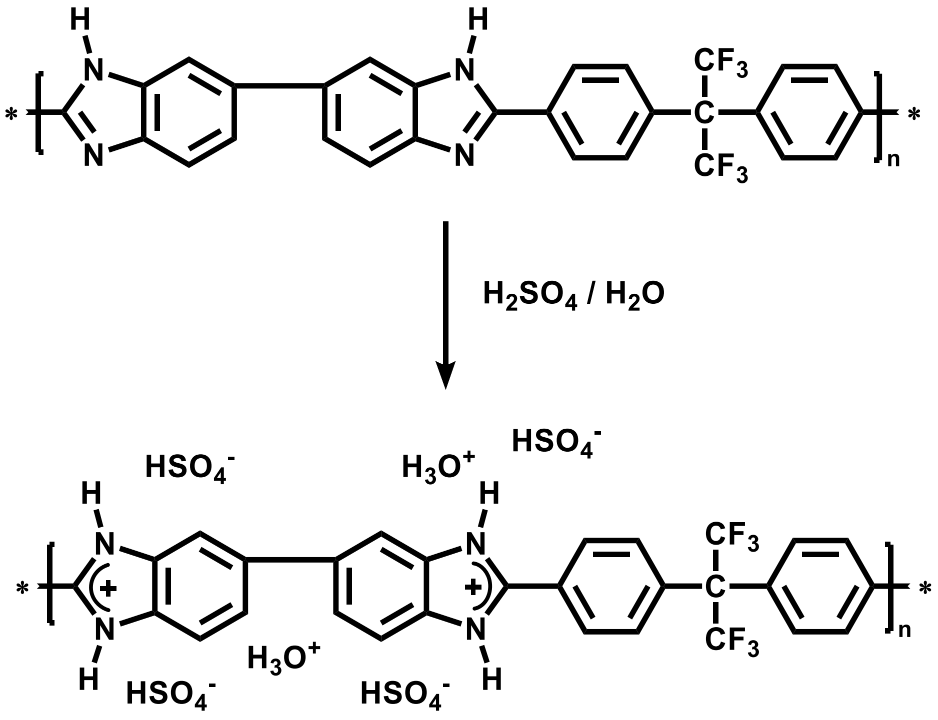

Figure 4. Protonation of F6-PBI when doped with sulfuric acid [31].

In order to investigate the thermal stability of the synthesized polymer and membranes, the weight loss was determined as a function of temperature using thermal gravimetric analysis (TGA). The TGA was operated with a highly oxidative atmosphere (70% oxygen, 30% nitrogen). According to Figure 5, PPFSt had a thermal resistance remaining stable up to 340 °C. After modification of the polymer (PPFSt-MTZ and M-PPFSt-MTZ), its thermal stability decreased. The first weight loss step at until around 150 °C for M-PPFSt-MTZ can be attributed to water evaporation. For PPFSt-MTZ the second weight loss step starts at 229 °C and can be ascribed to the loss of side chains due to the instability of mercaptotetrazole rings (See Figure S3 (a) in supporting information). After methylation, the second weight loss above 189 °C can be assigned to the loss of iodomethane via nucleophilic attack and mercaptotetrazole side chains (See Figure S3 (a) in supporting information). The temperature of polymers main chain degradation was indicated around 340 °C (See Figure S3 (b) in supporting information). However, in spite of the decline instability after modification, the synthesized anion exchange polymer and blend membranes showed sufficient thermal stability remaining stable up to 189 °C under harsh oxidative conditions.

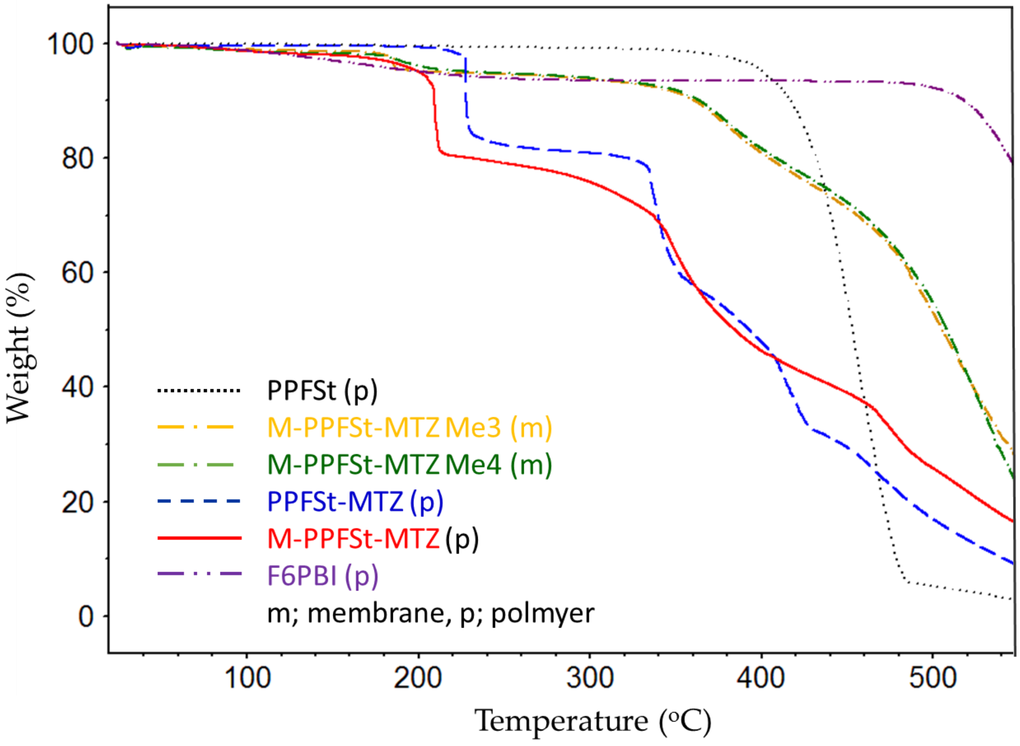

Figure 5. Thermal stabilities of polymers and membranes used in this study.

Vanadium redox flow battery evaluation

In order to evaluate the VRFB performance, a single VRFB cell was constructed as described in the literature [21]. It is important to note, that all the measurements were performed without electrolyte circulation in a stationary mode. This is allowing for a quick equilibration of the cell due to the relatively low electrolytes volume used (20 mL on each side). Thus, coulombic efficiencies (CEs) were investigated at various current densities. CE is determined by the ratio of charging time and discharging time. CE is influenced by the cross-over of vanadium ions through the membrane and increases with increasing current density due to the faster cross-over of vanadium ions [33]. As seen in Figure 6 (a), the CEs of blend membranes were higher than that of the Nafion membrane due to the Donnan exclusion effect as described above, while the Nafion membrane showed a low CE due to increased vanadium cross-over. It should be noted that AEMs do not always show high CEs, as this would also require a high dimensional stability of the membrane [21]. In addition, more dense PBI membranes have yielded higher CEs due to the low vanadium ion permeability [34]. Accordingly, the M-PPFSt-MTZ-Me 4 membrane with the highest F6-PBI content also showed the highest CE of almost 100%.

Voltage efficiencies (VEs) are governed by the ohmic resistances between two electrodes, which is mainly affected by the membrane resistance corresponding to its ionic conductivity [35]. As shown in Figure 6 (b), Nafion membrane showed the highest VE irrespective of the current density correlating with its highest conductivity among the membranes tested in this study. On the other hand, the M-PPFSt-MTZ-Me 4 showed the lowest VE again in line with its lowest conductivity of all membranes tested in this study.

The overall energy efficiencies (EEs) of the VRFBs are defined as the CE multiplied by the VE of which the results are shown in Figure 6 (c). The EE of M-PPFSt-MTZ-Me 3 showed slightly higher values than that of Nafion212 irrespective of the current density. This composition of blend membrane (60% M-PPFSt-MTZ and 40% F6-PBI) seemed to provide the best compromise between vanadium cross-over and membrane conductivity. On the other hand, the EE of M-PPFSt-MTZ-Me 4 was the lowest for all measured current densities due to the low VE in spite of the high CE.

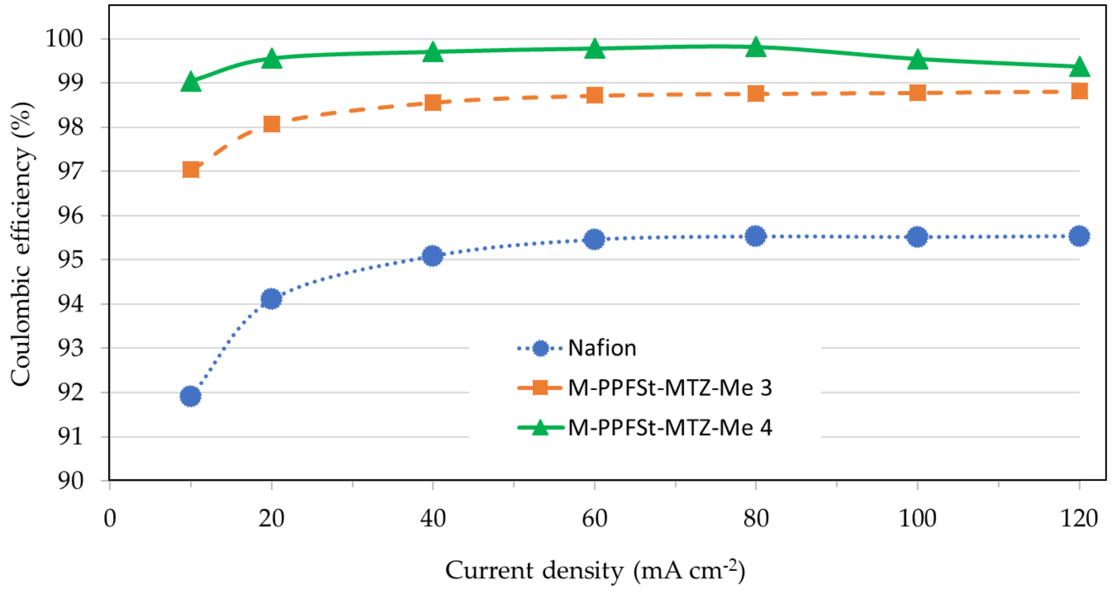

(a)

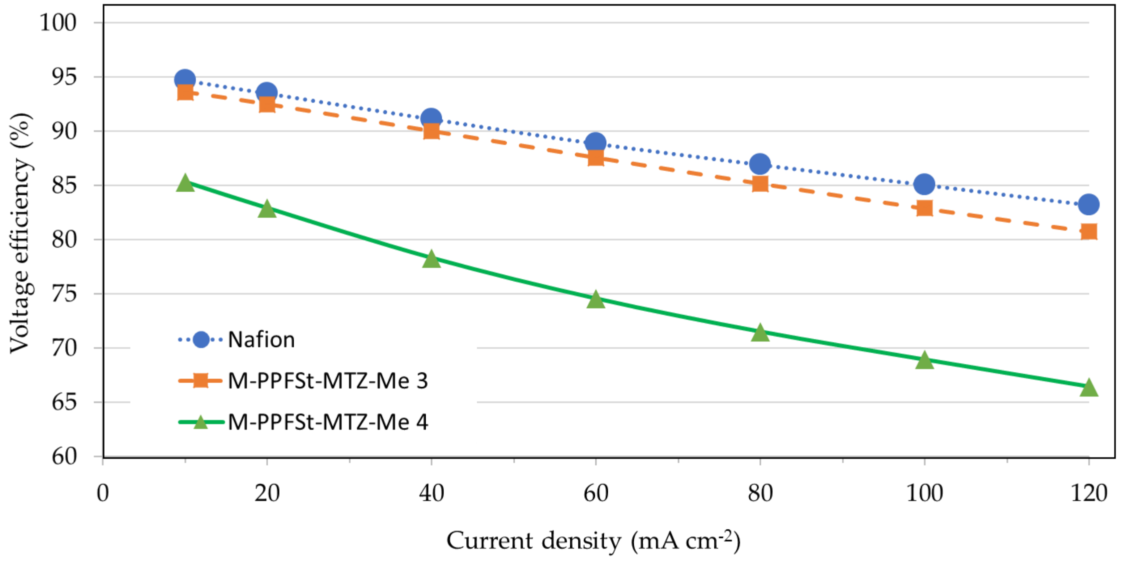

(b)

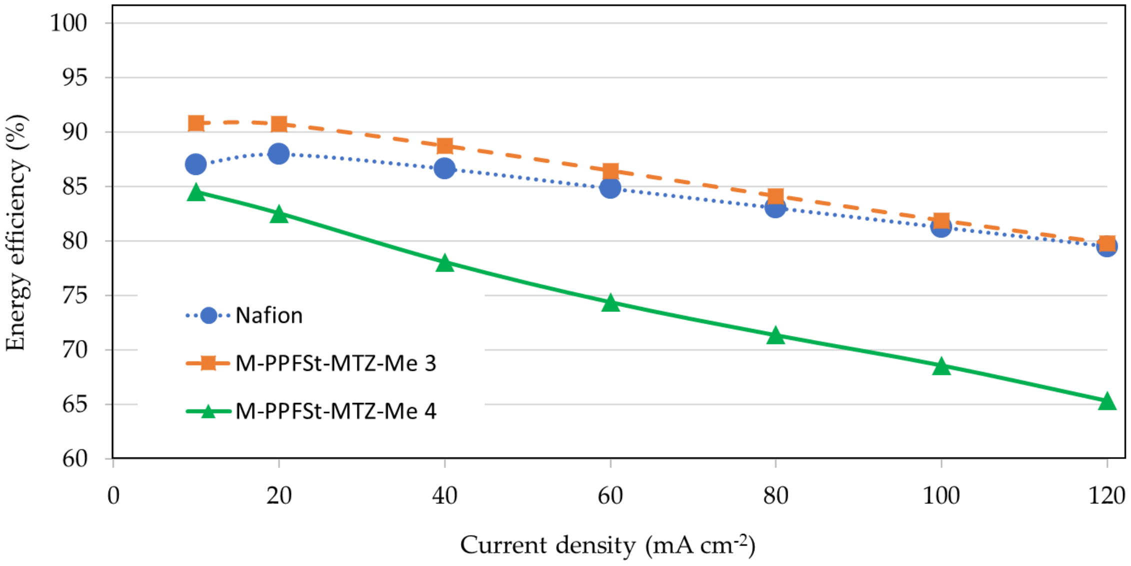

(c)

Figure 6. Coulombic efficiency (a), voltage efficiency (b) and energy efficiency (c) of VRFBs as a function of the current density.

Open circuit voltage (OCV) measurements can be used to indirectly measure the vanadium ion cross-over [36], as the cross-over through the membrane results in self-discharge which corresponds to a OCV drop in the performance of the VRFB [37]. Thus, self-discharge was monitored as a function of time. As seen in Figure 7, the OCV when using M-PPFSt-MTZ-Me 4 membranes remained nearly stable for over 200 hours indicating a low vanadium ion cross-over, as expected. When using Nafion212 in the VRFB, a fast self-discharge time of 27 h was observed due to fast cross-over. A VRFB with the M-PPFSt-MTZ-Me 3 membrane showed a slightly longer self-discharge time of 35 h, compared to that of Nafion. It is clear that the results of the OCV measurements are in accordance with the results obtained from the CE test.

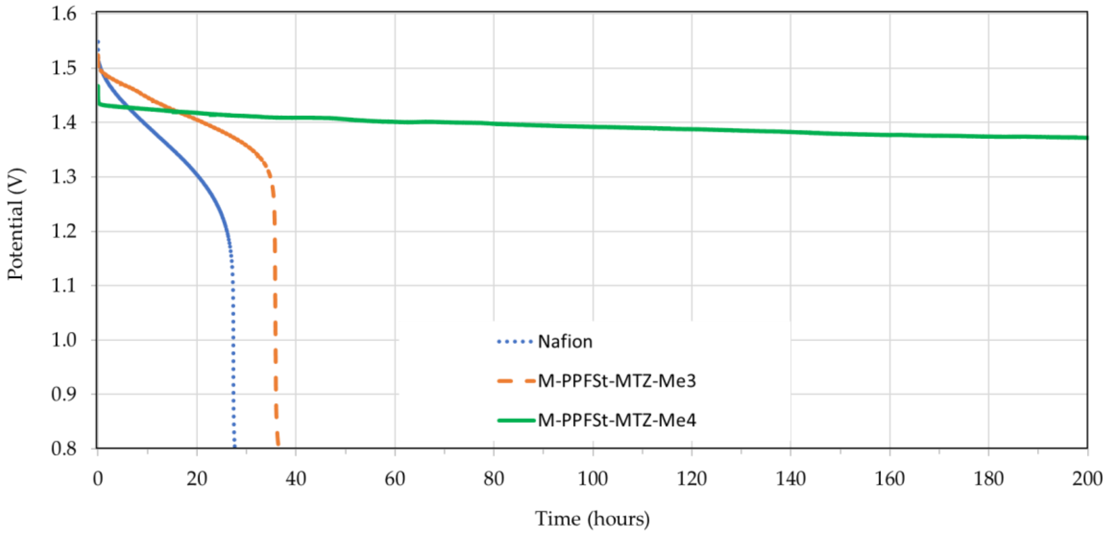

Figure 7. Open circuit voltage (OCV) of VRFBs with Nafion and blend membranes as a function of time.

Charging-discharging cycling performance operated at a constant current density of 40 mA/cm^2 for both charging and discharging of the blend membranes was measured and compared with Nafion212 (Figure 8). It has to be remembered that some capacity decay is inevitable during cycling tests due to the different permeabilities of the four vanadium ion states as well as the water transfer between electrolytes through the membrane [38,39]. While this capacity decay can be restored by simply remixing of the two electrolytes [40], this will add to the cost of maintaining the VRFBs. Thus, capacity retention is one of the most critical parameters in determining the success of a VRFBs application. As seen in Figure 8, the VRFB with Nafion showed a fast decay in capacity with most of its capacity lost in less than 100 cycles. In contrast, the VRFB with M-PPFSt-MTZ-Me 3 membrane showed a much better capacity retention with an 80% loss over 200 cycles, confirming considerably less vanadium ion cross-over. As in the previous experiment (CE and OCV), the VRFB with M-PPFSt-MTZ-Me 4 showed the highest capacity retention again confirming both its chemical and mechanical stability and consistently low vanadium ion cross-over rate.

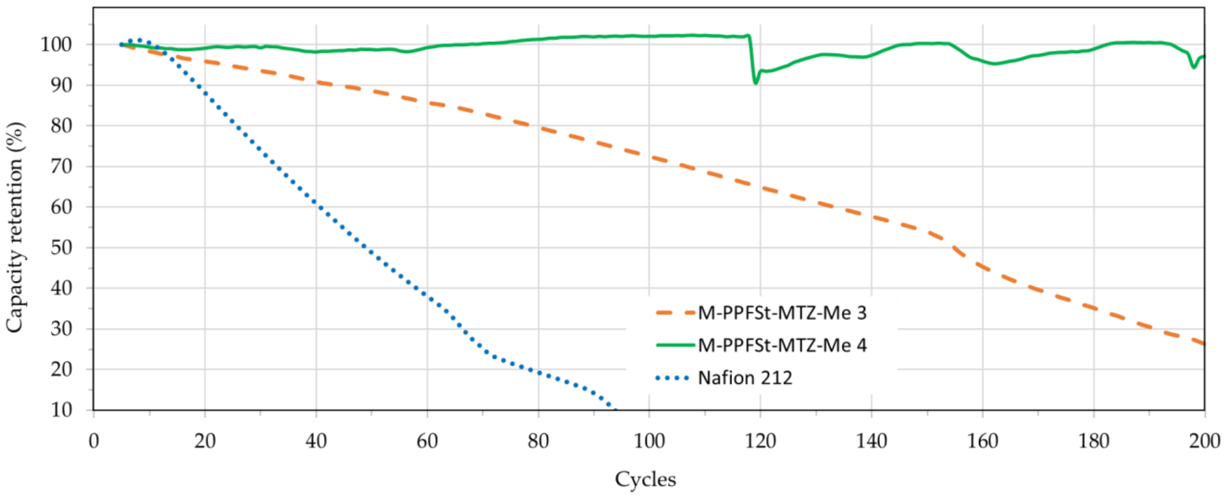

Figure 8. Charging-discharging cycling test.

5.4 Conclusions

In this study, a novel anion exchange polymer based on quaternary ammonium-functionalized poly(pentafluorostyrene) (PPFSt) was synthesized in two steps: 1) grafting of 1-(2-dimethylaminoethyl)-5-mercaptotetrazole by nucleophilic F/thiolate exchange and 2) quaternizing the 2-dimethylaminoethyl group using iodomethane. This polymer showed sufficient thermal stability for the VRFB application. However, no mechanically stable free-standing membranes could be prepared from this polymer. Therefore, the anion-exchange polymer was blended with F6-PBI. The blend membranes were characterized and applied in vanadium redox flow batteries. Specifically, the blend membranes containing 30 and 40% of F6-PBI demonstrated suitable membranes properties such as IEC, conductivity and swelling degree. During the VRFBs test, the blend membrane (M-PPFSt-MTZ-Me 3) yielded a better performance in VRFBs in terms of energy efficiency, OCV test and charging-discharging cycling test than a Nafion membrane, while the blend membrane M-PPFSt-MTZ-Me 4 displayed the highest OCV and capacity retention of all the membranes tested. It can therefore be concluded that these types of blend membranes are promising candidates for vanadium redox flow battery applications.

5.5 Supplementary Materials

Table S1. Optimization for PPFSt-MTZ synthesis.

Entry	Solvent	Equivalents of 1-(2-Dimethylaminoethyl)-5-mercaptotetrazole	Reaction conditions	Substitution Results*
1	NMP / MEK	5	80 °C, 18 hours	Low substitution (1% DOS)
2	MEK	1	55 °C, 72 hours	No substitution
3	NMP / MEK	5	80 °C, 72 hours	Low substitution (15% DOS)
4	NMP / MEK	5	95 °C, 72 hours	Used in this study (41% DOS)
5	NMP / MEK	5	95 °C, 168 hours	40 % DOS

* Degree of substitution (DOS) was calculated by F-NMR

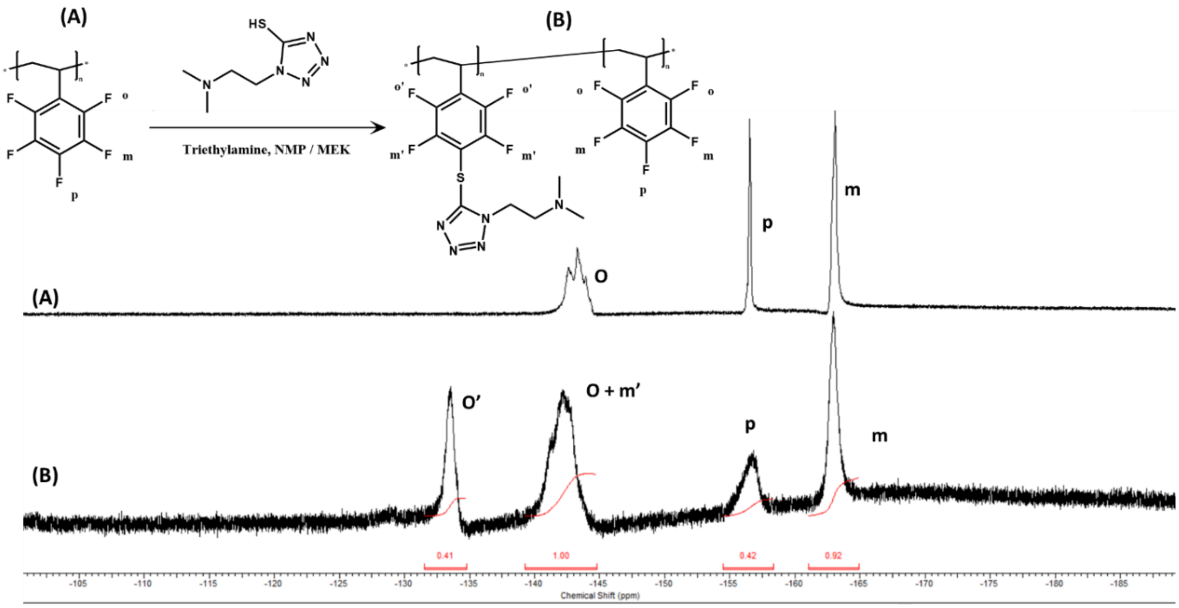

Figure S1. Calculation of degree of substitution confirming 41%.

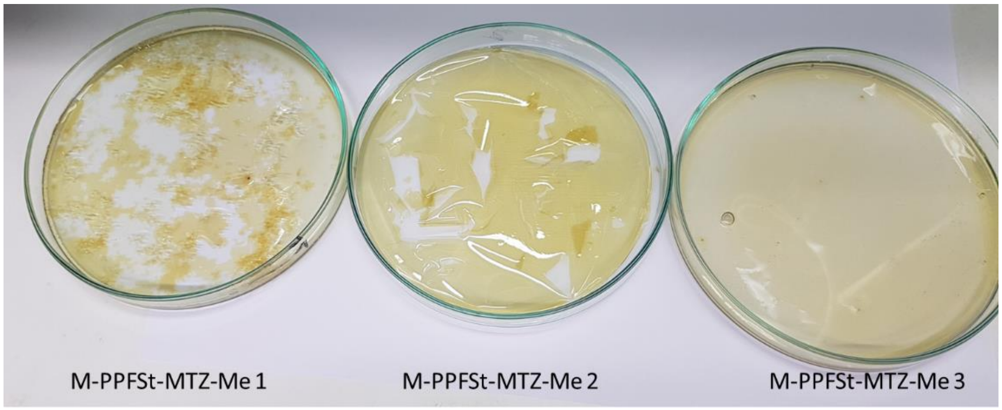

Figure S2. Photographs of the blend membranes.

Table S2. The blend membranes preparation.

Membrane	M-PPFSt-MTZ : F6-PBI (by weight)	Membrane formation (see Figure S2)
M-PPFSt-MTZ-Me 1	9 : 1	Brittle
M-PPFSt-MTZ-Me 2	8 : 2	Brittle
M-PPFSt-MTZ-Me 3	7 : 3	Ductile
M-PPFSt-MTZ-Me 4	6 : 4	Ductile

The blend membrane of M-PPFSt-MTZ-Me 3 was mechanically stable after drying the solvent. Therefore, blend membranes of M-PPFSt-MTZ-Me 3 and M-PPFSt-MTZ-Me 4 were prepared as larger membranes onto glass plate for the investigation in this study.

As seen in the Figure S3 (a), a strong peak 2957 cm^{-1} can be assigned to C-H vibration of N-CH_3 from the 1-(2-dimethylaminoethyl)-5-mercaptotetrazole. A strong peak at 1264 cm^{-1} can be assigned to the iodomethane by a nucleophilic substitution of iodide. The peaks at 2200 and 2400 cm^{-1} can be assigned to the loss of side chains,1-(2-dimethylaminoethyl)-5-mercaptotetrazole. Above 340^{o}C, polymer main back bone degradation was observed for all polymers, PPFSt, PPFSt-MTZ and M-PPFSt-MTZ (Figure S3 (b).

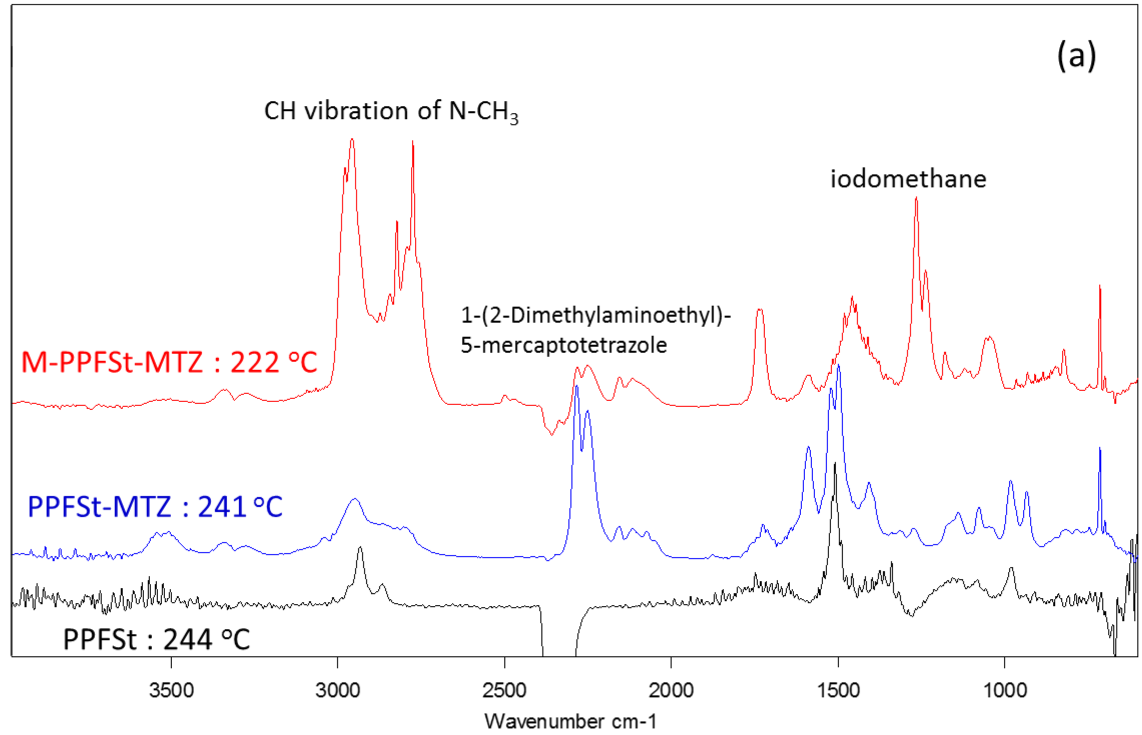

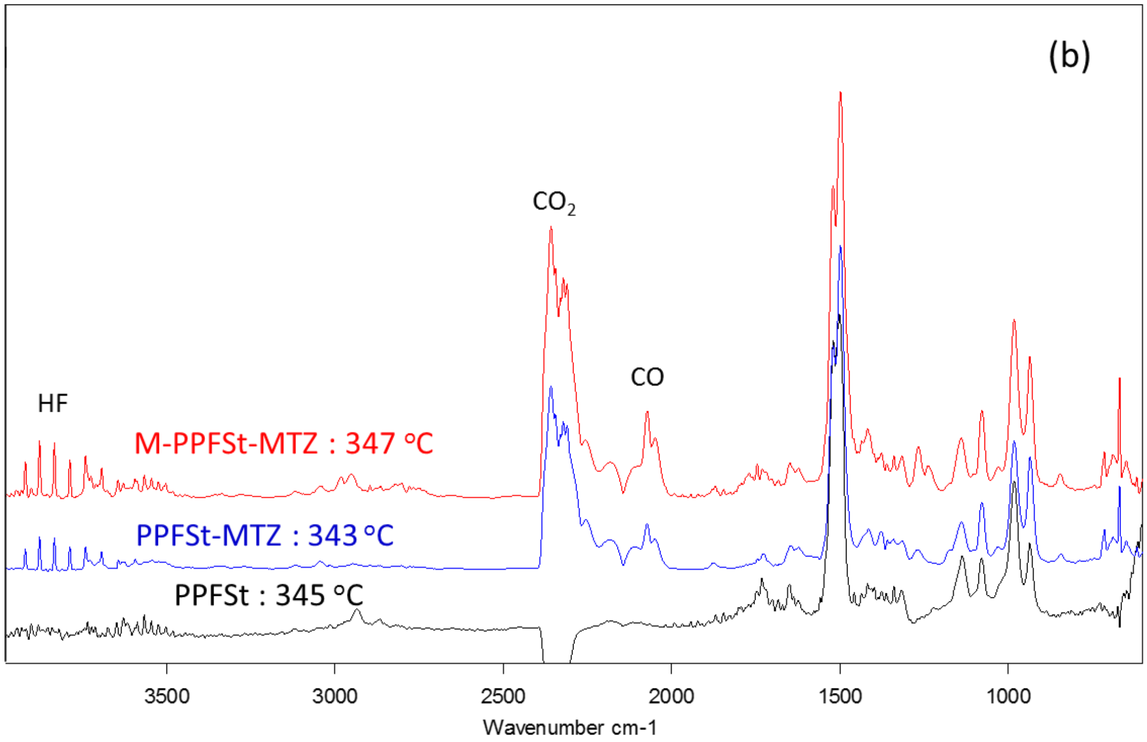

Figure S3. FT-IR spectrum of decomposed gases from first degradation step (a) and polymer main chain degradation (b).

5.6 Acknowledgments

The authors would like to thank Inna Kharitonova and Galina Schumski in performing the membrane characterization experiments.

5.7 References

1. Rychcik, M.; Robins, R.G.; Fane, A.G. THE New All-Vanadium Redox Flow Cell. *J. Electrochem. Soc.* **1986**, *133*, 1057–1058.

2. Kim, K.J.; Park, M.-S.; Kim, Y.-J.; Kim, J.H.; Dou, S.X.; Skyllas-Kazacos, M. A technology review of electrodes and reaction mechanisms in vanadium redox flow batteries. *J. Mater. Chem. A* **2015**, *3*, 16913–16933.

3. Prifti, H.; Parasuraman, A.; Winardi, S.; Lim, T.M.; Skyllas-Kazacos, M. Membranes for redox flow battery applications. *Membranes* **2012**, *2*, 275–306.

4. Schwenzer, B.; Zhang, J.; Kim, S.; Li, L.; Liu, J.; Yang, Z. Membrane development for vanadium redox flow batteries. *ChemSusChem* **2011**, *4*, 1388–1406.

5. Jiang, B.; Wu, L.; Yu, L.; Qiu, X.; Xi, J. A comparative study of Nafion series membranes for vanadium redox flow batteries. *J. Membr. Sci.* **2016**, *510*, 18–26.

6. Katzfuß, A.; Gogel, V.; Jörissen, L.; Kerres, J. The application of covalently cross-linked BrPPO as AEM in alkaline DMFC. *J. Membr. Sci.* **2013**, *425–426*, 131–140.

7. Marini, S.; Salvi, P.; Nelli, P.; Pesenti, R.; Villa, M.; Berrettoni, M.; Zangari, G.; Kiros, Y. Advanced alkaline water electrolysis. *Electrochim. Acta* **2012**, *82*, 384–391.

8. Kwon, T.; Lee, J.-W.; Cho, H.; Henkensmeier, D.; Kang, Y.; Hong, S.M.; Koo, C.M. Ionic polymer actuator based on anion-conducting methylated ether-linked polybenzimidazole. *Sens. Actuators B: Chem.* **2015**, *214 43-49*.

9. Lee, J.P.; Yoo, B.; Suresh, T.; Kang, M.S.; Vital, R.; Kim, K.J. Novel silane-substituted benzimidazolium iodide as gel electrolyte for dye-sensitized solar cells. *Electrochim.*

Acta **2009**, *54*, 4365–4370.

10. Pennline, H.W.; Granite, E.J.; Luebke, D.R.; Kitchin, J.R.; Landon, J.; Weiland, L.M. Separation of CO_2 from flue gas using electrochemical cells. *Fuel* **2010**, *89*, 1307–1314.

11. Mohammadi, T.; Skyllas Kazacos, M. Modification of anion-exchange membranes for vanadium redox flow battery applications. *J. Power Sources* **1996**, *63*, 179–186.

12. Hagesteijn, K.F.L.; Jiang, S.; Ladewig, B.P. A review of the synthesis and characterization of anion exchange membranes. *J. Mater. Sci.* **2018**, *53*, 11131–11150.

13. Atanasov, V.; Bürger, M.; Lyonnard, S.; Porcar, L.; Kerres, J. Sulfonated poly(pentafluorostyrene): Synthesis & characterization. *Solid State Ion.* **2013**, *252*, 75–83.

14. Atanasov, V.; Kerres, J. Highly phosphonated polypentafluorostyrene. *Macromolecules* **2011**, *44*, 6416–6423.

15. O'Hagan, D. Understanding organofluorine chemistry. An introduction to the C-F bond. *Chem. Soc. Rev.* **2008**, *37*, 308–319.

16. Dang, H.S.; Weiber, E.A.; Jannasch, P. Poly(phenylene oxide) functionalized with quaternary ammonium groups via flexible alkyl spacers for high-performance anion exchange membranes. *J. Mater. Chem. A* **2015**, *3*, 5280–5284.

17. Bakangura, E.; He, Y.; Ge, X.; Zhu, Y.; Wu, L.; Ran, J.; Cheng, C.; Emmanuel, K.; Yang, Z.; Xu, T. Tetrazole tethered polymers for alkaline anion exchange membranes. *Front. Chem. Sci. Eng.* **2018**, *12*, 306–310.

18. Morandi, C.G.; Peach, R.; Krieg, H.M.; Kerres, J. Novel morpholinium-functionalized anion-exchange PBI–polymer blends. *J. Mater. Chem. A* **2015**, *3*, 1110–1120.

19. Morandi, C.G.; Peach, R.; Krieg, H.M.; Kerres, J. Novel imidazolium-functionalized anion-exchange polymer PBI blend membranes. *J. Membr. Sci.* **2015**, *476*, 256–263.

20. Chromik, A.; dos Santos, A.R.; Turek, T.; Kunz, U.; Häring, T.; Kerres, J. Stability of acid-

excess acid-base blend membranes in all-vanadium redox-flow batteries. *J. Membr. Sci.* **2015**, *476*, 148–155.

21. Cho, H.; Krieg, H.M.; Kerres, J.A. Application of Novel Anion-Exchange Blend Membranes (AEBMs) to Vanadium Redox Flow Batteries. *Membranes* **2018**, *8*.

22. Chen, J.; Dumas, L.; Duchet-Rumeau, J.; Fleury, E.; Charlot, A.; Portinha, D. Tuning h-bond capability of hydroxylated-poly(2,3,4,5,6-pentafluorostyrene) grafted copolymers prepared by chemoselective and versatile thiol-para-fluoro “click-type” coupling with mercaptoalcohols. *J. Polym. Sci. Part A: Polym. Chem.* **2012**, *50*, 3452–3460.

23. Thomas, O.D.; Soo, K.J.W.Y.; Peckham, T.J.; Kulkarni, M.P.; Holdcroft, S. A Stable Hydroxide-Conducting Polymer. *J. Am. Chem. Soc.* **2012**, *134*, 10753-10756.

24. Henkensmeier, D.; Cho, H.; Brela, M.; Michalak, A.; Dyck, A.; Germer, W.; Duong, N.M.H.; Jang, J.H.; Kim, H.-J.; Woo, N.-S.; et al. Anion conducting polymers based on ether linked polybenzimidazole (PBI-OO). *Int. J. Hydrog. Energy* **2014**, *39*, 2842-2853.

25. Germer, W.; Leppin, J.; Kirchner, C.N.; Cho, H.; Kim, H.-J.; Henkensmeier, D.; Lee, K.-Y.; Brela, M.; Michalak, A.; Dyck, A. Phase separated methylated polybenzimidazole (O-PBI) based anion exchange membranes. *Macromol. Mater. Eng.* **2015**, *300*, 497-509.

26. Cho, H.; Hur, E.; Henkensmeier, D.; Jeong, G.; Cho, E.; Kim, H.J.; Jang, J.H.; Lee, K.Y.; Hjuler, H.A.; Li, Q.; et al. Meta-PBI/methylated PBI-OO blend membranes for acid doped HT PEMFC. *Eur. Polym. J.* **2014**, *58*, 135–143.

27. Lee, S.Y.; Kwon, Y.; Kim, B.H.; Chae, J.; Jang, J.H.; Henkensmeier, D.; Yoo, S.J.; Kim, J.Y.; Kim, H.J. Synthesis of high molecular weight sulfonated poly(arylene ether sulfone) copolymer without azeotropic reaction. *Solid State Ion.* **2015**, *275*, 92–96.

28. Yang, J.S.; Cleemann, L.N.; Steenberg, T.; Terkelsen, C.; Li, Q.F.; Jensen, J.O.; Hjuler, H.A.; Bjerrum, N.J.; He, R.H. High molecular weight polybenzimidazole membranes for high temperature PEMFC. *Fuel Cells* **2014**, *14*, 7–15.

29. Kerres, J.A.; Krieg, H.M. Poly(Vinylbenzylchloride) based anion-exchange blend membranes (AEBMs): Influence of PEG additive on conductivity and stability. *Membranes* **2017**, *7*.

30. Cho, H.; Krieg, H.M.; Kerres, J.A. Performances of Anion-Exchange Blend Membranes on Vanadium Redox Flow Batteries. *Membranes* **2019**,9.

31. Glipa, X.; Mula, B.; Jones, D.J.; Rozière, J. Comparison of the Conduction Properties of Phosphoric Acid Doped and Benzylsulfonate Grafted Polybenzimidazole. *Chemistry, Energy and the Environment, ed. Sequeira, C. A. C.; Moffat. J. B. Royal Society of Chemistry, Cambridge,* **1998**, pp. 249–256.

32. Zhang, B.; Zhang, S.; Xing, D.; Han, R.; Yin, C.; Jian, X. Quaternized poly(phthalazinone ether ketone ketone) anion exchange membrane with low permeability of vanadium ions for vanadium redox flow battery application. *J. Power Sources* **2012**, *217*, 296–302.

33. Teng, X.; Zhao, Y.; Xi, J.; Wu, Z.; Qiu, X.; Chen, L. Nafion/organically modified silicate hybrids membrane for vanadium redox flow battery. *J. Power Sources* **2009**, *189*, 1240–1246.

34. Jang, J.K.; Kim, T.H.; Yoon, S.J.; Lee, J.Y.; Lee, J.C.; Hong, Y.T. Highly proton conductive, dense polybenzimidazole membranes with low permeability to vanadium and enhanced H_2SO_4 absorption capability for use in vanadium redox flow batteries. *J. Mater. Chem. A* **2016**, *4*, 14342–14355.

35. Cha, M.S.; Jeong, H.Y.; Shin, H.Y.; Hong, S.H.; Kim, T.H.; Oh, S.G.; Lee, J.Y.; Hong, Y.T. Crosslinked anion exchange membranes with primary diamine-based crosslinkers for vanadium redox flow battery application. *J. Power Sources* **2017**, *363*, 78–86.

36. Liu, S.; Wang, L.; Li, D.; Liu, B.; Wang, J.; Song, Y. Novel amphoteric ion exchange membranes by blending sulfonated poly(ether ether ketone)/quaternized poly(ether imide) for vanadium redox flow battery applications. *J. Mater. Chem. A* **2015**, *3*, 17590–17597.

37. Sun, C.; Chen, J.; Zhang, H.; Han, X.; Luo, Q. Investigations on transfer of water and

vanadium ions across Nafion membrane in an operating vanadium redox flow battery. *J. Power Sources* **2010**, *195*, 890–897.

38. Gandomi, Y.A.; Aaron, D.S.; Mench, M.M. Coupled Membrane Transport Parameters for Ionic Species in All-Vanadium Redox Flow Batteries. *Electrochim. Acta* **2016**, *218*, 174–190.

39. Choi, C.; Kim, S.; Kim, R.; Choi, Y.; Kim, S.; Jung, H. young; Yang, J.H.; Kim, H.T. A review of vanadium electrolytes for vanadium redox flow batteries. *Renew. Sust. Energ. Rev.* **2017**, *69*, 263–274.

40. Cunha, Á.; Martins, J.; Rodrigues, N.; Brito, F.P. Vanadium redox flow batteries: a technology review. *Int. j. Energy Res.* **2015**, *39*, 889–918.

6. Overall discussion

AEBMs synthesized in this dissertation have shown promising performances in VRFBs. The AEBM was composed of 3 polymer components s. Firstly, PBI was used as a matrix polymer providing mechanical strength to membranes. A second polymer, as an anion exchange precursor, Br-PPO was used. A Br-PPO was used for both quaternized with TMIm and covalently cross-linking with PBIs. However, it should be note that most of Br-PPO was consumed by quaternization with TMIm, since the blend membrane composed of Br-PPO and PBI-OO (6/4 weight ratio) without TMIm showed a very low conductivity of 0.41 mS/cm in 1 M sulfuric acid (with TMIm: 65.2 mS/cm) and no performances in the VRFBs. A successful conversion of bromomethyl groups were confirmed by FT-IR analysis showing no peak of bromomethyl groups in blend membranes. As a third polymer, minor amount of sulfonated polymer was used for macromolecular ionical cross-linking to PBI.

AEBMs were optimized by varying the composition of polymers components. With increasing of an anion exchange precursor (Br-PPO) content in the blend membrane, the conductivity increased while the dimensional stability decreased due to the increased water uptake. The swelling properties of AEBMs can be controlled by varying anion exchange precursor amount or/and addition of a sulfonated polymer, where being regarded as a trade-off between the swelling property and ionic conductivity. Thus, blend membranes were optimized in terms of swelling ratio and conductivity in this study. In the battery test, all blend membranes showed better CE than that of commercial membranes (Nafion 212 for a CEM, FAP 450 for an AEM) due to the repelling of vanadium ions by AEMs which prevents vanadium ions cross-over thorough the membranes via Donnan exclusion effect. Since the CE mainly affected by vanadium ion cross-over. The VE is affected by ionic conductivity therefore, Nafion membrane showed highest VE than that of AEBMs. The overall EE of AEMBs showed comparable values to Nafion membrane. OCV test is commonly used as an indirect way to investigate the vanadium ion cross-over. The one optimized AEBM (BM-TMIm 4; 45 % Br-PPO, 45 % PBI-OO, 11 % sulfonated polymer) has shown much longer OCV time compared to Nafion membrane due to the less vanadium ion cross-over which is well correlated with the results of CE in the battery test.

The AEBMs have been optimized regarding compositions. Therefore, further developments for AEBMs have been studied with different polymers combinations in the blends. A Br-PPO was used as an anion exchange precursor. Two different matrix polymers based on PBI were used, one is non-fluorinated PBI (PBI-OO) and other is partially fluorinated PBI (F6-PBI). As a third component, two different polymers either non-fluorinated or partially fluorinated sulfonated polymer were used as macromolecular ionic cross-linker. For the blend membrane preparation, different combinations of the polymers used. All blend membranes showed similar ion exchange capacities and ionic conductivities since the same amount of anion exchange group was applied in each blend membrane during blend membrane preparation. In the VRFBs test, all AEBMs showed better CE than Nafion membrane because of the vanadium ions repelling by AEMs, named Donnan exclusion effect, as expected. Even though Nafion showed the highest VE due to the highest ionic conductivity among tested membranes, the most of AEBMs showed slightly higher EE than that of Nafion membrane due to the higher CEs. One of blend membranes composed of fluorinated polymers showed excellent capacity retention in the charge-discharge cycling test. This is probably due to the stable matrix polymer under the acidic conditions. F6-PBI membrane has shown that no significant changes of FT-IR spectrum were observed after 9 days in 30 % sulfuric acid solution. While PBI-OO has shown structural changes doped in 3 molar sulfuric acid solution in a few days which was confirmed by FT-IR spectrum by a sulfonation of the PBI-OO due to electron rich phenyl ether groups, which results in decreased ionic conductivity via ionical cross-linking of the sulfonated PBI and quarternary ammonium groups. Thus, it can be suggested that F6-PBI as a matrix polymer is more stable in VRFBs.

The novel anion exchange polymer was synthesized based on poly(pentafluorostyrene) (PPFSt) which was reported for the first time. Firstly, 1-(2-dimethylaminoethyl)-5-mercaptotetrazole was grafted on the *para*-position of PPFSt via nucleophilic substitution reaction. A successful synthesis was confirmed by NMR spectroscopy showing the degree of grafting of 41 %. Afterwards, tertiary amino group was quaternized by using methyliodide.

Because a mechanically stable free-standing membrane was not able to be prepared, the synthesized anion exchange polymer was blend with F6-PBI, since the F6-PBI was a suitable matrix polymer for VRFBs, which was concluded from the previous study. By blending, mechanically stable blend membranes were obtained. The obtained blend membranes showed relative low ion exchange capacities and chloride conductivities (around 0.04 mS/cm). But in 1 molar sulfuric acid solution, much higher conductivities were obtained from 13.5 to 19.1 mS/cm. Since they absorbed more sulfate or bisulfate ions, contributing to ion conductivity, per anion exchange group via hydrogen bridges. In the battery test, the synthesized blend membranes showed higher CEs than Nafion membrane due to the Donnan exclusion effect as mentioned previously. One of those blend membranes (70 % M-PPFSt-MTZ, 30 % F6-PBI) showed slightly higher overall EE than a Nafion membrane due to the higher CE. In the OCV measurement, the blend membranes showed longer time for voltage decay than that of Nafion membrane before OCV sharply drops, indicating low vanadium ions cross-over which was expected due to the enhanced Donnan exclusion effect. Those results are well correlated with CE results. The blend membranes showed better capacity retention than that of Nafion membrane measured by a charging-discharging cycling test at a constant current density of 40 mA/cm^2. The Nafion membrane showed a fast decay in capacity, losing most of its capacity in 100 cycles, while one blend membrane (70 % M-PPFSt-MTZ, 30 % F6-PBI) showed much better capacity retention of 80% loss over 200 cycles. It can be therefore conclude that blend membranes are promising candidate for VRFBs applications.

By considering the battery performances results, it can be concluded that anion exchange blend membranes are very promising candidates for VRFBs, if the proportion and type of the different components in the blend are carefully applied.

7. Summary and Outlook

In this dissertation, Anion Exchange Blend Membranes (AEBMs) were synthesized and applied in Vanadium Redox Flow Batteries (VRFBs). In the first paper, AEBMs were systematically optimized for VRFBs by varying the composition of polymers components. A bromomethylated poly (2, 6-dimethyl-1,4-phenylene oxide) (Br-PPO) was used as an anionic exchange precursor which was quaternized with 1,2,4,5-tetramethylmidazole (TMIm). A Polybenzimidazole-OO (PBI-OO, produced by Fuma-Tech) was used as a matrix polymer to provide mechanical strength. A minor amount of sulfonated polymer was used as an ionical cross-linker. Those AEBMs showed comparable Energy Efficiency (EE) with Nafion 212 membranes and one of the synthesized AEBMs (BM-TMIm 4) showed a superior Coulombic Efficiency (CE) of almost no decreasing after 300 charging-discharging cycles with a significant capacity retention of 77% of the initial value for after 300 charging-discharging cycles at a current density of 40 mA/cm^2. Therefore, AEBMs are promising candidates for long-term operation in VRFBs if the proportion and type of the different components in the blend system is carefully adjusted.

In the first paper, the composition of AEBMs were optimized for use in VRFBs. In the second paper, AEBMs were prepared with different polymer combinations. These AEBMs consisted of 3 polymer components. 1) F6-PBI (fluorinated PBI) or PBI-OO (non-fluorinated PBI): PBI was used as a matrix polymer, 2) Br-PPO: Br-PPO was used as an anion exchange polymer precursor by quaternizing with TMIm to provide anion exchange sites, 3) a partially fluorinated polyether or a non-fluorinated poly (ether sulfone): sulfonated polymer was used as an ionical cross-linker. The same weight ratios of three components were used in blend membranes, while different combinations of polymers were used. Similar properties of blend membranes such as ion exchange capacity, conductivity and swelling behavior showed since same amount of anion exchange polymer in each blend membrane was used. In VRFB test, all blend membranes showed better performances than the commercial membranes (Nafion: a cation exchange membrane and FAP 450: an anion exchange membrane) in terms of coulombic-, voltage- and energy efficiencies. One of the blend membranes (BM-TMIm4 FF), which is composed fluorinated polymers, exhibited excellent capacity retention showing no capacity decay over 550 charging-discharging cycles run at a current density of 40 mA/cm^2. The outstanding performance of fluorinated polymers-based blend membranes probably is due to the highly stability of F6-PBI in an acidic condition. A pure F6-PBI membrane showed no structural changes in 30 % sulfuric acid solution for 9 days confirmed by Fourier-Transfrom Infrared Spectroscopy (FT-IR spectra), while a PBI-OO membrane was sulfonated after few days. Thus, it can be concluded that if proper matrix polymer chosen for blend membrane, the AEBMs in VRFBs are expected to exhibit superior performance.

In the paper 3, AEBMs were synthesized by 3 steps based on Poly(pentafluorostyrene) (PPFSt) for use in VRFBs. Firstly, 1-(2-dimethylaminoethyl)-5-mercaptotetrazole was grafted onto PPFSt by nucleophilic substitution on the para-position. Secondly, the tertiary amino groups were quaternized with iodomethane to provide anion exchange sites. Thirdly, AEBMs were fabricated by blending of synthesized anion exchange polymer with F6-PBI. The blend membrane containing of 30% F6PBI showed better VRFBs performance that Nafion membrane in terms of energy efficiency, Open Circuit Voltage (OCV) and charging-discharging cycling. While the blend membrane containing of 40% F6-PBI displayed much longer OCV time and capacity retention by a charging-discharging test than that of Nafion membrane. It can be concluded that AEBMs are strong candidate for VRFB applications.

The AEBMs tested in VRFBs have shown better performances than that of commercial reference membranes of a cation exchange membrane (Nafion) and an anion exchange membrane (FAP 450). By considering the battery test results of AEBMs in this study, therefore, it can be concluded that the AEBMs are very promising candidates as separators in VRFBs if the matrix polymer is chosen properly. One further potential application of those blend membranes can be used in phosphoric acid doped high temperature proton exchange membrane fuel cells (PA-doped HT-PEMFCs), since the AEBMs in this dissertation showed high thermal stability. In recent paper (Nat Energy 1, 16120 (2016)), anion exchange membrane showed very promising results in PA-doped PEMFCs displaying much better performances than that of a polybenzimidazole membrane (a standard membrane for PA-doped HT-PEMFCs) in the FC test. The results in our patent have shown also that those anion exchange membranes exhibited promising performances in the fuel cell test. Therefore, anion exchange blend membranes synthesized in this study are expected to excellent performances for phosphoric acid doped HT-PEMFCs.

8. Zusammenfassung und Ausblick

In dieser Dissertation wurden Anionenaustauscherblendmembranen (AEBMs) synthetisiert und in Vanadium Redox Flow Batterien (VRFBs) eingesetzt. In der ersten Arbeit wurden die AEBMs systematisch für VRFBs optimiert, indem die Zusammensetzung der Polymerkomponenten variiert wurde. Als anionischer Austauschvorläufer wurde ein brommethyliertes Poly(2,6-dimethyl-1,4-phenylenoxid) (Br-PPO) verwendet, das mit 1,2,4,5-tetramethylimdazole (TMIm) quaternisiert wurde. Polybenzimidazole-OO (PBI-OO, Hersteller: Fuma-TecH) wurde als Matrixpolymer verwendet, um die mechanische Stabilität zu unterstützen. Eine geringe Menge an sulfoniertem Polymer wurde als ionischer Vernetzer verwendet. Diese AEBMs zeigten vergleichbare Energieeffizienz (EE) mit Nafion 212-Membranen und eines der synthetisierten AEBMs (BM-TMIm 4) zeigte eine überlegene Coulombeffizienz (CE), die nach 300 Lade-Entlade-Zyklen fast nicht abnahm, mit einer signifikanten Kapazitätserhaltung von 77% des Anfangswertes bei einer Stromdichte von 40 mA/cm^2. Daher sind AEBMs vielversprechende Kandidaten für den Langzeitbetrieb in VRFBs, wenn das Verhältnis und die Art der verschiedenen Komponenten im Mischungssystem sorgfältig angepasst werden.

Im ersten Teil dieser Arbeit wurde die Kombination von AEBMs für den Einsatz in VRFBs optimiert. Im zweiten Teil wurden AEBMs mit verschiedenen Polymerkombinationen hergestellt. Diese AEBMs bestanden aus 3 Polymerkomponenten. 1) F6-PBI (fluoriertes PBI) oder PBI-OO (nicht fluoriertes PBI): PBI wurde als Matrixpolymer verwendet, 2) Br-PPO: Br-PPO wurde als Anionenaustauscherpolymer-Vorläufer durch Quaternisierung mit TMIm verwendet, um Anionenaustauschergruppen bereitzustellen, 3) ein teilfluoriertes Polyether oder ein nichtfluoriertes Poly(ethersulfon): sulfoniertes Polymer wurde als ionischer Vernetzer verwendet. In den Blend-Membranen wurden die gleichen Gewichtsverhältnisse der drei Komponenten verwendet, während unterschiedliche Kombinationen von Polymeren eingesetzt wurden. Es zeigten sich ähnliche Eigenschaften der Blend-Membranen bezüglich der Ionenaustauscherkapazität, der Leitfähigkeit und des Quellverhaltens, da in jeder Blend-Membran die gleiche Menge an Anionenaustauscherpolymer verwendet wurde. Im VRFB-Test zeigten alle Blend-Membranen bessere Leistungen als die kommerziellen Membranen (Nafion: eine Kationenaustauschmembran und FAP 450: eine Anionenaustauschmembran) in Bezug auf die Coulomb-, Spannungs- und Energieeffizienzen. Eine der Blend-Membranen (BM-TMIm4 FF), die aus fluorierten Polymeren besteht, zeigte eine exzellente Kapazitätserhaltung und keinen Leistungsabfall über 550 Lade-/Entladezyklen bei einer Stromdichte von 40 mA/cm^2. Die herausragende Leistung der auf fluorierten Polymeren basierenden Blend-Membranen ist wahrscheinlich auf die hohe Stabilität von F6-PBI im sauren Medium zurückzuführen. Eine reine F6-PBI-Membran zeigte keine strukturellen Änderungen in 30 %iger Schwefelsäurelösung für 9 Tage, was durch Fourier-Transformations-Infrarotspektroskopie (FT-IR-Spektren) bestätigt wurde, während eine PBI-OO-Membran nach wenigen Tagen sulfoniert wurde. Daraus lässt sich schließen, dass AEBMs in VRFBs eine überlegene Leistung aufweisen können, wenn das richtige Matrixpolymer für die Blend-Membran gewählt wird.

Im dritten Teil dieser Arbeit wurden AEBMs in 3 Stufen auf Basis von Poly(pentafluorstyrol) (PPFSt) für die Verwendung in VRFBs synthetisiert. Erstens wurde 1-(2-Dimethylaminoethyl)-5-mercaptotetrazol durch nukleophile Substitution an der para-Position auf PPFSt aufgepfropft. Zweitens wurden die tertiären Aminogruppen mit Iodmethan quaternisiert, um Anionenaustauschergruppen zu bilden. Drittens wurden AEBMs durch Mischen des synthetisierten Anionenaustauscherpolymers mit F6PBI hergestellt. Die Blend-Membran, die 30 % F6PBI enthält, zeigte eine bessere VRFB-Leistung als die Nafion-Membran in Bezug auf Energieeffizienz, Leerlaufspannung (OCV) und Lade-/Entladezyklen. Die Blend-Membran, die 40% F6PBI enthält, zeigte eine viel längere OCV-Zeit und Kapazitätserhaltung bei einem Lade-Entlade-Test als die Nafion-Membran. Daraus kann geschlossen werden, dass AEBMs vielversprechende Kandidaten für VRFB-Anwendungen sind.

Die AEBMs, die in VRFBs getestet wurden, zeigten bessere Leistungen als die kommerziellen Referenzmembranen einer Kationenaustauschermembran (Nafion 212) und einer Anionenaustauschermembran (FAP 450). Unter Berücksichtigung der Batterietestergebnisse der AEBMs in dieser Studie kann daher festgestellt werden, dass die AEBMs sehr vielversprechende Kandidaten als Separatoren in VRFBs sind, wenn das Matrixpolymer richtig gewählt wird. Eine weitere mögliche Anwendung dieser Blend-Membranen kann in einer phosphorsäuredotierten Hochtemperatur-Protonenaustauschmembran-Brennstoffzellen (HT-PEMFCs) gefunden werden, da die AEBMs in dieser Dissertation eine hohe thermische Stabilität zeigten. In einer kürzlich erschienene Arbeit (Nat. Energy 1, 16120 (2016)) zeigte die Anionenaustauschermembran sehr aussichtsreiche Ergebnisse in PA-dotierten HT-PEMFCs, die im FC-Test deutlich bessere Leistungen als die einer PBI-Membran (eine Standardmembran für PA-dotierte HT-PEMFCs) zeigten. Die Ergebnisse in einem Patent, mit dem Autor als Koerfinder, haben auch gezeigt, dass diese Anionenaustauschermembranen vielversprechende Leistungen im Brennstoffzellentest zeigten. Daher wird erwartet, dass die in dieser Studie synthetisierten Anionenaustauschermembranen hervorragende Leistungen für Phosphorsäure-dotierte HT-PEMFCs erbringen.

9. Acknowledgements

There have been many people who have supported and assisted throughout working on this dissertation. Firstly, I wish to show my gratitude to Prof. Friedrich who accepted me as a doctoral student and gave me an opportunity to publish this dissertation.

I would like to express my sincere appreciation to Dr. Kerres who offered place to fulfill experiments and to write dissertation. Without his guidance and supporting during my Ph D, this dissertation may not be able to be written. I have learned a lot under his supervision and his teaching has improved my ability to think academically.

I wish to express my deepest gratitude to Dr. Atanasov, a group leader, who supported me to make possible my work until finish my dissertation with valuable discussions. I thank all of his efforts that made my work in ICVT possible. And I would like to thank Johannes Bender who helped me a lot in the lab and office whenever I had some troubles. I would also like to thank to Inna Kharitonova and Galina Schumski for valuable assistance which made publications in the scientific journals possible.

I would like to express my gratitude to Prof. Nieken, head of ICVT and Prof. Merten, deputy head of ICVT and all members at ICVT, providing me kind atmosphere and friendly feelings during my stay in ICVT.

I would like to thank to Dr. Henkensmeier who was my supervisor during my master thesis and recommended to carry out my Ph D in Stuttgart, Germany and appreciate regarding kind responding whenever I asked something.

Finally, I would like to thank my friends and family, specially I deeply appreciate my family in Korea. Even though I could not visit them often due to the long distance, I know that they always love me. All my achievements reflect of their support and sacrifice. I would like to give all the best things wholeheartedly and gratefulness to my father, mother and family of my older brother, who always stood on my side.

I would like to thank again to everyone who supported me. I have many people that I should thank. Even though I could not mention all the names, I will always remember for their attitudes to me.